ALMA MATER STUDIORUM
UNIVERSITÀ DI BOLOGNA

DIPARTIMENTO DI INGEGNERIA CIVILE, CHIMICA, AMBIENTALE E DEI MATERIALI

CORSO DI LAUREA

TESI DI LAUREA

in
Ingegneria chimica e di processo

Experimental characterization of mechanical properties of thermal insulation materials in cryogenic and vacuum conditions

CANDIDATO:
Marco Carboni

RELATORE:
Giordano Emrys Scarponi

CORRELATORE:
Robert Eberwein
Finn Harwege

Anno Accademico 2024/2025
Sessione III

INDEX

1. ABSTRACT

The energy transition toward hydrogen as an energy carrier requires the development of cryogenic storage systems capable of containing liquid hydrogen (LH_2) at –253 °C with minimal evaporation losses.
Conventional cryogenic tanks and vacuum insulation panels (VIPs) employ powdered insulating materials, glass microspheres, filtered perlite, cryoperlite, and fumed silica, in the insulating interspace.
However, the mechanical behavior of these materials under operating conditions (vacuum, cryogenic temperature) remains poorly characterized in the literature, representing a critical knowledge gap for the structural design of next-generation large-scale storage tanks.
This work aims to experimentally and quantitatively characterize the compressive mechanical behavior of the four aforementioned insulating materials under atmospheric, vacuum, and cryogenic conditions, with the objective of extracting comparable parameters and identifying the prevailing densification mechanisms.
Tests were conducted through uniaxial compression using a purpose-built instrumented apparatus, applying loading–unloading cycles up to maximum pressures of approximately 0.45 MPa.
Experimental data were analyzed by applying the Heckel and Kawakita equations, widely used in pharmaceutics and powder technology, here extended to highly porous materials (porosity >90%, bulk density 0.05–0.16 g/cm³) that lie outside their traditional applicability ranges.
Results show that the Kawakita equation better suits the characteristics of the tested materials, achieving R^2 coefficients above 0.94 in the majority of material–condition combinations where plastic deformation is attained.
The Heckel equation demonstrated limited applicability, strongly dependent on environmental conditions, with acceptable R^2 (>0.90) only in specific cases; it was therefore retained as a comparative tool for literature positioning.
Among the tested materials, fumed silica confirmed itself as the most compressible under all conditions, with maximum strains up to 82% under cryogenic conditions and Kawakita yield pressures of approximately 0.09–0.15 MPa.
Filtered perlite and cryoperlite exhibit intermediate resistance (Py ≈ 0.32–0.48 MPa), with cryoperlite displaying anomalous behavior at cryogenic temperature, interpretable as catastrophic collapse of the porous structure followed by recompaction of fragments.
Glass microspheres exhibited the mechanically stiffest behavior, with reduced strains and absence of permanent consolidation within the investigated pressure range, confirming the inadequacy of the experimental setup for their full characterization.
The study identifies fumed silica as the material at greatest risk of performance degradation under load in VIP applications, where core material compressibility is a critical parameter for maintaining internal vacuum and dimensional stability.
Glass microspheres, despite showing the highest mechanical stiffness, require higher pressures for complete characterization.
The results contribute to bridging the knowledge gap regarding the cryogenic mechanical behavior of these insulators, providing a quantitative basis for the design of large-volume LH_2 tanks and for the selection of core materials in VIPs intended for advanced cryogenic applications.

2. INTRODUCTION

2.1 Context and motivation of the study

With the growing need for a stable and widespread energy transition, hydrogen is emerging as an energy carrier, a potential solution for energy storage and transport thanks to its mass energy density (which is 120 MJ/kg compared to 44 MJ/kg for gasoline) and the possibility of producing it from renewable sources [1].
It is essential to upgrade infrastructure and conduct an in-depth analysis of new techniques for storage and long-distance transport, as current technologies would not allow for national or global implementation of this molecule. Indeed, with today's tank volumes, transport would not be economically sustainable for processes that currently rely on other energy carriers or fuels.
Among the various methods under study for hydrogen transport—such as compression, adsorption on solid materials, or chemical carriers—liquid hydrogen stands out for its higher mass energy density.
This makes it an interesting option for large-scale and long-distance applications, despite the technical challenges associated with its cryogenic management.
To date, the largest liquid hydrogen storage tanks ever built are located in the United States and Japan, specifically at the Kennedy Space Center (Florida, USA) and at Kobe Airport.
The reasons behind their construction are different: the first was developed to support the Apollo program, while the second is used to support the hydrogen supply chain arriving by air from Australia.
The American tanks are the largest, with a capacity of 3,200 m^3 of hydrogen [2].
Furthermore, a new tank is under construction, equipped with advanced insulating materials such as microspheres, combined with a vacuum pumping and integrated refrigeration system, and an expected volume of 4,700 m^3 [3].
Despite the listed dimensions, hydrogen storage volumes are still an order of magnitude lower than those required for industrial-scale storage comparable to LNG (Liquefied Natural Gas).
For reference, LNG tanker ships typically carry between 125,000 and 266,000 cubic meters of liquefied gas, with Q-Max class ships representing the upper end of this range.
On land, full containment LNG tanks can reach capacities up to 200 million liters (200,000 cubic meters), such as those managed by Toho Gas and Osaka Gas.

2.2 Cryogenic hydrogen storage: thermal challenges

Storage tanks for cryogenically liquefied gases are normally composed of an inner and an outer vessel, separated by an insulating layer.
This layer can consist of various materials, including perlite, microspheres, and multilayer insulation (MLI).
This layer is also placed under vacuum, which significantly improves thermal insulation by minimizing heat transfer by conduction and convection through the gap.
Its purpose is to reduce heat transfer in all its forms (conduction, convection, and radiation), thus ensuring minimal heating of the liquid and maintaining its temperature while minimizing material loss due to boiling.
Therefore, it is essential to deepen the study of the mechanical properties of insulating materials such as perlite and microspheres under operating conditions.
This will enable the design of larger volume tanks with sustainable evaporation rates, which is fundamental for the expansion of hydrogen infrastructure.

To achieve this goal, it is necessary to understand how these materials behave under mechanical stress and cryogenic temperatures, especially in configurations such as vacuum insulation panels (VIPs).
VIPs are composite insulating systems consisting of a highly porous core material enclosed within a gas-tight envelope that is evacuated and sealed, offering extremely low thermal conductivities that depend on the core material and vacuum level which are being explored to simplify the construction of large LH_2 tanks without requiring a global vacuum.

2.3 Thesis objectives

Unlike conventional double-walled cryogenic tanks, VIPs apply mechanical stress to the core insulating materials, however traditional cryogenic insulators such as perlite and microspheres are rarely studied under mechanical load.
This knowledge gap must be filled to ensure structural integrity and thermal performance.
Even in conventional tank designs, problems can arise, as demonstrated by NASA's investigation of a poorly performing LH_2 sphere [4], in which voids in the perlite insulation compromised tank efficiency.
For large-scale tanks, it is generally assumed that the same insulation mechanism will be used [3].
However, the stress applied to materials frequently used in the insulating gap must be characterized under operating conditions.
Currently, the literature includes a study that analytically and numerically characterizes the behavior of microspheres under load [5].
However, it is important to provide an experimental basis to confirm this behavior.
This study therefore aims to investigate the mechanical properties of insulating powders under vacuum and at cryogenic temperatures by subjecting them to uniaxial loading.

3. STATE OF THE ART

3.1 Insulating materials for cryogenic applications

These materials are commonly used in the interstitial space between the inner and outer tank to reduce heat transfer from the environment to the liquid, limiting thermal conduction and the consequent evaporation of hydrogen [6].
A comparison of the thermal insulating capabilities of microspheres and perlite has already been conducted in the literature using a 1000 L tank, in which the evaporation rate of liquid hydrogen and liquid nitrogen was measured, obtaining a reduction of 34% for the former and 46% for the latter [7].
Despite the clear results obtained, this study involves the comparison of all four powders. Indeed, with the aim of constructing large-volume tanks that would enable the use of hydrogen as an energy vector on a global scale, the possibility of employing vacuum insulation panels (VIPs) is currently being investigated.
The advantages of these panels include modularity, the presence of an external envelope containing the core material, and the presence of opacifiers and porosity within the core material, which further reduce heat transmission by radiation and conduction [8].
The mechanical properties of VIPs therefore depend on the material chosen as the core, among which the most commonly used are the powders analyzed in this study.
In order to verify which material can best withstand the cyclic thermal and mechanical stresses imposed on tanks for liquid hydrogen containment, it is necessary to conduct this study not only on the most thermally efficient material, but also on materials with lower efficiency that can nevertheless be used with good insulating results and potentially superior mechanical capabilities.
Expanded perlite exhibits thermal conductivity values that vary significantly as a function of the applied vacuum level.
Under high vacuum conditions ($P < 10^{-3}$ Pa), perlite achieves a thermal conductivity of approximately 0.95 mW/m·K, comparable to that of multi-layer insulation at the same pressure.
However, as pressure increases, insulating performance progressively decreases: at moderate vacuum (10^{-3} Pa $< P < 10^{-1}$ Pa) conductivity rises to approximately 1 mW/m·K, while at ambient pressure ($P = 10^{5}$ Pa) it reaches values of 44 mW/m·K, indicating a sharp reduction in insulating effectiveness in the absence of vacuum [3].
A critical limitation of perlite in cryogenic applications is represented by the phenomenon of settling and compaction over time.
This aspect is particularly problematic in applications subject to vibrations, such as in tanks for maritime transport, or to repeated thermal cycles.
Settling occurs when perlite particles shift or compress, reducing the effective insulation thickness and forming voids that lead to increased thermal conductivity.
Thermal cycling, characterized by repeated cooling and heating, causes expansion and contraction of the tank walls, resulting in particle shifting and compaction.
Perlite tends to compact more at the tank bottom, creating gaps that constitute thermal bridges and significantly reduce insulating capability over time [9].
From a mechanical perspective, expanded perlite particles are hollow and porous, resulting in low bulk density (ranging from 32 to 150 kg/m³).
This property, along with its low thermal conductivity, makes perlite an attractive material for various applications.
However, perlite has relatively low compressive strength due to its porous structure and thin-walled hollow particles [10], [11].

Hollow glass microspheres (HGMs) represent a promising alternative to perlite due to their excellent resistance to compaction and settling.
Road transport tests, simulating real-world vibrations, have demonstrated that glass microspheres maintain their insulating properties with minimal performance degradation.
This compaction resistance is crucial for cryogenic tanks that may experience vibrations during their lifecycle, ensuring consistent insulating effectiveness without significant loss of performance due to settling [9].
From a thermal perspective, glass microspheres exhibit exceptionally low thermal conductivity under high vacuum conditions, with minimum values of 0.9 mW/m·K ($P < 0.13$ Pa), proving particularly effective in cryogenic environments.
Even at moderate vacuum levels ($0.13\ Pa < P < 13.3\ Pa$), microspheres continue to provide stable insulation with typical conductivity of 1.5 mW/m·K, showing lower thermal conduction compared to alternative materials such as perlite and aerogel [3].
Glass microspheres consist of heat-resistant materials with high melting temperatures, ranging from 1400 to 1600 °C, making them well-suited for applications requiring structural stability and resilience to extreme temperatures.
The density of glass microspheres ranges between 65 and 350 kg/m³ depending on the size and morphology of the spheres [9].
Furthermore, in applications involving repeated thermal cycling, glass microspheres maintain their thermal performance.
Unlike materials prone to compaction during thermal cycling, microspheres remain largely unchanged, avoiding the formation of gaps or thermal bridges that could increase heat transfer [9].
Fumed silica represents the primary material used in Vacuum Insulation Panels (VIP) due to its exceptionally low thermal conductivity, approximately 4 mW/m·K under vacuum conditions [12].
VIPs are insulating systems composed of a highly porous core material enclosed in a gas-tight envelope, which is evacuated and sealed.
This structure minimizes conductive, convective, and radiative heat transfer, offering extremely low thermal conductivities that depend on the core material and vacuum level [13].
The thermal performance of VIPs is influenced by several factors, including internal pressure and moisture content.
As internal pressure increases, the thermal conductivity of the core material also rises. Similarly, the presence of moisture can significantly degrade thermal performance, with an observed increase of 0.5 mW/m·K per mass percent of water in fumed silica [12].
Radiative heat transfer is reduced by incorporating opacifiers such as silicon carbide powder, which make the core material opaque to infrared radiation.
Solid conduction within the core is minimized due to the high porosity and small pore size of fumed silica.
To mitigate the effects of degradation over time, getters and desiccants are often added to the core material to absorb residual gases and moisture, thereby prolonging the service life of the panels.
As a result of this progressive degradation, the effective thermal conductivity of fumed silica VIPs ranges from 7 to 9 mW/m·K over a timespan of approximately 25 years [14].

3.2 Mechanical behavior of insulating powders

Insulating powders used in cryogenic systems are subjected to mechanical loads during filling operations, transport and thermal cycles.

Understanding the mechanical behavior of these materials is essential to ensure the structural integrity and thermal performance of insulation systems.
This section analyzes the deformation mechanisms, elastic properties, stress distribution and effects of dynamic loading on insulating powders under uniaxial compression.

3.2.1 Fundamental Mechanisms of Powder Compaction

During confined uniaxial compression, powders undergo progressive porosity reduction through different deformation mechanisms that operate sequentially or simultaneously[15].
In the initial stage, at low applied loads, particle rearrangement prevails: particles reposition themselves occupying available void spaces through geometric rearrangement requiring minimum energy.
This mechanism is particularly effective for powders with spherical or regular particles.
As the applied load increases, when particles have already reached a denser packing configuration, local deformation mechanisms intervene.
For ductile materials, such as metallic powders, localized plastic deformation occurs in interparticle contact zones, with progressive flattening of contact points and consequent increase of contact area [15].
For brittle materials, such as glass microspheres and ceramic powders, the dominant mechanism is particle fracture, with formation of fragments that fill residual interstices[16] [17].
The nature of the material profoundly influences the compaction path.
It has been demonstrated that plastically deformable powders show a more gradual and partially reversible compaction, while brittle powders present discontinuities in the load-displacement behavior corresponding to fracture events of individual particles [15].

3.2.2 Elastic Properties and Stress Distribution

The elastic properties of powders during compaction have been investigated through elastic wave velocity measurements [18].
During uniaxial compression, the Young's modulus of powders increases progressively with porosity reduction, reflecting the increase of contact points between particles and material densification.
However, the elastic properties of powders depend not only on total porosity, but also on pore geometry and contact distribution.
For spheroidal metallic powders (copper, stainless steel, aluminum) the Young's modulus normalized to the solid material value (E/E_{solid}) collapses onto a single curve as a function of porosity, indicating that the elastic properties of the solid material dominate the macroscopic behavior when particle geometry is similar [18].
Conversely, powders with irregular or dendritic particles show greater compliance at equal porosity, due to the presence of less efficient contacts and more rugged pores.
Regarding Poisson's ratio (ν), a concave trend has been evidenced during compaction: ν initially decreases with porosity reduction, reaches a minimum in an intermediate porosity region, and subsequently increases approaching the solid material value when porosity tends to zero [18].
This behavior is attributed to the fact that, at high porosity, local lateral deformations are "absorbed" by void spaces rather than transmitted through the bulk, making the macroscopic behavior relatively insensitive to the Poisson's ratio of the solid material.
With progressive densification, instead, the elastic properties of the solid material assume an increasing role.
The stress distribution within confined powder columns under uniaxial compression is not uniform.

Detailed experimental measurements using capacitive sensors have characterized radial stresses on container walls and axial stresses at the base [19].
The results show that:

- **Axial stresses**: decrease exponentially with depth from the load application surface, according to Janssen's relation.
  For sufficiently tall columns (height/diameter ratio > 0.6), stress at the base becomes uniform; for shorter columns, localized stress concentrations are observed.

- **Radial stresses**: immediately below the loading piston, very high radial stresses develop (up to 40-50% higher than the applied axial stress), indicating a radial distribution of stresses in the surface region [19].
  This phenomenon is particularly relevant for brittle materials, as it can induce tensile fracture in particles near the container walls.

3.2.3 Effects of Vibration and Settling

Dynamic loading induced by vibrations represents a critical factor for applications where insulating powders are subjected to transport, tank filling or high-energy transient events such as space launches.
The behavior of glass microspheres (glass bubbles) and perlite under random vibrations with intensity up to 42.8 G_{rms} (root mean square) for durations of 3-15 minutes has been investigated simulating space shuttle launch environments [20].
The main results highlight:

- **Vibration-induced compaction**: glass microspheres show the lowest compaction (2.5-4% volume reduction), while perlite presents higher values (13-17.5%) [20].
  This behavior is correlated with particle morphology: spherical and smooth particles reorganize less compared to irregular particles.

- **Vibration transmissibility**: glass microspheres show the best vibration attenuation at high frequency (300-5000 Hz), thus representing an advantageous material for applications subjected to dynamic loading [20].

- **Phase separation**: in stratified mixtures of microspheres and perlite, prolonged vibrations (14 hours at 30 Hz) do not induce significant mixing, maintaining a sharp interface between the two materials [20].
  This indicates good dimensional stability for multilayer applications.

Settling effects are particularly relevant for powders with high surface roughness, which tend to mechanically interlock, and for low-permeability powders, which hinder air backflow during post-compression expansion [19].

3.3 Mechanical models for powders

The Heckel and Kawakita equations represent two complementary approaches for characterizing the mechanical behavior of powders under compression, each developed with different theoretical assumptions.
The Heckel equation, based on first-order kinetics for porosity reduction, assumes that densification occurs through continuous plastic flow of particulate material, making it particularly suitable for metallic and pharmaceutical powders at relatively high density.

The Kawakita equation, conversely, describes the behavior of materials that compact through particle rearrangement and void space reduction, proving optimal for soft, highly compressible powders (fluffy powders).

3.3.1 Heckel model

The Heckel equation $\ln\left(\frac{1}{\varepsilon}\right) = KP + A$

(1)$\ln\left(\frac{1}{\varepsilon}\right) = KP + A$

(1 was applied to experimental compression data to characterize the mechanical behavior of the powders and determine their yield pressure.

$$\ln\left(\frac{1}{\varepsilon}\right) = KP + A \quad (1)$$

where ε represents the material porosity, P the applied pressure, K the proportionality constant, and A the intercept.
In the experimental data, porosity was calculated as ε = 1 - D, where D is the relative density of the sample, obtained from the ratio between the apparent density and the theoretical density of the material as if it had no porosity the substitution resulted in $ln\left(\frac{1}{1-D}\right) = KP + A$ (2).

$$ln\left(\frac{1}{1-D}\right) = KP + A \quad (2)$$

The Heckel equation is based on the assumption that porosity reduction follows first-order kinetics with respect to the applied pressure, making it particularly suitable for describing the behavior of materials that compact primarily through plastic deformation[21].
However, as reported in the literature, Heckel profiles typically show initial curvature attributable to particle rearrangement and possible granule fragmentation, followed by a linear region where plastic deformation dominates [22].
Yield pressure (P_H) represents the fundamental parameter extracted from Heckel analysis and corresponds to the inverse of the constant K obtained from the slope of the linear region:

$$P_H = \frac{1}{K} \quad (3)$$

This parameter is correlated to the material's yield strength according to the relationship

$$P_H = 3\sigma_0 \quad (4)$$

where σ_0 represents the intrinsic yield strength of the material.
Yield pressure provides a quantitative measure of the material's resistance to plastic deformation under compression and allows materials to be classified based on their mechanical behavior.
According to the classification proposed by Roberts and Rowe, materials with $P_H < 40$ MPa are considered "very soft", those with $40 < P_H < 80$ MPa "soft", materials with $80 < P_H < 200$ MPa "moderately hard", and those with $P_H > 200$ MPa "hard"[22].

An alternative classification proposed by Denny distinguishes plastic materials ($P_H < 60$ MPa), those with intermediate deformation mechanisms ($60 < P_H < 120$ MPa), and brittle materials ($P_H > 120$ MPa)[21].
Accurate determination of P_H is therefore essential for understanding the mechanical behavior of insulating powders under the operating conditions expected for cryogenic tanks.
Correct identification of the linear region of the Heckel profile is crucial for obtaining reliable yield pressure values. In the present study, the linear region was identified by selecting a pressure range between 60% and 95% of the maximum pressure reached during the experiment. This approach, based on fixed fractions of the maximum pressure, automatically excludes the initial curved region dominated by particle rearrangement and the possible final region where work hardening effects might manifest.
The quality of the linear fit was evaluated using the R^2 coefficient, requiring values greater than 0.90 to consider the analysis acceptable.
The starting point of the analysis was defined using the initial relative density of the sample, calculated from the bulk density measured experimentally by vibration.

3.3.2 Kawakita model

The Kawakita equation $\frac{P}{C} = \frac{1}{ab} + \frac{P}{a}$ (5) was applied to experimental compression data to characterize the mechanical behavior of powders through a relationship between pressure and degree of volumetric compression.

$$\frac{P}{C} = \frac{1}{ab} + \frac{P}{a} \quad (5)$$

where P represents the applied pressure, C the degree of volume reduction, and a and b are material-characteristic constants[23].
In its non-linearized form, the equation is expressed as seen in $C = \frac{abP}{(1+bP)}$ (6).

$$C = \frac{abP}{(1+bP)} \quad (6)$$

which directly describes the relationship between compression and applied pressure.
The parameter C represents the volumetric reduction of the sample and was calculated as:

$$C = \frac{(V_0 - V)}{V_0} \quad (7)$$

Considering that the cross-sectional area of the compression chamber remains constant during the experiment, the volumetric reduction can be equivalently expressed in terms of sample height reduction:

$$C = \frac{(H_0 - H)}{H_0} \quad (8)$$

where H_0 is the initial sample height and H the height under pressure P.

This simplification was used in the experimental data analysis, calculating the piston displacement measured by the laser sensor to determine the height variation.
The Kawakita equation was originally developed for soft and highly compressible powders (fluffy powders), making it particularly suitable for describing the behavior of materials that compact through particle rearrangement and deformation in the initial phases of compression [21], [23]
The linearized form of the equation allows characteristic parameters a and b to be obtained through linear regression of the $\frac{P}{C}$ plot as a function of P, where the slope provides $\frac{1}{a}$ and the intercept provides $\frac{1}{ab}$.
From Kawakita analysis, three fundamental parameters can be extracted to characterize powder compressibility: parameter a (maximum compressibility), parameter b (inverse of characteristic pressure), and Kawakita yield pressure, defined as $P_y = \frac{1}{b}$.
Yield pressure P_y represents the pressure necessary to achieve half of the maximum compression and provides a quantitative measure of the material's resistance to densification[23].
This parameter is particularly useful for comparing different materials and experimental conditions, as it allows materials to be classified based on their ease of compression.
An additional derived index is the product ab, proposed as a classification index for compression behavior [22]
Materials with high ab values (typically > 0.1 MPa^{-1}) are classified as "Class I" and show significant particle rearrangement during compression, while materials with low ab values (≤ 0.1 MPa^{-1}) are classified as "Class II" with limited particle rearrangement and mainly plastic deformation.
It is important to emphasize that the Kawakita equation, while developed for pharmaceutical powders and soft materials at relatively low pressures [23], can be applied as an empirical descriptive model even for materials with very high porosity such as cryogenic insulating powders, provided that the extracted parameters are interpreted with due caution and used primarily for relative comparisons between materials and conditions rather than as absolute values with rigorous physical meaning[21].
The parameters a and b extracted from Kawakita analysis provide complementary information on the mechanical behavior of powders.
Parameter a theoretically represents the maximum degree of compression that the material can reach when pressure tends to infinity, and is therefore correlated to the maximum compressibility of the material.
From a theoretical perspective, for piston compression where the material cannot escape laterally, the value of a should correspond to the initial porosity ε_0 of the material.
Indeed, Kawakita & Lüdde (1970) demonstrate that:

$$a = \frac{(V_0 - V\infty)}{V_0} \quad (9)$$

where $V\infty$ is the material volume at infinite pressure, which theoretically should correspond to the volume of solid particles, making a equal to the initial porosity.
However, in experimental practice, a values often do not correspond exactly to the measured initial porosity, as also reported by Nordström et al. (2011).
This discrepancy can be attributed to several factors: first, for materials with very high initial porosity such as cryogenic insulating powders (with porosities typically exceeding 90%), accurate determination of the initial volume V_0 is problematic and strongly depends on sample loading and vibration conditions.

Kawakita & Lüdde (1970) emphasize that "particular attention must be paid to the experimental measurement of the initial volume of the powder" and that "deviations from this expression are sometimes due to fluctuations in the measured value of V_0".
Second, parameter a represents compressibility extrapolated to infinite pressure, while experiments are necessarily limited to a finite pressure range; this extrapolation can introduce significant discrepancies, especially when the material does not reach a complete densification state within the tested pressure range.
Third, for materials undergoing complex densification mechanisms, such as fragmentation of hollow particles or collapse of internal porous structures, the very concept of "solid volume" becomes ambiguous and parameter a assumes a more empirical than rigorously physical meaning.
Fourth, deviation from linearity of the Kawakita equation at high pressures, due to work hardening phenomena or changes in the dominant deformation mechanism, can influence the value of a obtained from linear fitting.
Kawakita & Lüdde (1970) observe that "the plot of P/C against P will be considered to deviate negatively from linearity in the initial stages of the compression, i.e. at low pressures", indicating that linearization is a valid approximation only within a certain pressure range.
For these reasons, parameter a must be interpreted primarily as a comparative indicator of relative compressibility between different materials and experimental conditions, rather than as an absolute measure of initial porosity.
Parameter b, which has dimensions of inverse pressure [MPa^{-1}], represents the pressure necessary to achieve compression equal to half the maximum value (a/2) and provides a measure of the material's resistance to compression.
High values of b indicate that the material compresses easily even at low pressures, while low values suggest greater resistance to compression [21]
Kawakita & Lüdde (1970) suggest that parameter b is correlated to cohesive forces between particles, observing that there exists a relationship between b and parameter k in Kuno's tapping equation, which represents "the ease of compression" and is related to the cohesive forces of powder particles.

3.3.3 Comparison between the two models

As highlighted by Denny (2002), "the Kawakita equation is best used for low pressures and high porosities", conditions that differ significantly from the application field of the Heckel equation, which requires sufficiently high pressures to induce significant plastic deformation.
In the context of the tested cryogenic insulating materials—glass microspheres, filtered perlite, cryoperlite, and fumed silica—the experimental conditions fall in a limiting region relative to traditional application fields.
With initial porosities > 90%, bulk densities of 0.05-0.16 g/cm³, and maximum pressures of approximately 0.5 MPa, the observed densification mechanisms primarily include particle rearrangement, fragmentation of hollow particles (microspheres and perlites), or collapse of aggregate structures (fumed silica).
Nordström et al. (2011) describe the typical Heckel profile as characterized by an "initial curved region due to particle rearrangement" followed by a "linear region where plastic deformation dominates".
For the tested materials, rearrangement dominates the entire experimental range, compromising identification of the linear region required by Heckel analysis and making rigorous application of the model problematic.
Despite these limitations, the Heckel equation was applied as a comparative tool for two main reasons.

First, yield pressure P_y provides a standardized parameter enabling qualitative comparisons with existing literature, positioning cryogenic materials within established classification frameworks such as Roberts and Rowe's.
Extracted parameters are interpreted as comparative indicators between materials and conditions, avoiding attributions of absolute physical meaning not justified by model assumptions.
This pragmatic approach maximizes the informational value of both methodologies—Kawakita's specificity for high compressibility and Heckel's universality for bibliographic comparisons—providing robust and complete characterization of insulating materials for cryogenic applications.

4. MATERIALS AND METHODS

4.1 Tested materials

In order to evaluate and compare the performance of different insulating materials, four powders composed predominantly of silicon dioxide were selected, which differ in production method and secondary components.
The chosen materials are glass microspheres, filtered perlite, cryoperlite, and fumed silica.

4.1.1 Glass microspheres

The microspheres used in this experiment are manufactured by 3M, specifically the K1 model.
The chemical structure is similar to that of soda-lime-borosilicate glass.
This type of hollow spheres is produced by adding a blowing agent to molten glass which, upon reaching high temperatures, generates a vacuum inside, rendering the sphere hollow with good insulating properties.

4.1.2 Filter perlite

The filtered perlite used is manufactured by KNAUF, specifically the D12 model.
The composition is 60-80% SiO2, 12-16% Al2O3, 5-10% Na2O, with the remaining percentage consisting of other oxides.
The production process employs thermal expansion: volcanic perlitic rock is placed in a furnace that reaches temperatures up to 1000 °C, heating it rapidly.
This temperature increase causes instantaneous evaporation of the water trapped in the material, which expands the volume by 15-20 times and creates the characteristic porosity.
Once expanded, the material is crushed and classified by particle size.
The presence of pores makes this material an excellent thermal insulator.

4.1.3 Cryoperlite

The cryoperlite used is manufactured by KNAUF, specifically the Cryoperl EL model. The chemical composition and production method are identical to those of filtered perlite D12.
The main difference lies in the particle size distribution: after expansion and crushing, the material is classified into a coarser size distribution, specifically optimized for cryogenic applications.
The larger particle size, combined with the characteristic porosity, makes this material particularly suitable as a thermal insulator for cryogenic fluid storage.

4.1.4 Fumed silica

The fumed silica used is manufactured by EVONIK, specifically the AEROSIL 200 model.
The chemical composition consists of >99.8% SiO2.
This material is produced through controlled combustion of silicon tetrachloride ($SiCl_4$) in an oxyhydrogen flame.
The high-temperature process enables the formation of silica particles that accumulate as an extremely fine amorphous powder.
The high purity and nanometric particle size confer excellent thermal insulating properties to this material.

Material	Microsphere	Filter Perlite	Cryoperlite	Fumed Silica
Diameter	65 µm	20 µm	0.5 mm	2,5 – 50 nm
Density	2.4 g/cm³	2.2 g/cm³	2.2 g/cm³	2.2 g/cm³
Bulk Density	0.083 g/cm³	0.163 g/cm³	0.074 g/cm³	0.049 g/cm³
Thermal conductivity	0.047 W/m·K	0.055 W/m·K	0.055 W/m·K	/

Table 1: Properties of materials

Figure 1: Photos of the materials: a) SEM photo of an assembly of microspheres [5] b) Filter perlite c) Fumed silica

4.2 Experimental setup

The experimental setup consists of several mechanical and electrical components that ensure the mechanical stability of the system and the recording of data necessary for the analysis of compression tests.
The load-bearing structure comprises an aluminum profile frame that provides rigid support for the entire experimental configuration.
This frame supports the load application system, composed of an actuator that applies uniaxial force first to the measurement sensors and subsequently to a second piston.
The measurement instruments include load cells for detecting the applied force and a laser sensor for continuous monitoring of piston displacement.
The lower piston transmits the load to the powder contained in the cylindrical compression chamber, enabling the study of the mechanical behavior of the material under uniaxial compression.
Below the compression apparatus, as can be observed in the three following images (Figure 3) there is a cryogenic containment system.
The configuration consists of a basin with an external plastic container, inside which a layer of lava rock bricks is positioned to serve as thermal insulation. This arrangement allows for thermal insulation of the stainless steel chamber that will contain the liquid nitrogen, reducing heat losses from the external environment and ensuring stable temperature conditions during cryogenic tests.

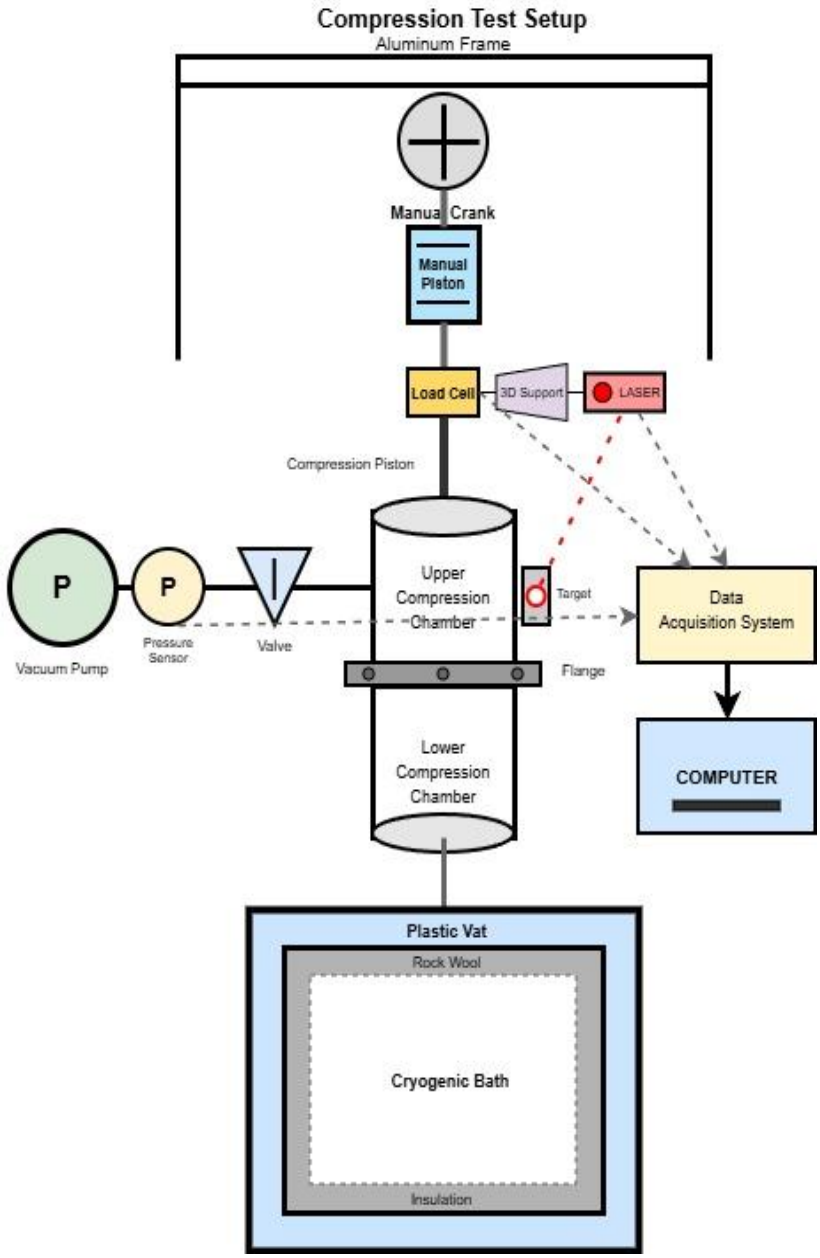

Figure 2: Scheme of the setup

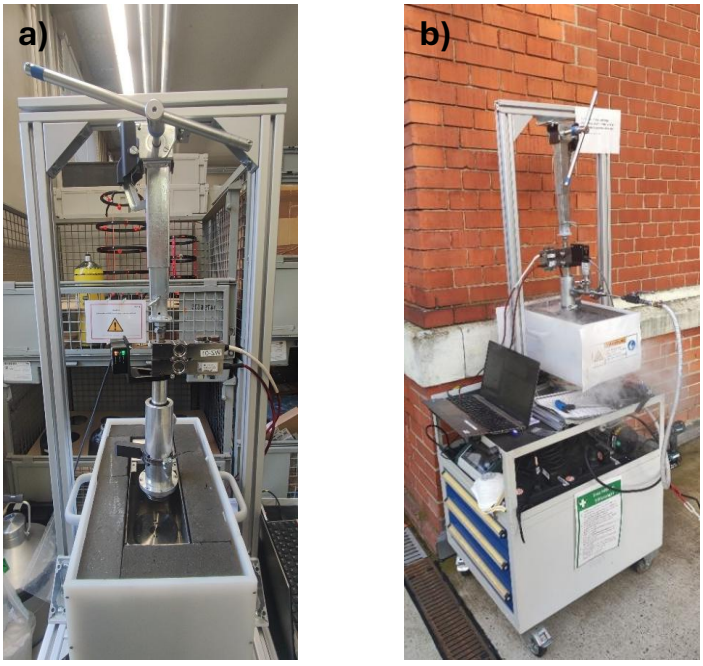

Figure 3: Frontal view of the structure (a) and complete view of the structure (b)

4.2.1 Uniaxial compression system

As can be observed in Figure 3, the first element present on the aluminum profile structure is a screw piston actuated by a manual crank.
This represents one of the main limitations of the instrumentation, as it does not allow high precision on the applied force compared to an automatic actuator.
However, for the load ranges used in these experiments, namely up to 1000 N, a variation of ±20-30 N is not problematic.
Between the upper piston and the compression chamber are positioned the load cells for measuring the applied force and the laser sensor for monitoring displacement, whose technical details will be described in the following paragraph.
Below in Figure 4 is the compression chamber.
It is equipped with a piston at whose end there are two rings that, during compression, prevent the upward movement of the powders.
The external chamber features a connection to which the valve system, filter, and vacuum pump are attached to create the necessary test conditions.
The upper and lower parts of the compression chamber are connected by means of a flange that uses 8 bolts to ensure the maintenance of vacuum conditions during tests, and a plastic ring as an additional sealing element.

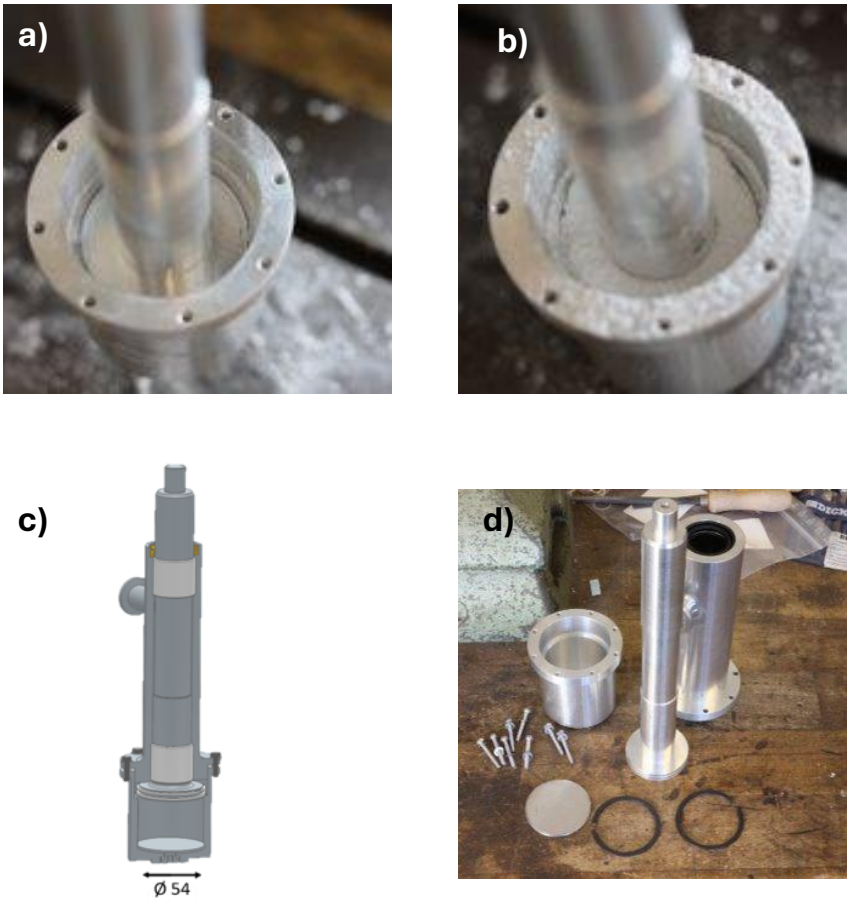

Figure 4: a) Compression with rings b) Compression without rings c) Compression chamber scheme d)General view of the components

The lower chamber contains the powders and features a bolt at the bottom which, once removed, allows the displacement of a movable base using a tool for the removal of samples at the end of the test.
The lower chamber also fits, through a dedicated circular hole, into the steel basin which provides additional stability during compression.

4.2.2 Instrumentation and data acquisition

In order to monitor and record parameters during the experiments, the setup is equipped with several measurement sensors.
There are two load cells manufactured by HBK, model HLCB2, with a maximum capacity of 110 kg, from which the 1000 N limit during compression is derived. Of the two load cells, only the first is used for data acquisition, while the second serves as a support plate on which the first performs measurements.

Indeed, the presence of suitable attachments and a flat surface made it optimal as a support base.
For displacement measurement, there is a laser sensor manufactured by BAUMER, model OM70-L1000, supported by a holder fabricated by 3D printing.
This sensor is used during experiments to measure the displacement of the piston relative to a fixed reference, also 3D printed and secured to the compression chamber by means of a metal clamp.
After the valve, there is also a sensor to determine the degree of vacuum in the compression chamber and ensure suitable conditions for the experiment.
The various sensors were connected to a data logger, specifically the Almemo 710, which allows data recording simultaneously with the experiment.
The data logger also enables the graphical representation of two recorded variables as a function of time or against each other.
Specifically, for this experiment, force as a function of displacement was displayed. This function is not available directly through the Almemo 710, but through dedicated software from the same manufacturer, Ahlborn.
Once recorded, the data were exported in Excel format so that they could be used in Python software to perform the necessary analyses.

Figure 5: Almemo 710

4.2.3 Test conditions (atmospheric, vacuum, cryogenic)

Since these materials are intended for use in tanks for cryogenic hydrogen storage, it is necessary to define test conditions that allow the evaluation of mechanical properties in a manner similar to real applications.
In particular, these tanks are subjected to cycles of thermal stress, vacuum conditions in the gap between the inner and outer tank, and, in the case of VIP usage, compression stress due to pressure differences.
The experimental conditions designed to reproduce these stress sources on the material consist of uniaxial compression under cryogenic and vacuum conditions.
The vacuum condition was achieved by maintaining the compression chamber below 10 mbar, while the cryogenic condition was obtained by cooling the compression chamber by immersing it for 25 minutes in liquid nitrogen.
The 25-minute timeframe was determined experimentally using the most insulating material, namely the microspheres, and waiting to detect a temperature decrease of the insulating material down to -177 °C, measured by a thermocouple inserted directly inside the sample.

Since 25 minutes proved sufficient for cooling the most insulating material, this timeframe is assumed to be conservative in order to ensure that the other materials also reached cryogenic conditions within the same time.
Regarding the maximum applicable pressure, this was imposed by the setup itself, as the availability of load cells with a maximum load of 110 kg imposes a maximum limit of 1000 N which, in some cases, proved insufficient.
In order to compare the data with each other and verify whether environmental conditions actually affect the mechanical properties, the conditions chosen for the experiments were: atmospheric compression, compression under vacuum, and compression under vacuum in cryogenic conditions.
In this way, it is possible to evaluate whether either vacuum or low temperature alone has direct effects on the mechanical behavior of the material.

Material	Conditions	Test	Applied Force (N)	Test duration* (min)
Microsphere	Atmospheric	3	900-1000	2
	Vacuum	3		15
	Cryo-vacuum	3		40
Filter Perlite	Atmospheric	7		2
	Vacuum	4		15
	Cryo-vacuum	5		40
Cryoperlite	Atmospheric	8		2
	Vacuum	3		15
	Cryo-vacuum	3		40
Fumed Silica	Atmospheric	3		2
	Vacuum	5		15
	Cryo-vacuum	4		40
TOTAL		51		

Table 2:The following table summarizes the timeframes, quantities of material used, and maximum force applied in tests conducted for each material under each experimental condition. It is important to note that the reported timeframes refer exclusively to the compression phase and do not include sample preparation times, which are approximately 10 minutes per test. This preparation time is mainly due to the vibration phase, which alone requires 5-6 minutes to ensure achievement of reference bulk density and elimination of air trapped

4.3 Experimental procedures

In order to achieve a good compromise between testing time and number of tests performed, it was decided to conduct 3 compression tests for each material under each condition.
For some materials, additional tests were performed both to compensate for the fact that the load on the sample was applied manually and therefore not always identically, and to ensure the reliability of the results obtained.
Once the timeline and minimum number of tests were planned, it was necessary to define the methodology to ensure that the quantity of sample inside the compression chamber was always the same, both in terms of mass and volume.
To do this, the bulk density was first measured, i.e., the density of the material once subjected to vibration, the values of which are reported in the tables at the beginning of this section.

For each material, a measured mass was placed inside the JEL STAV II by J.ENGELSMANN and, after 1250 vibrations, the volume was measured using a graduated cylinder.

Figure 6: JEL STAV II Jolting Volumeter

Material	Measured mass (g)
Microspheres	5.7
Filter Perlite	11.3
Cryoperlite	5.1
Fumed Silica	3.4

Table 3: Masses of the samples

By repeating this procedure three times for each material and averaging the results obtained by dividing the inserted mass by the final volume, the density was calculated.
Assuming that only 30 mm of the 54 mm height of the compression chamber were filled, in order to leave 24 mm for the proper
insertion of the piston, it was possible to calculate the mass to be inserted into the lower compression chamber.
The masses obtained are different for each material, as the particle size and compaction mode of the material after vibration affect the final volume.
Once compression is completed, it is important to consider that, in the case of vacuum conditions, it is necessary to return the compression chamber to atmospheric pressure before proceeding, while in the cryogenic case it is necessary to allow the temperature of the compression chamber to increase to make it manageable and avoid ice formation on the upper sleeve and in the flange, which would prevent vacuum formation in subsequent experiments.

4.3.1 Sample preparation

The preparation of samples for the experiments always follows the same procedure to ensure reproducibility of results.
The first step, when proceeding from a previous experiment, consists of removing the previous sample, washing and thoroughly drying the lower compression chamber so that it does not remain moist, as moisture could affect the experimental results.
Once the container is dried, it is placed on a balance with an uncertainty of 0.1 g or less (this uncertainty is not sufficient to produce significant uncertainty in the final sample height variations) and the mass indicated in the table is inserted.

The compression chamber is then positioned on the JEL STAV II with an adapted support fabricated by 3D printing and vibrated for 1250 cycles in order to reproduce the bulk density conditions initially obtained and thus determine the starting height of the sample.

Figure 7: JEL STAV II with lower compression chamber

Once the vibration process is completed, the chamber is inserted into the basin, the piston is slowly lowered onto the powder, and the flange is bolted.
Subsequently, depending on the conditions under which the experiment is being conducted, different preparations are necessary.
In the atmospheric case, compression can begin directly.
In the vacuum case, it is necessary to slowly open the valve with the vacuum pump on, in order to gradually decrease the pressure and avoid sudden suction that could damage the pump itself.
In the cryogenic case, using all necessary safety equipment, it is necessary to fill the basin with liquid nitrogen a first time and, after waiting approximately 10 minutes from the first filling, refill the basin due to boil-off.
Before starting cryogenic compression, it is always necessary to check for and remove any ice that may have formed due to ambient humidity.

4.3.2 Compression protocol

The compression procedure must also be repeated uniformly across the various experiments so that the data are reproducible.
Compression is performed by turning the manual crank positioned on top of the piston attached to the aluminum structure.
The piston inside the compression chamber must already be resting on the powder and channeled into the lower compression chamber in order to prevent the plastic rings, which block the upward movement of the powder, from jamming and deforming, causing the experiment to fail.
Compression then begins and proceeds uninterrupted until reaching 950-1000 N, as indicated by the software used for data recording.
It is necessary to compress at a relatively rapid rate, otherwise there is a risk of obtaining an oscillatory force trend due to further rearrangement of the granules under pressure, which would prevent subsequent data analysis.
Once compression has occurred, rapid decompression can be performed so that the detachment from the force peak is sharp and therefore more easily identifiable for the data analysis program.

It is then possible to proceed, adopting the necessary safety measures in the cryogenic case, to unbolt the flange of the compression chamber and prepare the setup for a new experiment.

4.3.3 Loading-unloading cycles

The choice of a single loading cycle rather than multiple cycles with increasing final force is motivated by two reasons.
The first reason, of an applicative nature, is due to the fact that the application of the chosen equations requires a single loading curve and it would therefore have been necessary, during data analysis in the case of multiple loadings, to separate the loading and unloading segments to form a single continuous curve.
The second reason is that, starting from the second loading cycle, some materials still in the elastic phase could partially re-expand and it was not possible to precisely identify the new starting point of compression.
A single uniaxial loading was therefore chosen, which does not effectively reproduce the cyclic mechanical loading and unloading conditions that can occur in a tank, caused by thermal expansion and contraction. However, this approximation should not significantly affect the results since the forces applied in the experiments are greater than those normally generated by these phenomena.

4.3.4 Selection and justification of the compression models

The choice to apply both the Heckel and Kawakita equations in this study reflects the specific characteristics of the tested materials and the absence of an established methodology for cryogenic insulating powders.
With initial porosities exceeding 90% and bulk densities in the range of 0.05–0.16 g/cm³, glass microspheres, filtered perlite, cryoperlite, and fumed silica fall outside the traditional application domain of the Heckel equation, which was developed for denser, plastically deforming powders such as metallic and pharmaceutical materials. In contrast, the Kawakita equation is better suited to highly compressible, low-density powders at low pressures, conditions that more closely match the experimental context of this work.
For this reason, Kawakita serves as the primary tool for quantitative characterization of mechanical parameters, while the Heckel equation is retained as a secondary reference to enable comparison with existing literature and cross-validation of results in particular through the correlation between the yield pressure P_y derived from Kawakita and the yield pressure derived from Heckel.
This dual approach maximizes the informational content of the experimental data while acknowledging the limitations inherent in applying both models outside their ideal validity ranges.
The equations used in the model are therefore the linearized ones $ln\left(\frac{1}{1-D}\right) = KP + A$ (2) for Heckel and $C = \frac{abP}{(1+bP)}$ (6) for Kawakita respectively.

5. DATA ANALYSIS

5.1 Processing methodology

Once one of the experiments is completed, what is obtained is an Excel spreadsheet in which, depending on the column examined, the data from the load cell, laser sensor, or vacuum sensor are found.
As row headers, there is instead the exact time at which each data point was acquired, with a time difference from the following row equal to the interval set on the ALMEMO 710 as the sampling frequency.
This temporal structure allows precise tracking of the experiment's evolution over time.
However, this raw data contains not only the actual compression phase, but also the waiting periods necessary for vacuum formation and cooling of the compression chamber and the contained material, as well as the rapid unloading period following the achievement of the peak force. Obviously, all these portions must be identified and removed in order to obtain a curve usable for quantitative data analysis.
The data were therefore made available as input to a code developed in the Spyder development environment using Python language.
The developed code has two versions: a simpler one for the atmospheric case and a more complex one for the vacuum and cryogenic cases, necessary to manage the additional preparation phases present in the latter.
The program allows, in the first instance, to acquire the measured data, select the appropriate physical parameters based on the material and experimental conditions used, and identify, through predetermined parameters and conditions, which data are useful for subsequent calculations.
This pre-processing phase is fundamental to eliminate noise and non-significant data that could negatively influence the analysis.
Once the data to be processed are obtained, the necessary calculations are performed to fit the curves identified as descriptive of powder behavior in the literature, namely the Kawakita and Heckel equations.
These mathematical models allow the extraction of characteristic parameters of the mechanical behavior of powders under compression, such as compressibility and resistance to plastic deformation.
Since the program was designed to analyze in batch mode all Excel files present within a specific folder (i.e., all experiments conducted on that material), an output image containing 5 graphs is obtained for each file, specifically: pressure-strain, relative density-pressure, force-displacement, Heckel curve, and Kawakita curve.
The first three graphs serve primarily to verify that the experiment occurred correctly and that the data are consistent with physical expectations, while the last two represent data calculated from those experimentally recorded and constitute the core of the analysis of the mechanical behavior of the materials.
In addition to the graphs, the program returns a text file containing all the most important values extracted from the analysis, such as the parameters of the Kawakita and Heckel equations and the characteristic values of density and pressure.
These data were subsequently provided as input to a second program developed specifically to visually analyze the differences between the various experimental conditions and different materials through comparative graphs, thus allowing a systematic evaluation of the mechanical performance of the four insulating materials under different operating conditions.

5.1.1 Data filtering

The data cleaning and filtering process represents a crucial phase of the analysis, implemented through a series of sequential filters that allow isolation of the actual compression curve by eliminating non-relevant portions of the recording.
The filtering procedure varies according to the experimental conditions, presenting additional steps for vacuum and cryogenic experiments compared to the atmospheric case.

Vacuum condition filter: This filter is applied exclusively to vacuum and cryogenic experiments. For vacuum experiments, all data points acquired when the chamber pressure exceeds 10 mbar are discarded, while for cryogenic experiments the threshold is set at 20 mbar. This automatically eliminates all data recorded during the pumping phase, ensuring that the analysis includes only data acquired under the correct environmental conditions. In the case of atmospheric experiments, this filter is not applied as there is no vacuum creation phase.
Force offset application: This step is applied exclusively to vacuum and cryogenic experiments. Before proceeding with subsequent filters, a systematic correction is applied to force values to compensate for the load sensor offset, due to the pressure applied on the piston during vacuum generation. This correction amounts to +65 N for vacuum experiments and +75 N for cryogenic ones, values determined through calculation of the area subjected to the pressure difference. In atmospheric experiments, as there is no pressure difference, this correction is not applied.
Positive force filter: This filter is applied to all experimental conditions. After the possible offset application (for vacuum and cryogenic) or directly on raw data (for atmospheric), all data points where the force is negative or zero are eliminated. This filter typically removes the initial data, corresponding to the piston approach phase to the powder before the actual start of compression. Only data with strictly positive force are retained for subsequent analysis.
Extreme displacement filter: This filter is applied to all experimental conditions. A physical consistency check is implemented on displacement values measured by the laser sensor. All data points presenting displacement greater than 55 mm are eliminated, as they are physically impossible considering that the initial sample height is 30 mm. This filter removes any outliers due to momentary laser sensor malfunctions.
Peak identification and unloading phase removal: This final filter is applied to all experimental conditions. The program identifies the maximum force value in the entire cleaned dataset and uses this as the endpoint of the compression phase. All data subsequent to the peak, corresponding to the rapid decompression phase, are removed from the analysis as they are not representative of the material's behavior under increasing load.

The final result of this filtering sequence is a clean curve that represents exclusively the monotonic compression phase of the material, from negligible initial force up to reaching the maximum load of approximately 1000 N, ready for the application of the Kawakita and Heckel equations.

Filter Name	Atmospheric	Vacuum	Cryogenic	Removed phase
Vacuum conditions	-	< 10 mbar	< 20 mbar	Pumping phase
Force offset	-	+65 N	+75 N	-
Positive force	> 0 N	> 0 N	> 0 N	Piston approach
Extreme displacement	< 55 mm	< 55 mm	< 55 mm	Anomalous data
Peak identification	Maximum value	Maximum value	Maximum value	Decompression

Table 6: Summary table

5.1.2 Application of the equations

The experimental pressure-strain data obtained from compression tests were analyzed using two semi-empirical equations: the Heckel equation and the Kawakita equation.
These models represent two complementary approaches for characterizing the mechanical behavior of powders under compression, each developed with different theoretical assumptions and application domains.
Data preprocessing was performed prior to model application to ensure reliability of the analysis.
Raw force and displacement measurements were converted to engineering stress (pressure) and volumetric strain, accounting for the initial powder bed height and the cross-sectional area of the compression cylinder.
Outlier detection was implemented using residual analysis with a threshold of 2 standard deviations from the fitted models, and identified outliers were excluded from the regression analysis to prevent distortion of the derived parameters.

The **Heckel equation**, expressed as $\ln[1/(1-D)] = kP + A$, where D is the relative density, was applied to the high-pressure region of the compression curves, typically corresponding to pressures above 0.1-0.15 MPa.
This equation, based on first-order kinetics for porosity reduction, assumes that densification occurs through continuous plastic flow of particulate material, making it particularly suitable for metallic and pharmaceutical powders at relatively high density.
Linear regression was performed on the linearized data, and the quality of fit was assessed through the coefficient of determination (R^2).
The slope k provides the reciprocal of the mean yield pressure ($\sigma y = 1/k$), which represents the material's resistance to permanent deformation, while the intercept A is related to the initial packing density and low-pressure densification by particle rearrangement.

The **Kawakita equation**, written in its linearized form as $P/C = P/a + 1/(ab)$, where $C = (h_0 - h)/h_0$ is the degree of volume reduction, was applied to the same high-pressure region used for Heckel analysis.
This model describes the behavior of materials that compact through particle rearrangement and void space reduction, proving optimal for soft, highly compressible powders.

The parameter *a* represents the maximum achievable compression or initial porosity of the powder bed, while the parameter *b* (or its reciprocal $P_y = 1/b$) indicates the pressure required to reduce the void volume by 50%. Linear regression of P/C versus P yielded both parameters from the slope (1/a) and intercept (1/ab).

Both models were implemented in automated Python scripts that process multiple datasets in batch mode, enabling systematic analysis of different materials and environmental conditions. The scripts generate standardized output including fitted parameters with their uncertainties, regression statistics (R^2, adjusted R^2), diagnostic plots, and comparative visualizations.

In the context of the tested materials—glass microspheres, filtered perlite, cryoperlite, and fumed silica—the experimental conditions (initial porosities > 90%, bulk densities 0.05-0.16 g/cm³, maximum pressures ~0.5 MPa) fall outside the traditional application domains of these models.

Densification occurs primarily through particle rearrangement and fragmentation rather than plastic flow, compromising the identification of the linear Heckel region.

Despite these limitations, both equations were applied: Kawakita as the primary tool for quantitative characterization given its suitability for highly compressible powders at low pressures, and Heckel as a secondary reference for benchmarking literature data and cross-validation.

6. RESULTS

6.1 Compression behavior of individual materials

In this section, the results of compression tests for each studied insulating material are presented and discussed. The objective is to characterize the individual mechanical behavior of each powder before proceeding to the comparative analysis in section 6.2, allowing identification of deformation mechanisms and the influence of structural properties on compression behavior.
For each material, experimental data of applied pressure and volumetric strain were analyzed through application of the Heckel and Kawakita equations, described in Chapter 3.
Compression tests were conducted under three distinct conditions: atmospheric, vacuum, and cryogenic vacuum, allowing evaluation of the combined effect of temperature and pressure on the mechanical behavior of the powders.
For each condition, a representative graph containing experimental data from one of the conducted experiments is presented, along with five analysis plots: pressure-strain, relative density-pressure, force-displacement, Heckel curve, and Kawakita curve.
Complete data from all repeated tests are available in Appendix A for reference.
Materials are presented in the following order: glass microspheres (6.1.1), filtered perlite (6.1.2), cryoperlite (6.1.3), and fumed silica (6.1.4).
This order corresponds approximately to increasing bulk density and a progressive transition from more rigid and spherical particulate structures (microspheres) toward more irregular, porous, and compressible structures (fumed silica).
For each material, experimental curves, parameters derived from application of theoretical models, and interpretation of the behavior observed under different experimental conditions are presented.

6.1.1 Glass microspheres

It is important to emphasize from the outset that the experimental setup proved inadequate for glass microspheres, a material significantly more resistant to compression than the others tested.
Comparing the obtained results with data reported by Fesmire et al. (2008), it is observed that the maximum pressure of 0.45 MPa applied by the piston is insufficient to induce significant plastic deformation, barely reaching the limit of the elastic zone of the material.

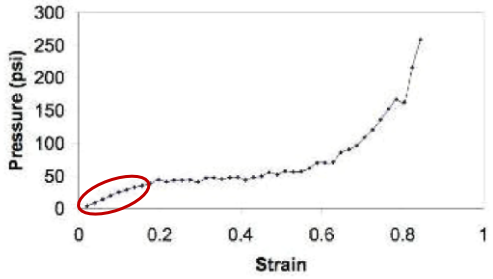

Figure 8: Fesmire graph Pressure-Strain Microsphere [2]

Referring to the pressure-strain graph of Fesmire et al. (2008), the experimental conditions of this study fall in the initial zone of the curve (circled in red in the Figure 12), characterized by

predominantly elastic behavior and particle rearrangement, without reaching the region of fracture and marked densification observed at higher pressures.
This observation is confirmed by visual analysis of the material: microspheres removed from the compression chamber after all tests, regardless of environmental conditions, maintain their fluid-like behavior without evidence of compaction into clusters or formation of cohesive aggregates.

Atmospheric conditions:

The three curves: pressure-strain, relative density-pressure, force-displacement serve to verify the correct progress of the experiment and the material's behavior under mechanical stress.
As observed from the pressure-strain and force-displacement graphs, the powder layer undergoes volumetric compression: despite macroscopic behavior similar to that of a fluid, the powder experiences measurable volume reduction.
This variation generates, however, a very steep curve, indicative of the high mechanical resistance opposed by microspheres up to the fracture point.
Fesmire et al. (2008) show that, once the critical fracture pressure of hollow spheres is exceeded, the behavior becomes much more similar to that observed in other insulating materials, with progressive and less steep densification.
The experimental curves obtained under atmospheric conditions are therefore consistent with literature data for the pre-fracture elastic zone, confirming the correctness of the experimental methodology.
The graph showing density increase further confirms that the experiment is proceeding correctly, as the relative density increases almost doubling after a few tenths of MPa.
This is indicative of the characteristic behavior of microspheres that are already in contact with each other and are rapidly approaching the fracture threshold, confirming the transition from the rearrangement phase toward the pre-fracture elastic phase.
The absence of a significant plastic deformation zone causes, however, substantial problems for the application of theoretical models.
For analysis using the Heckel equation, the fundamental assumptions of the model are not satisfied, as the equation was developed to describe densification in the region of permanent plastic deformation.
Although the Heckel curve appears to present apparent linearity in a certain pressure range, the extracted parameters (yield pressure P_H) are significantly different from those reported in previous analyses of glass microspheres at higher pressures, suggesting that the extrapolation is not physically representative of the plastic behavior of the material.
Regarding the Kawakita curve, the P/C vs P plot does not present the increasing linear region expected from theory, instead showing anomalous or decreasing behavior.
This anomalous behavior makes reliable extraction of parameters a and b through linear regression impossible.
Also in this case, the fundamental problem is insufficient applied pressure to reach the plastic deformation and fracture zone of microspheres, limiting the analysis to only the initial elastic region where powder compression models are not applicable.

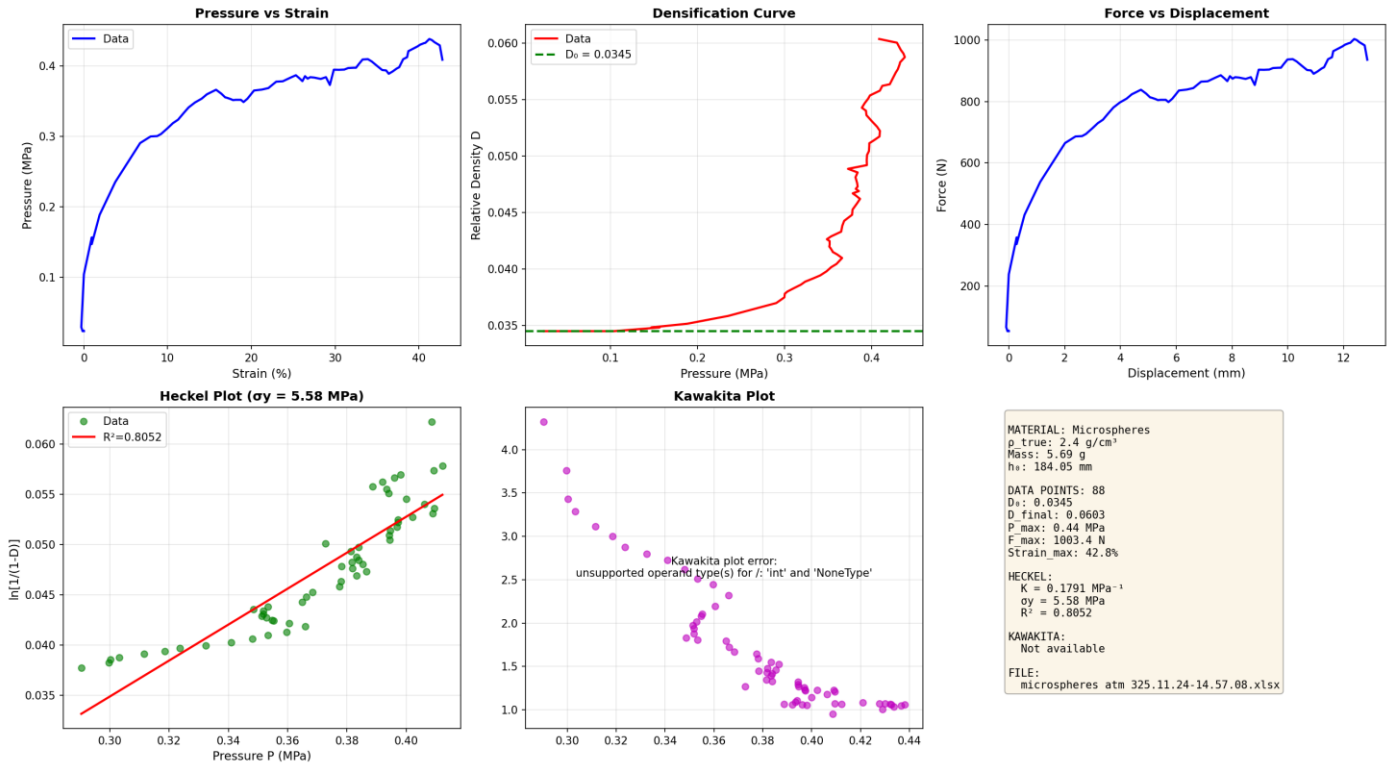

Figure 9: Graph Microsphere Test 3 atmospheric

Vacuum conditions:

Results obtained under vacuum conditions show behavior substantially similar to that observed under atmospheric conditions.
The maximum applied pressure (0.45 MPa) remains insufficient to reach the plastic deformation and fracture zone of microspheres, confining the analysis to the initial elastic region.
Pressure-strain and force-displacement curves again present a steep trend, characteristic of the high mechanical resistance of microspheres up to the fracture point.
The relative density graph confirms rapid density increase within a few tenths of MPa, indicating that particles are in contact and approaching the fracture threshold without reaching it.
Consequently, also under these conditions, application of the Heckel and Kawakita equations proves problematic: extracted parameters do not represent the plastic behavior of the material and curves show anomalies relative to expected theoretical trends.
However, an improvement in experimental data quality is observed compared to atmospheric tests.
The curves are noticeably smoother, with reduced or absent abrupt oscillations.
This phenomenon is attributable to preventive vacuum creation in the compression chamber, which allows complete elimination of interstitial air between particles before compression begins.
During compression under atmospheric conditions, air trapped between microspheres can cause sudden jumps or irregularities in the force-displacement curve when expelled under pressure.
The absence of air under vacuum conditions eliminates this contribution, producing more regular curves that better reflect the intrinsic mechanical behavior of the particulate material.
It is important to note that the initial sample height remains substantially unchanged compared to atmospheric conditions, despite air elimination, indicating that the contribution of air to the macroscopic porosity of the powder bed is negligible for this material.

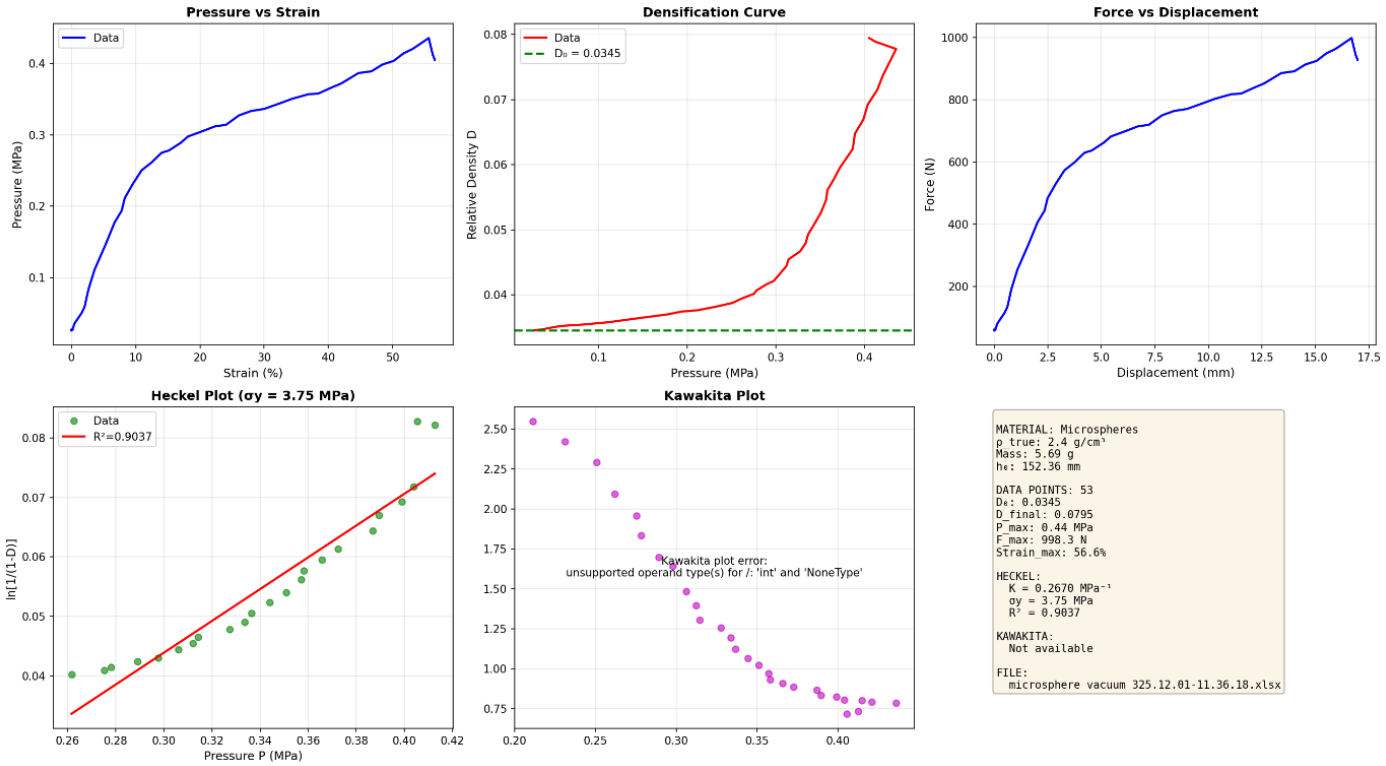

Figure 10: Graph Microsphere Test 3 vacuum

Cryogenic vacuum conditions:

Results obtained under cryogenic conditions further confirm the inadequacy of the experimental setup for characterizing the mechanical behavior of glass microspheres in the plastic deformation regime.
As in previous conditions, the maximum pressure of 0.45 MPa is insufficient to induce fracture of hollow spheres, limiting observation to only the initial elastic region.
However, cryogenic conditions introduce peculiar effects that are clearly manifested in the experimental data.
The relative density graph shows an extremely limited increase, with a rise of only 0.01 from the initial value.
This behavior indicates that, at low temperatures, the stiffness of microspheres increases further and the resistance to compression in the elastic phase becomes even more pronounced, reducing the material's capacity to densify under applied load.
Pressure-strain and force-displacement curves present a markedly segmented trend, with jumps more evident than in atmospheric and vacuum conditions.
This phenomenon is attributable to ice formation on the piston surface and in the compression chamber, despite preventive air pumping.
Residual moisture present in the system, exposed to the cryogenic temperatures of liquid nitrogen (-196°C), condenses and solidifies on metal surfaces, creating ice deposits that interfere with regular piston movement.
Unlike vacuum conditions, where air elimination produces smoother curves, cryogenic conditions therefore show a worsening of data quality due to these ice formation effects.
Analysis using the Heckel equation proves even more problematic than in previous conditions.
The Heckel plot does not present any identifiable linear region, instead showing a completely irregular trend that confirms the absence of plastic deformation in the tested pressure range.
Parameters extracted under these conditions are therefore completely unreliable and devoid of physical meaning.
The Kawakita curve also presents anomalous behavior distinctly different from the atmospheric and vacuum cases: the P/C vs P plot initially shows a decreasing trend, followed by a local peak, then becoming decreasing again.
This morphology does not correspond to any of the theoretical behaviors predicted by the equation and makes application of the linear regression method for extraction of parameters a and b impossible.
Also under cryogenic conditions, therefore, insufficient maximum applied pressure prevents any reliable characterization of microspheres through powder compression models, highlighting the need for an experimental setup capable of reaching significantly higher pressures for this specific material.

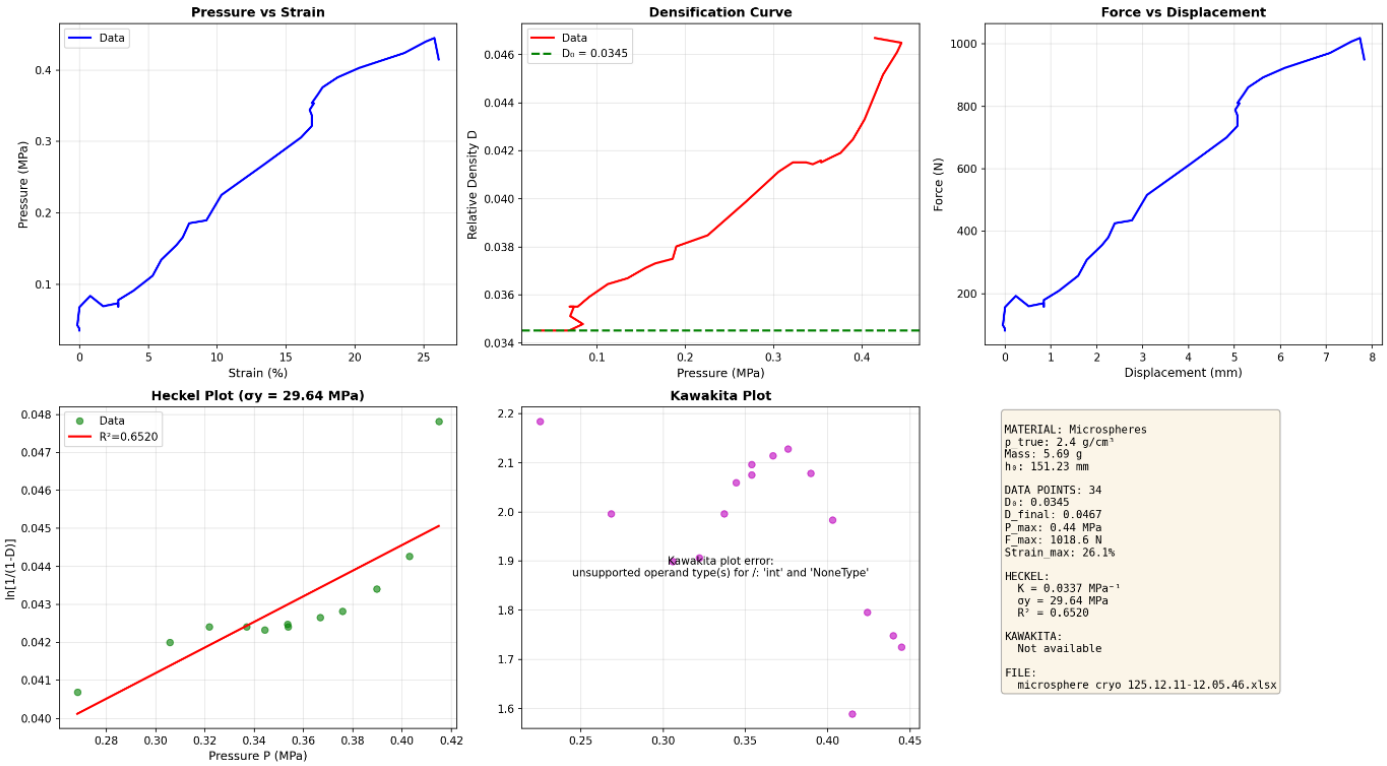

Figure 11: Graph Microsphere Test 1 cryo-vacuum

In order to provide a comprehensive overview of the obtained data, the following table presents the relevant parameters extracted from all experiments conducted on glass microspheres, with their respective variations across the three tested experimental conditions.

Condition	N° test	D_0	Max strain %	σ_y (MPa)	P_y (MPa)	Force (N)
Atmospheric	3	0.0345	42 ±1.2	6.69±1.12	N/A	N/A
Vacuum	3	0.0345	51.1±5.5	5.68±1.78	N/A	N/A
Cryogenic	3	0.0345	22.6±5.2	31.86±8.46	N/A	N/A

Table 4: Microspheres allexperiment data

6.1.2 Filter perlite

Filtered perlite presents itself as a powder with "floury" consistency, easily compactable and capable of entrapping large quantities of air that is eliminated through vibration during sample preparation.
This material represents the second in order of compression resistance among those tested: at the maximum applied pressure (0.45 MPa), a completely consolidated solid disk of compacted powder does not form, but the presence of partially cohesive powder clusters is observed.
The ease of compaction is evidenced by the fact that, once extracted from the compression chamber, the sample initially maintains the cylindrical shape impressed by the piston.

Figure 12: Example of filter perlite after compression

However, applying minimal manual pressure easily crumbles this structure, revealing the presence of small localized clusters that do not constitute an extended cohesive network.
This behavior suggests that, in the tested pressure range, filtered perlite is in an intermediate condition between pure particle rearrangement and the beginning of stable mechanical bond formation between particles, without reaching true permanent plastic densification of the material.

Atmospheric conditions:

The trend of pressure-strain and force-displacement curves differs markedly from that observed for microspheres and reflects the characteristic behavior of materials that form or begin to form a solid disk during compression.
Unlike the steep, almost linear curve of microspheres, filtered perlite shows an exponential-type compression profile (similar to e^x), with an initial phase characterized by relatively gradual compression that progressively accelerates with increasing load.
This type of curve is attributable to the collapse of internal porous structures of perlite particles, which yield under load and begin to compact together, offering decreasing resistance as void spaces are progressively reduced and particles rearrange into denser configurations.
The relative density graph confirms that the material is easily compactable, showing significant increase during compression.
However, relative density does not manage to double its initial value in the tested pressure range, indicating that greater forces would be necessary to achieve complete densification and form a consolidated solid.
This result is consistent with the experimental observation that the sample extracted from the chamber maintains only partially the cylindrical shape without constituting a completely solid disk.
Given the exit conditions of the sample from tests, it is evident that permanent plastic deformation has not occurred completely.
This conclusion is supported by analysis using the Heckel equation: the plot presents a not completely linear trend, with deviations from linearity indicating the presence of multiple densification mechanisms (rearrangement, structural collapse, beginning of plastic deformation) that overlap in the tested pressure range.
Consequently, parameters extracted from Heckel linear regression, while showing better fit quality compared to microspheres, cannot be considered fully reliable as descriptors of the plastic behavior of the material.
However, the presence of an approximately linear region suggests that the experimental setup approaches, though without completely reaching, the applicability zone of the Heckel model.
Analysis using the Kawakita equation presents significantly more promising results.
The P/C vs P curve shows a well-defined linear trend on which regression can be applied with good statistical reliability.
The extracted parameters, particularly yield pressure $P_y = 1/b$, provide physically sensible values indicating the beginning of cohesive structure formation around a pressure corresponding to approximately 700 N of applied load.
This value is consistent with experimental observations: reaching a maximum load of 900-1000 N in tests, one is only slightly beyond the yield threshold identified by Kawakita, explaining why localized cluster formation is observed but not a completely solid and consolidated cylinder.
The good linearity of the Kawakita curve confirms that this model, specifically developed for highly compressible powders, is more suitable for describing the behavior of filtered perlite in the tested pressure range.
It is important to emphasize that use of a greater compression force range would allow more complete material characterization, probably revealing a higher effective yield pressure corresponding to completely consolidated solid formation, and allowing application of the Heckel model in its theoretical validity region.

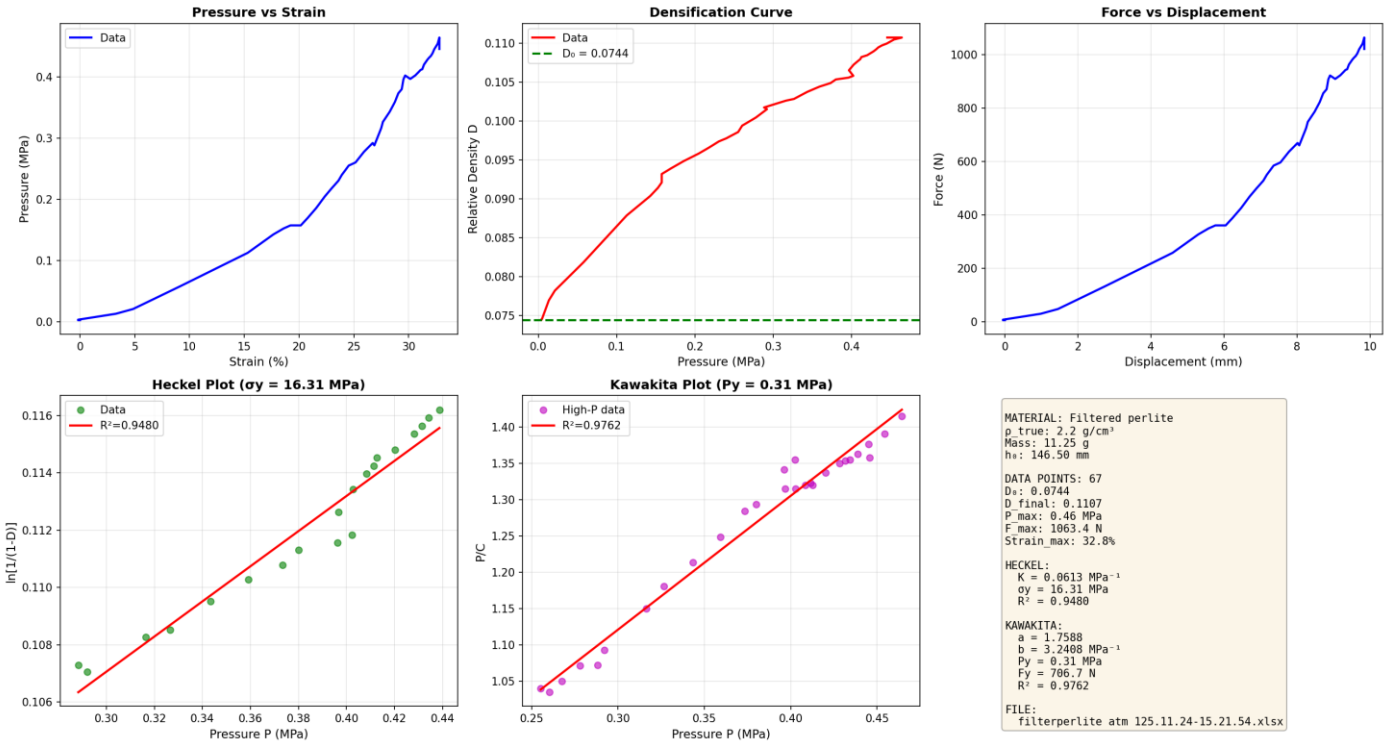

Figure 13: Graph Filter perlite Test 1 atmospheric

Vacuum Condition:

Results obtained under vacuum conditions show behavior substantially similar to that observed under atmospheric conditions, confirming the mechanical characteristics of filtered perlite in the tested pressure range.
As for atmospheric tests, also in this case more complete data and more accurate characterization of the plastic deformation regime would be obtained using an experimental setup capable of reaching greater forces.
The relative density graph remains essentially unchanged compared to atmospheric conditions. This behavior is attributable to the easily compactable nature of the material: vibration applied during sample preparation is already sufficient to eliminate most of the air trapped between particles and within void spaces of the porous structure.
Consequently, vacuum pumping does not produce further appreciable densification of the powder bed, since residual porosity essentially consists of structural void spaces between particles already in contact, rather than easily removable interstitial air.
Pressure-strain and force-displacement curves, which already presented a relatively smooth exponential-type profile under atmospheric conditions, maintain this characteristic under vacuum conditions with slight improvement in data regularity.
The absence of residual air between particles eliminates small jumps or irregularities that could derive from expulsion of air pockets during compression, producing slightly more regular curves that more faithfully reflect the intrinsic mechanical behavior of the material.
Analysis using the Heckel equation confirms results obtained under atmospheric conditions.
The plot presents a sufficiently linear trend in the medium-high pressure region, allowing parameter extraction through linear regression.
Yield pressure P_H values obtained are similar to those from atmospheric tests, indicating that vacuum conditions do not significantly alter the mechanical resistance of the material in the tested range.
However, the limitations already highlighted for the atmospheric case regarding the reliability of these parameters remain, given the incompleteness of plastic deformation in the applied force range.
The Kawakita equation also reports behavior analogous to that observed under atmospheric conditions. The P/C vs P curve maintains a well-defined linear trend, with parameters a and b that are consistent with those extracted from atmospheric tests.
Yield pressure P_y remains around 700 N, confirming that the threshold for beginning formation of cohesive structures is not significantly influenced by the presence or absence of air in the system.
The consistency of results between the two experimental conditions strengthens the validity of applying the Kawakita model for this material and suggests that the dominant densification mechanisms (collapse of porous structures, particle rearrangement) are essentially mechanical in nature and are not influenced by the presence of interstitial air.

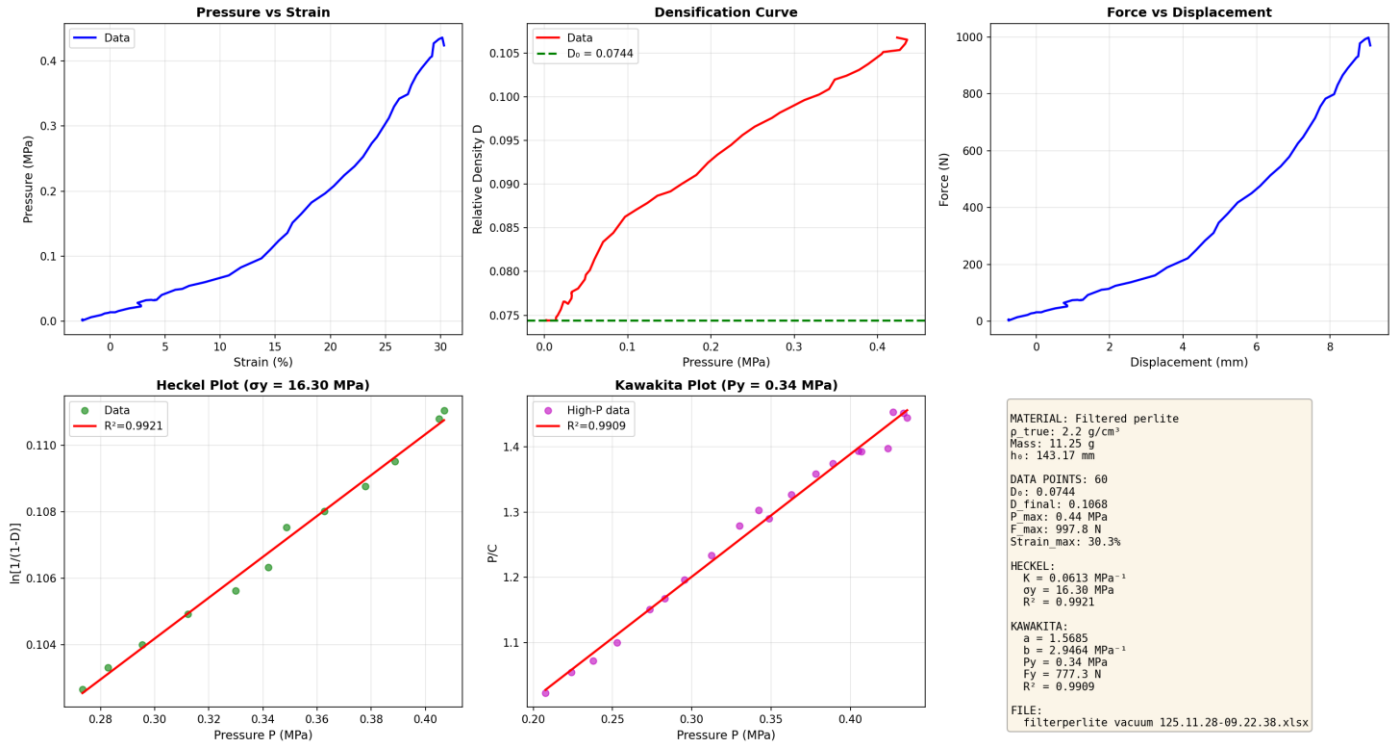

Figure 14: Graph Filter perlite Test 1 vacuum

Cryogenic vacuum conditions:

The powder behavior in relation to relative density remains substantially unchanged compared to atmospheric and vacuum conditions.
This result suggests that, for filtered perlite, the ease of compaction and effective air elimination during the vibration phase make the contribution of interstitial air negligible even at cryogenic temperatures.
Unlike microspheres, where the presence of air trapped inside spherical cavities can influence mechanical behavior, the open and interconnected porous structure of perlite allows complete air evacuation, minimizing effects related to its presence or absence under different experimental conditions.
Pressure-strain and force-displacement curves present, however, a segmented trend during compression.
This phenomenon, already observed for microspheres under cryogenic conditions, is attributable to ice formation on the piston surface and in the compression chamber.
This effect partially compromises data quality compared to vacuum conditions at ambient temperature, where curves were more regular.
Analysis using the Heckel equation shows defined linearity in the medium-high pressure region, allowing parameter extraction through linear regression.
The obtained yield pressure P_H confirms values calculated under atmospheric and vacuum conditions.
This maintenance of the same mechanical limit could be partly influenced by the lower quantity of data available for analysis compared to previous conditions, making extracted parameters less sensitive to possible variations induced by cryogenic temperature.
The Kawakita equation maintains a well-defined linear trend, confirming its applicability even under cryogenic conditions.
However, interesting variations are observed in extracted parameters compared to previous conditions: the calculated yield pressure P_y is lower, while parameter a (maximum compressibility) shows an increase.
This combination of effects is indicative of a change in the mechanical behavior of the material induced by temperature decrease.
The reduction in yield pressure and increase in compressibility suggest that the porous structure of perlite becomes more fragile at cryogenic temperatures, with internal cavity walls yielding more easily under load compared to ambient temperature.
This behavior can be attributed to thermal embrittlement of the glassy material constituting perlite particles, a phenomenon known for ceramic and glassy materials exposed to low temperatures, where reduced atomic mobility favors brittle fracture mechanisms over plastic deformation.

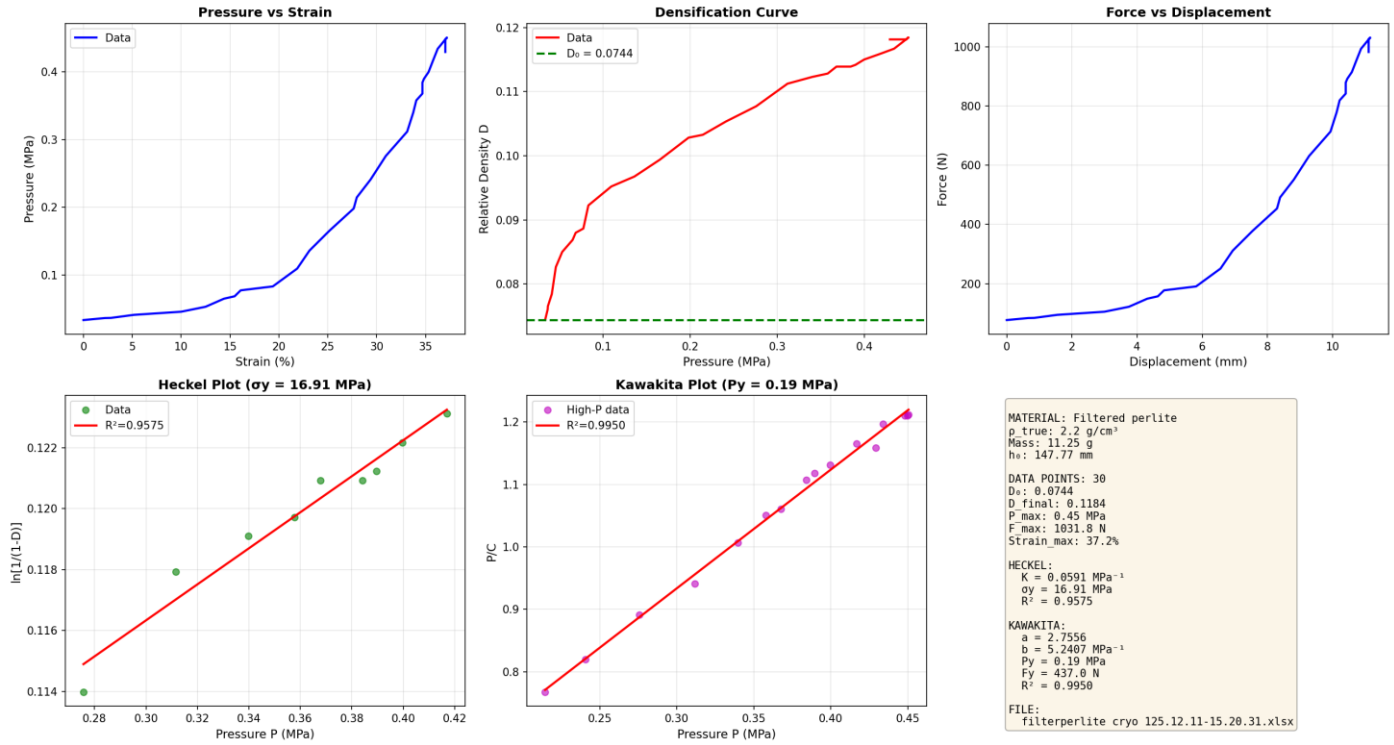

Figure 15: Graph Filter perlite Test 1 cryo-vacuum

Condition	N° test	D_0	Max strain %	σ_y (MPa)	P_y (MPa)	Force (N)
Atmospheric	4	0.0744	35.0±2.4	15.22±1.75	0.3234±0.0998	740.6±228.6
Vacuum	3	0.0744	27.0±3.2	31.87±25.20	0.3639±0.1251	833.4±286.6
Cryogenic	3	0.0744	34.1±6.2	11.75±6.23	0.2123±0.0606	486.3±139.0

Table 5: Filter perlite all experiment data

Data presented in the table were obtained from a selection of tests conducted under each experimental condition: atmospheric (tests 1, 3, 5, 6), vacuum (tests 1, 2, 3), and cryogenic (tests 1, 2, 3).
The remaining tests from the total number of experiments conducted (indicated in Table 2) were not included in the analysis as they return evidently incorrect results that cannot be attributed to the real mechanical behavior of the material.
These anomalous results manifest primarily in two ways: some tests provide yield pressure values derived from Heckel and Kawakita regressions exceeding the applied force range, a physically impossible result considering that plastic deformation was observed; other tests return excessively low yield pressure values, which would imply formation of a completely solid and cohesive disk already at reduced forces, a condition not experimentally verified.
These anomalous tests were therefore excluded from analysis to ensure validity and physical consistency of extracted parameters.

6.1.3 Cryoperlite

Cryoperlite, although chemically identical to filtered perlite, presents substantially different physical characteristics and mechanical behavior due to significantly coarser particle size distribution.
Granules are clearly visible to the naked eye and give the material a consistency similar to that of expanded polystyrene, with grain sizes smaller than the latter but much larger than those of filtered perlite.
This morphological difference is reflected in distinct mechanical behavior during compression. The highly porous structure of cryoperlite granules introduces a significant methodological complication in the experimental procedure.
Slow compression during piston descent returns data characterized by evident jumps, caused by progressive fracture of internal hollow structures and collapse of granules under load.

These discrete fracture events produce discontinuities in force-displacement curves that compromise experimental data quality.

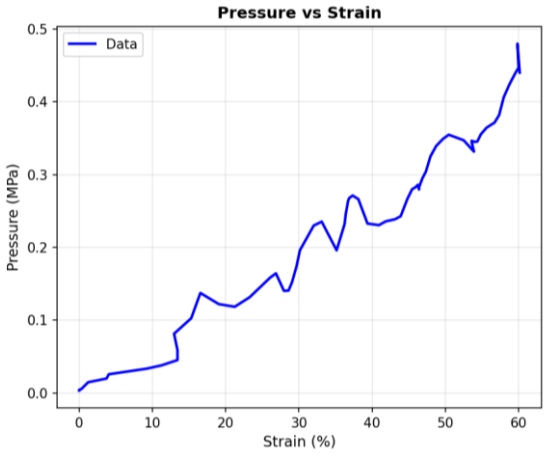

Figure 16:example of low speed compression.

It was therefore necessary to adopt a rapid compression procedure, which minimizes jumps allowing more continuous material densification.
However, this strategy entails greater difficulty in accurate data recording, as high compression speed reduces the number of points acquired during the process and may introduce dynamic effects in the measured mechanical response.
Unlike filtered perlite, the maximum pressure applied by the experimental setup (0.45 MPa) proved sufficient to induce formation of a consolidated disk once extracted from the compression chamber.
This represents an important result, indicating that cryoperlite reaches, in the tested pressure

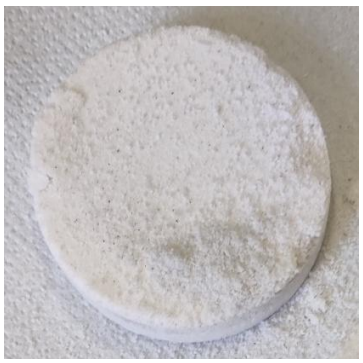

Figure 17: Entire extracted sample

range, a degree of densification and cohesion between particles superior to that observed for filtered perlite, where mainly localized clusters formed.

However, the formed disk is very fragile to the touch, easily crumbling under minimal manual solicitation.

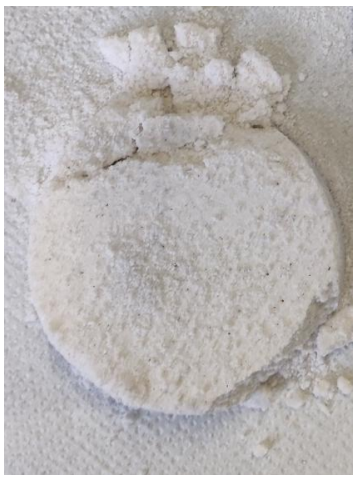

Figure 18: Fractured sample after handling

This behavior suggests that, although densification sufficient to create mechanical continuity between particles has been reached, the bonds formed remain weak and the structure has not yet achieved complete consolidation.
After repetition of several experiments and consistent obtaining of a disk at the end of tests, it is evident that the transition limit to the plastic phase must fall within the tested pressure range.
Analysis of experimental curve morphology provides a more precise indication of this transition: the force-displacement graph presents a slope increase in the final part of compression, due to an increase in compression resistance that signals the transition from the collapse and rearrangement phase toward the true plastic phase.
Based on this observation, it can reasonably be assumed that the yield threshold is located beyond 500 N, in the final portion of the tested force range.
It is reasonable to hypothesize that further compression, beyond the current setup limit, would increase the mechanical resistance of the disk, strengthening contact points between granules and increasing overall structural cohesion.
Conditions for application of the theoretical Heckel and Kawakita models are substantially satisfied for this material.
Formation of a continuous disk, even if fragile, and identification of a transition toward the plastic regime indicate that the material has exceeded the yield threshold and has begun to develop a network of permanent contacts between particles, a necessary condition for applicability of powder compression equations.
This places cryoperlite in an intermediate position between microspheres, for which the experimental setup proved inadequate, and more compressible materials such as fumed silica, allowing more reliable characterization of mechanical behavior through available theoretical models.

Atmospheric conditions:

The trend of pressure-strain and force-displacement curves for cryoperlite more closely resembles that observed for filtered perlite rather than microspheres.
This similarity resides both in the chemical identity of the two perlitic materials, despite structural differences due to particle size, and in the fact that in both cases plastic deformation is observed, unlike microspheres where the tested pressure range was limited to only the elastic phase.
The compression profile again presents an exponential-type trend, similar to that of filtered perlite, although with less pronounced slope in the final part of the curve.
This lower slope in the final phase of compression suggests that cryoperlite offers increasing resistance more gradually compared to filtered perlite, probably due to the larger granule size which entails different collapse and rearrangement mechanisms.
The relative density graph shows significant increase, with values doubling between the initial and final configuration of the compressed sample.
This substantial increase in relative density indicates good material densification, such as to allow formation of the disk observed at the end of compression.
The doubling of density confirms that the material has undergone significant porosity reduction through collapse of internal hollow structures of granules and particle rearrangement into more compact configurations.
Consistent disk formation at the end of tests constitutes clear evidence that plastic deformation was reached in the applied pressure range.
However, the fragility of the obtained disk, which easily crumbles under minimal manual solicitation, indicates that densification, while sufficient to create mechanical continuity, has not yet produced particularly strong bonds between granules.
This behavior suggests that application of slightly higher pressure could significantly improve the quality of the formed disk, further consolidating contact points between particles and increasing overall mechanical resistance of the structure.
One of the main problems in characterizing this material is due to jumps caused by the highly porous structure of granules.
As discussed in the introduction, progressive collapse of internal cavities during compression generates discrete fracture events that manifest as discontinuities in experimental curves.
These jumps partially compromise data quality, making curves less smooth compared to those observed for filtered perlite.
Consequently, data obtained for application of Heckel and Kawakita equations appear slightly more dispersed and less perfectly linear compared to the previous material, introducing greater uncertainty in extraction of characteristic parameters.
Analysis using the Heckel equation shows greater difficulty in identifying a clearly linear region.
Dispersion of experimental points and presence of deviations from linearity make regression less reliable, suggesting that fracture and collapse events of granules introduce multiple densification mechanisms that overlap in the tested pressure range.
Although it is possible to extract parameters from linear regression, their reliability is lower compared to materials presenting more regular curves.
The Kawakita equation, while not presenting perfect linearity as in the case of filtered perlite, nevertheless shows a sufficiently regular trend to allow application of linear regression.
However, the stepped profile of the curve introduces considerable variability in extracted parameters: different atmospheric tests return highly dispersed yield pressure P_y values, ranging between 600 N and 1300 N.

This wide difference is directly attributable to the irregular profile of curves, where sudden fracture events significantly influence the slope and intercept of linear regression, compromising the reliability of individual extracted values.
However, averaging results from different tests yields a value of approximately 900 N, which appears physically sensible because: (a) it falls within the applied force range (900-1000 N), consistently with the observation that yield pressure must necessarily be reached in the tested range to allow disk formation; (b) it is compatible with analysis of curve morphology indicating transition toward plastic regime beyond 500 N.
Despite complications introduced by the highly porous nature of the material, averaging of results provides reasonably reliable characterization of the mechanical behavior of cryoperlite under atmospheric conditions.

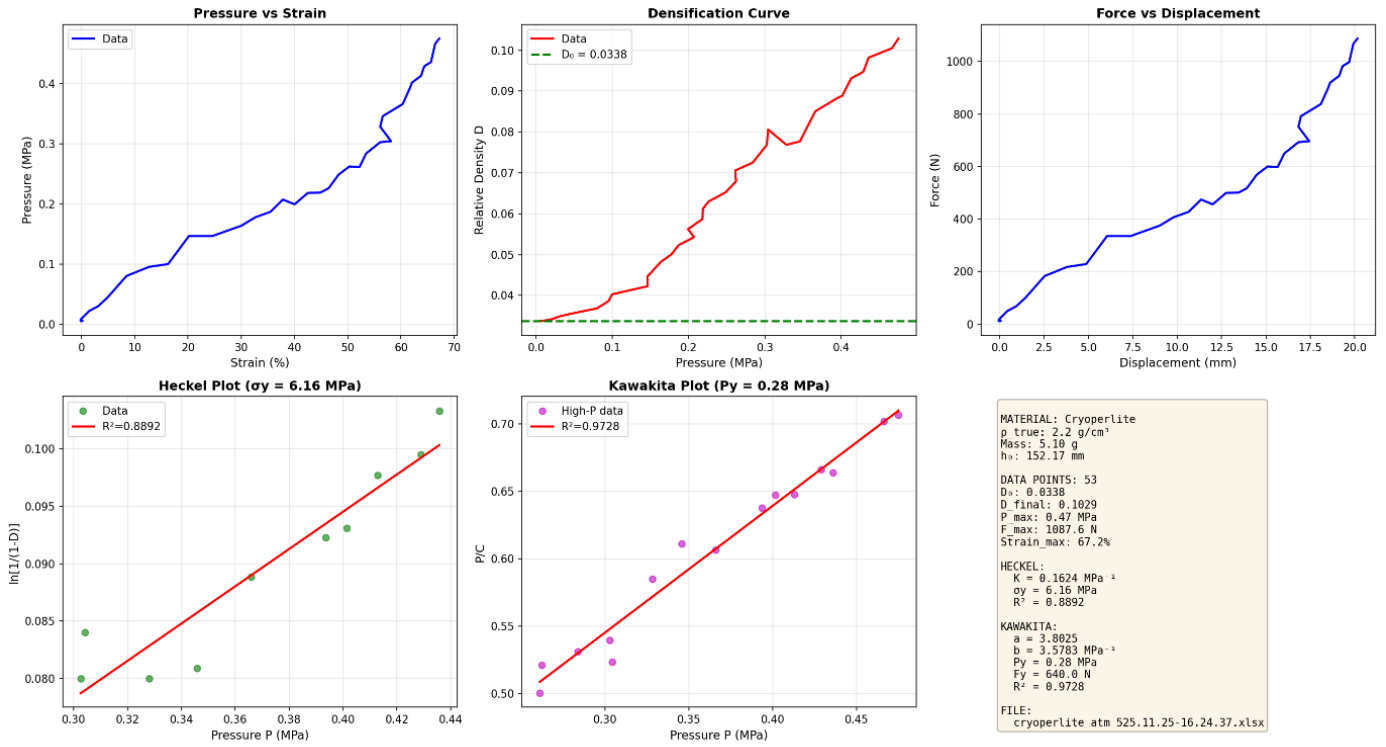

Figure 19: Graph Cryoperlite Test 5 atmospheric

Vacuum Condition:

The behavior of cryoperlite under vacuum conditions shows significant improvements in experimental data quality compared to atmospheric tests.
Pressure-strain and force-displacement curves are noticeably smoother, with marked reduction in jumps observed under atmospheric conditions.
This improvement in data regularity is attributable to elimination of interstitial air between porous granules, which reduces sudden fracture events and inhomogeneous collapse phenomena during compression, allowing more gradual and continuous material densification.
The relative density graph shows that compaction conditions similar to atmospheric ones are reached, with comparable final values confirming disk formation at the end of the experiment.
The absence of significant variations in final density between the two conditions indicates that vacuum pumping does not substantially alter the degree of densification achievable in the tested pressure range, but primarily improves the quality and regularity of the compression process by eliminating air that could cause heterogeneous behaviors during collapse of porous structures.
Data obtained from analysis using the Heckel equation are significantly improved compared to atmospheric conditions.
The plot presents a well-defined clearly linear region, free from dispersions and deviations from linearity observed in the presence of air.
This marked linearity allows application of regression with greater reliability, extracting more accurate and statistically robust parameters.
The improvement in Heckel fit quality confirms that air elimination allows clearer observation of plastic deformation mechanisms of the material, reducing disturbance effects related to sudden fracture events.
Analysis using the Kawakita equation also returns significantly improved data and more marked linearity in the P/C vs P curve.
The reduction in jumps in the experimental curve is reflected in lower dispersion of extracted parameters between different tests.
Obtained yield pressure P_y values converge around 900 N with greater consistency compared to atmospheric conditions, where strong dispersion (600-1300 N) required averaging to obtain a reliable estimate.
The improvement in data quality under vacuum conditions allows more accurate and repeatable estimation of yield pressure, confirming that the effective value is indeed around 900 N.
This result indicates that vacuum conditions do not substantially alter the mechanical resistance of the material, but allow measuring it with greater precision by eliminating artifacts due to air presence and sudden jumps in experimental curves, thus providing more reliable characterization of the mechanical behavior of cryoperlite
.

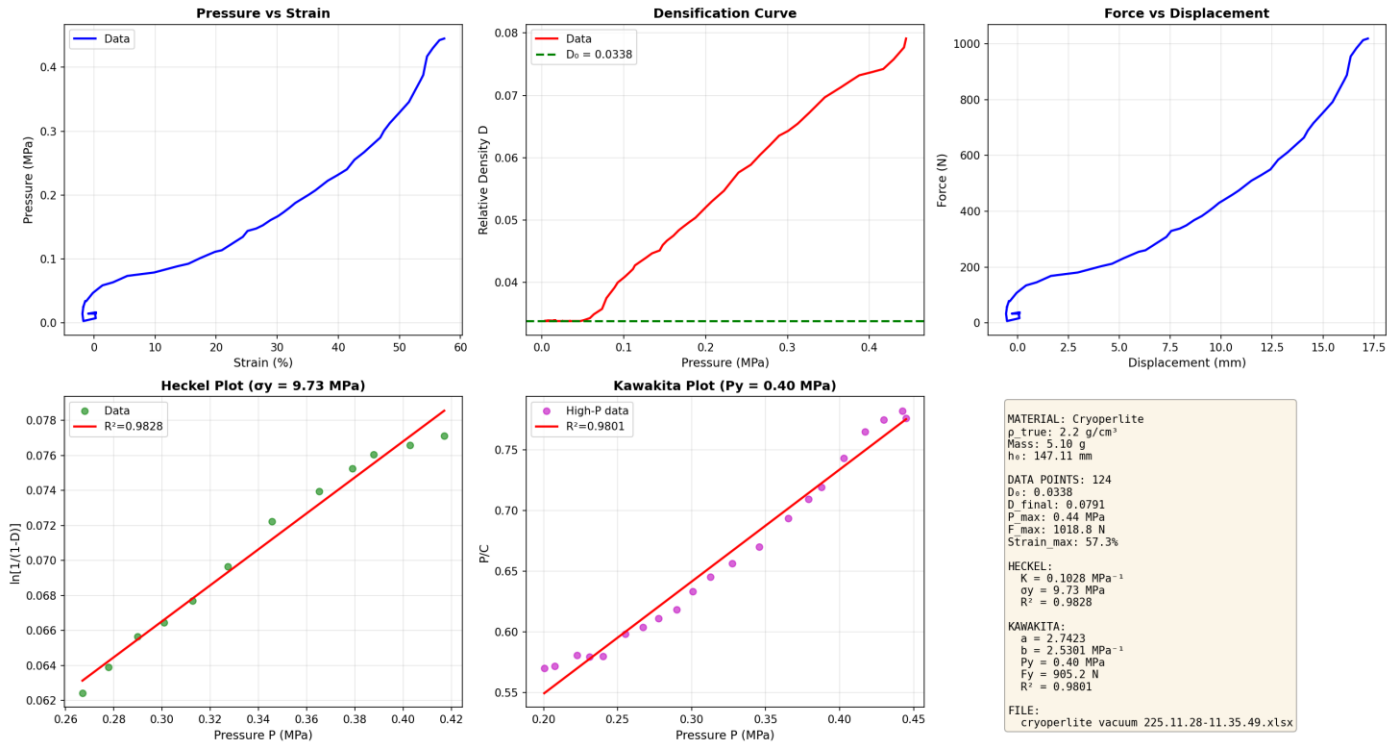

Figure 20: Graph Cryoperlite Test 2 vacuum

Cryogenic vacuum conditions:

In the cryogenic vacuum case, the behavior of cryoperlite changes substantially compared to previous conditions.
Thanks to vacuum creation, pressure-strain and force-displacement curves no longer present the marked jumps observed under atmospheric conditions, maintaining the regularity acquired in the vacuum-only case at ambient temperature.
However, curve morphology is profoundly different: the profile is no longer exponential-type as observed in other conditions, but assumes an almost rectilinear trend.
This change in curve shape indicates substantial modification in material densification mechanisms induced by temperature decrease.
The relative density graph reveals lower overall densification compared to atmospheric and vacuum conditions at ambient temperature.
However, density decrease is much more sensitive than that observed when moving from atmospheric to vacuum conditions.
This result suggests that cryogenic temperature has a marked effect on the material's ability to compact: the glassy structure of perlite, stiffened by low temperatures, offers greater resistance to deformation and collapse of internal cavities, limiting volumetric reduction achievable in the tested pressure range.
Analysis using the Heckel equation still presents a sufficiently linear region that allows parameter extraction through regression.
Yield pressure P_H values obtained are quite in line with those from the vacuum case, suggesting that, at least regarding the Heckel model, cryogenic temperature does not drastically alter the mechanical resistance of the material in the transition regime toward plastic deformation.
This consistency of Heckel parameters between vacuum and cryogenic conditions could indicate that the model, while being applicable, does not fully capture changes in densification mechanisms induced by temperature.
Analysis using the Kawakita equation instead presents a completely unexpected and anomalous profile. The P/C vs P curve no longer maintains the linear trend expected from theory, but forms a characteristic "U" curve that makes application of the standard linear regression method for extraction of parameters a and b impossible.
This behavior represents a fundamental deviation from Kawakita model predictions and indicates that compression mechanisms at cryogenic temperatures no longer follow the volumetric reduction kinetics described by the equation.
The U shape suggests that the material goes through distinct phases during compression: an initial phase where resistance decreases (descending branch of U), followed by a phase where resistance increases again (ascending branch of U), behavior incompatible with Kawakita's assumption of monotonic porosity reduction with pressure.
Although this anomalous profile may seem like an experimental error, the same behavior repeats consistently in all three cryogenic tests conducted, with U curves more or less marked but always present.
This repeatability confirms that the phenomenon is real and representative of material behavior at cryogenic temperatures.
The physical origin could be related to thermal embrittlement of the glassy structure, which favors brittle fracture rather than gradual deformation, highlighting the limits of applicability of classical compression equations under extreme temperature conditions for highly porous materials.

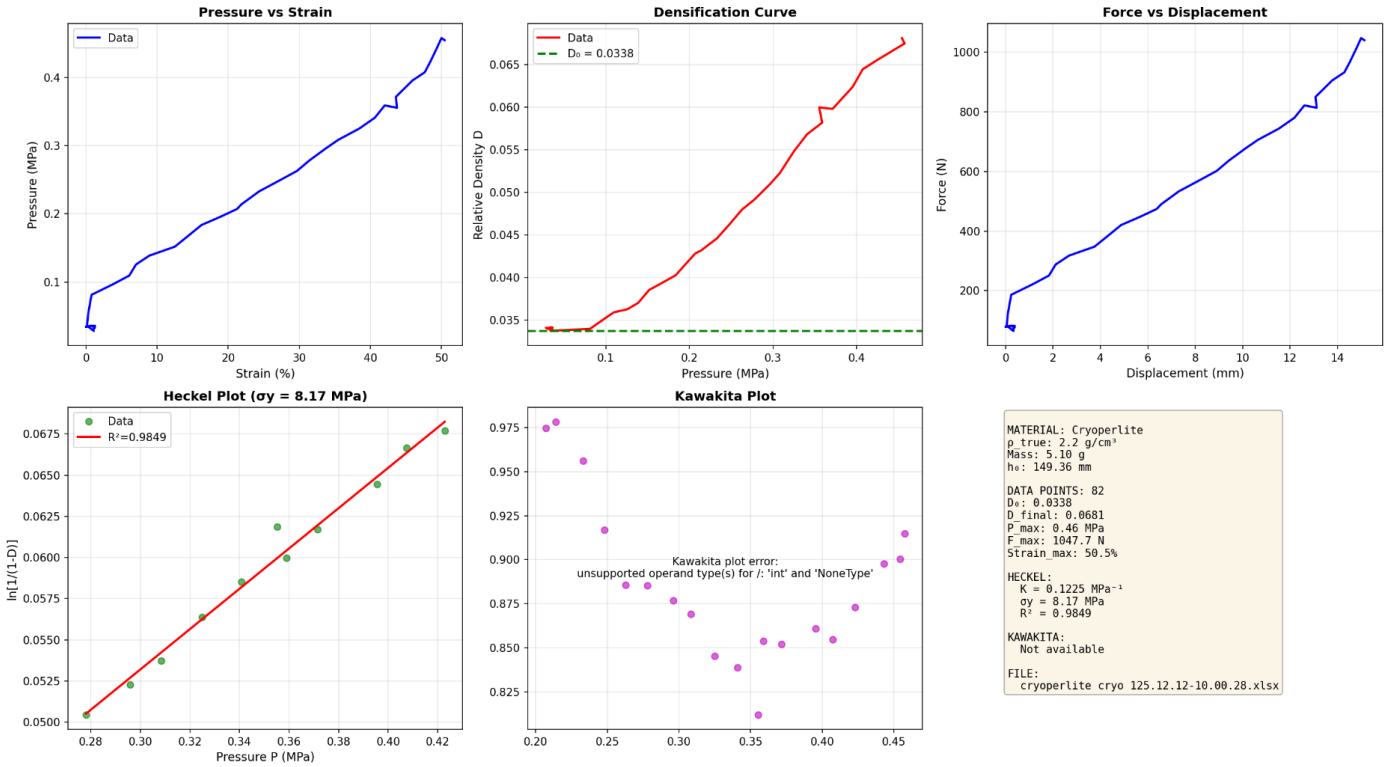

Figure 21: Graph Cryoperlite Test 1 cryo-vacuum

Condition	N° test	D_0	Max strain %	σ_y (MPa)	P_y (MPa)	Force (N)
Atmospheric	3	0.0338	65.4±1.6	5.63±0.87	0.4818±0.1764	1103.3±404.1
Vacuum	3	0.0744	59.0±4.1	7.57±1.69	0.4617±0.1267	1057.4±290.2
Cryogenic	**3**	**0.0744**	**34.1±6.2**	**9.04±3.94**	**N/A**	**N/A**

Table 6: Cryoperlite all experiment data

Data presented in the table were obtained from a selection of tests conducted under each experimental condition: atmospheric (tests 4, 5, 6), vacuum (tests 1, 2, 3), and cryogenic (tests 1, 2, 3).
For vacuum and cryogenic conditions, all conducted tests were included in the analysis as they provided consistent and physically coherent results.
However, for atmospheric tests, a significant number of tests (tests 1, 2, 3, 7, 8) were excluded from analysis as they returned evidently incorrect results that cannot be attributed to the real mechanical behavior of the material.
The high number of discarded atmospheric tests is directly correlated to the highly porous nature of cryoperlite granules: under atmospheric conditions, sudden jumps caused by collapse of hollow structures occurred frequently during compression, compromising the quality of acquired data and introducing marked discontinuities in force-displacement curves.
These jumps produced artifacts in Heckel and Kawakita regressions, making analyses inapplicable or returning excessively high yield pressure values devoid of physical meaning (exceeding the applied force range).
Elimination of interstitial air in vacuum and cryogenic tests significantly reduced these sudden fracture events, allowing acquisition of regular data and reducing the need to discard anomalous tests.
Atmospheric tests included in the analysis (4, 5, 6) were selected as they presented sufficiently regular curves to allow extraction of reliable parameters, while maintaining the characteristic stepped profile of the material that made averaging of results discussed previously necessary.

6.1.4 Fumed silica

Fumed silica represents the most suitable material among those tested for characterization through Heckel and Kawakita equations in the applied pressure range.
It is an extremely soft and compressible powder that fully respects the theoretical assumptions of Kawakita equation applicability, specifically developed for highly compressible "fluffy powders".
This theoretical suitability is directly verified by the experimental result: at the end of compression, a solid disk is obtained with mechanical resistance significantly superior to the other tested materials.
Unlike the fragility observed for perlites, the fumed silica disk presents cohesion such as to require application of appreciable manual force to be fractured in half, indicating formation of a network of stable bonds between nanometric particles.
The high capacity of fumed silica to remain suspended in air, a characteristic shared with glass microspheres but even more pronounced due to nanometric particle dimensions, required adoption of specific experimental measures.

Two plastic rings were positioned around the piston to prevent powder escape during compression: without this precaution, applied pressure could force very fine particles through small tolerances between piston and chamber, causing material loss and compromising test validity.
This same measure, already necessary for microspheres, proves even more critical for fumed silica given the almost aeriform behavior of uncompacted powder.
The compression procedure for fumed silica presented no particular operational difficulties and the applied force range (900-1000 N, corresponding to approximately 0.45 MPa) proved more than sufficient to completely characterize the mechanical behavior of the material.
Obtained data are fully consistent with the observed physical result: formation of a consolidated disk confirms achievement of permanent plastic deformation, a necessary condition for applicability of theoretical models.
Fundamental assumptions of both Heckel and Kawakita equations are verified for this material: densification occurs through particle rearrangement mechanisms followed by plastic deformation, experimental curves present morphologies expected from models, and extracted parameters show physical consistency and repeatability between different tests.
Fumed silica therefore represents the most suitable material among those tested for application of this mechanical characterization methodology in the experimented pressure range, providing reliable results and parameters with clear physical meaning that allow direct comparisons with literature data on similar materials.

Atmospheric conditions:

Pressure-strain and force-displacement curves of fumed silica present an exponential-type profile that qualitatively reflects the behavior observed by Fesmire [2] for similar insulating materials, although their study used a significantly broader pressure range.
The exponential trend, characterized by initial gradual compression that progressively accelerates with increasing load, is indicative of the densification mechanism typical of nanometric powders with high porosity: an initial phase of particle rearrangement and reduction of macroscopic void spaces, followed by a plastic deformation phase that produces rapid increase in compression resistance.
At the end of the experiment, a well-formed solid disk is consistently obtained, with appreciable mechanical resistance confirming achievement of permanent plastic deformation in the tested pressure range.
The relative density graph shows substantial increase, with values doubling between the initial and final configuration of the compressed sample.
This significant increase is fully consistent with experimental observations: formation of a consolidated and resistant disk confirms marked porosity reduction, with transition from an extremely expanded configuration to a compact configuration where nanometric particles form a cohesive network.
The formed disk represents the ideal result of this methodology, validating both the testing range and instrumentation adequacy.
Unlike microspheres (insufficient pressure) and perlites (fragile disks or localized clusters), fumed silica produces a solid, cohesive, and manipulable disk demonstrating correct experimental setup functioning.
This confirms that the applied force range (900-1000 N) is appropriate to characterize highly compressible materials in the plastic deformation regime.
The material presents no operational difficulties during the compression procedure and experimental curves are remarkably smooth, free from jumps and discontinuities observed for other materials such as cryoperlite.

The absence of sudden fracture events or abrupt collapse is attributable to the uniform nanometric structure of fumed silica: extremely fine particles rearrange and deform continuously and gradually under load, without the macroscopic hollow structure rupture phenomena that characterized perlites.
This exceptional regularity of experimental data translates into high-quality curves that allow optimal application of theoretical models.
Analysis using the Heckel equation presents practically perfect linearity in the medium-high pressure region, with extremely high determination coefficients R^2 indicating excellent model fit to experimental data.
Yield pressure P_H extracted from regression is reliable and physically significant, confirming that the material behaves according to Heckel model assumptions in the plastic deformation region.
Similarly, the Kawakita equation shows perfect linearity in the P/C vs P curve, with R^2 values indicating almost ideal adherence between experimental data and theoretical predictions. Parameters a and b extracted are stable and repeatable between different tests, providing robust characterization of mechanical behavior.
Yield pressure P_y calculated from the Kawakita equation is located around 200 N, a value significantly lower than the other tested materials and fully consistent with the extremely compressible nature of fumed silica.
This value indicates that the material begins to develop permanent cohesive bonds already at relatively low forces, well within the tested range, explaining solid disk formation and confirming that the experimental setup operated in the optimal region for this material.
The consistency between Heckel and Kawakita parameters and their coherence with experimental observations make fumed silica the ideal reference material to validate the characterization methodology developed in this study.

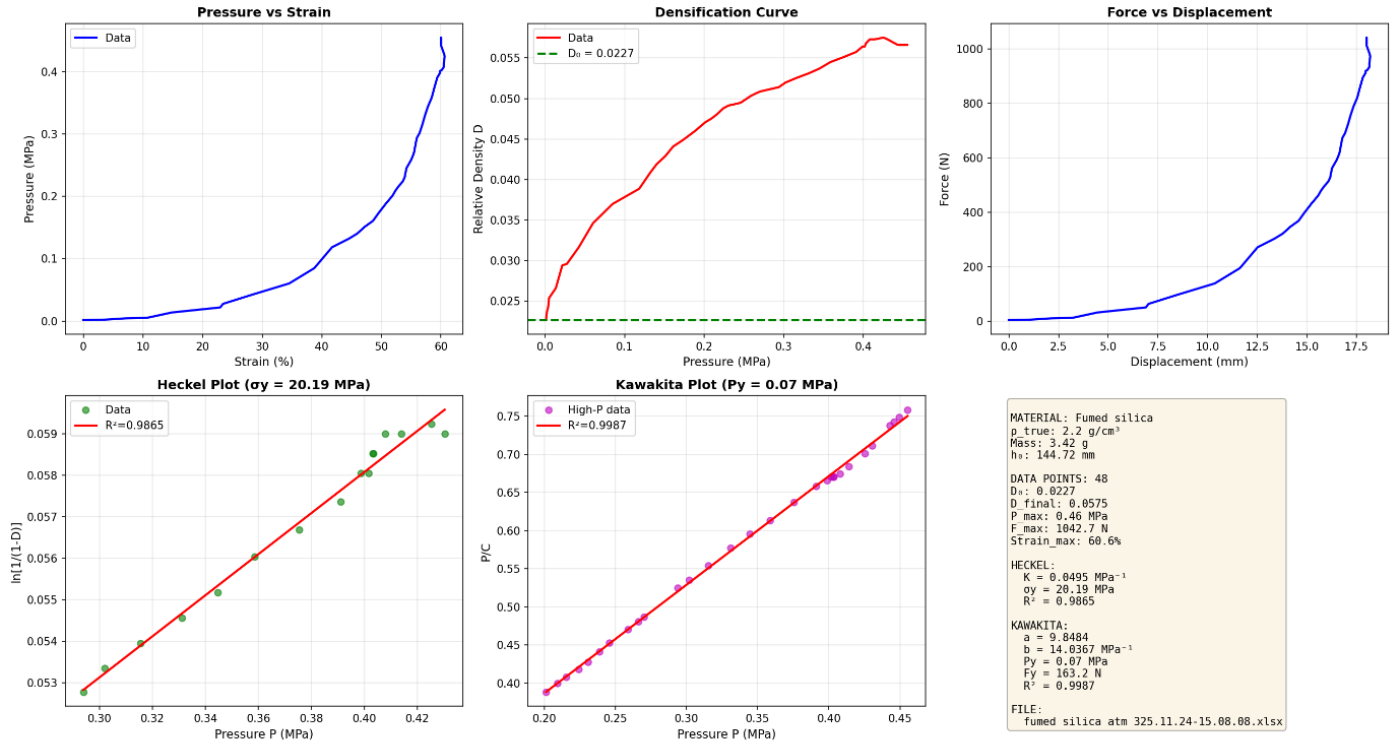

Figure 22: Graph Fumed silica Test 3 atmospheric

Vacuum Condition:

Under vacuum conditions, pressure-strain and force-displacement curves maintain the smooth trend already observed in atmospheric tests.
Unlike materials such as cryoperlite, where air elimination produced marked improvement in data regularity, for fumed silica the curves were already free from discontinuities and jumps under atmospheric conditions.
Vacuum creation therefore does not introduce qualitative variations in curve profile, confirming that the uniform nanometric structure of the material produces intrinsically regular mechanical behavior regardless of the presence or absence of interstitial air.
The relative density graph reveals more pronounced increase compared to atmospheric conditions, with values exceeding doubling between the initial and final configuration of the compressed sample.
This superior increase indicates that preventive air elimination from the compression chamber results in greater final material densification.
Air trapped between nanometric particles of fumed silica, despite preliminary vibration during sample preparation, evidently still occupied a non-negligible fraction of total volume.
By removing this air through vacuum pumping, the material reaches a slightly denser initial configuration and, under compression, can densify further compared to atmospheric conditions, producing a disk with higher final density.
Analyses using Heckel and Kawakita equations maintain the high quality observed under atmospheric conditions.
Both models present perfectly linear curves in their respective representations, allowing easy execution of linear regressions with excellent determination coefficients R^2.
Yield pressure extracted from the Kawakita equation is slightly above 200 N, a value very similar to that obtained under atmospheric conditions.
This substantial invariance of yield pressure between the two conditions suggests that, for fumed silica, mechanical resistance to formation of permanent bonds between particles is not significantly influenced by the presence or absence of air, but is mainly determined by direct interactions between nanometric silica particles.
The consistency of extracted parameters between atmospheric and vacuum conditions further strengthens the reliability of mechanical characterization of this material and confirms that obtained yield pressure values accurately reflect intrinsic material properties rather than experimental artifacts.

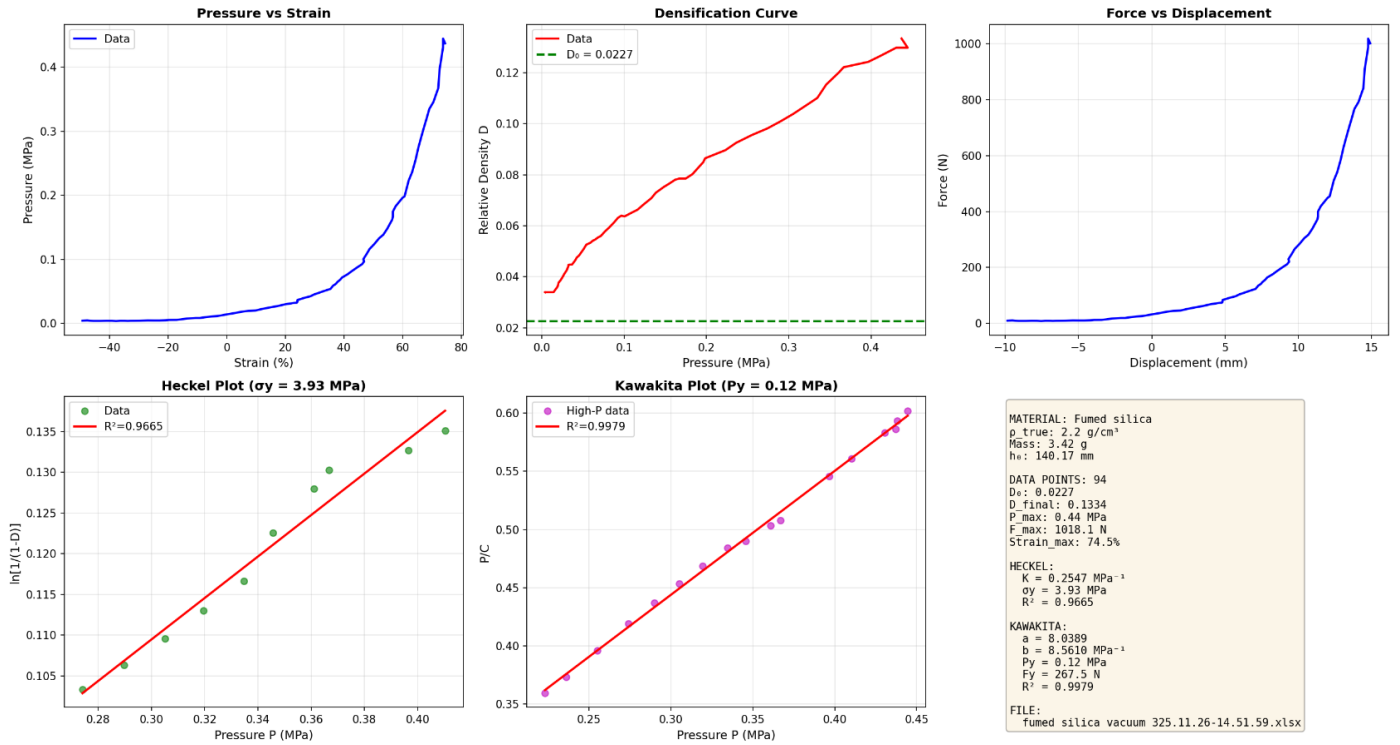

Figure 23: Graph Fumed silica Test 3 vacuum

Cryogenic vacuum conditions:

Under cryogenic conditions, the mechanical behavior of fumed silica remains substantially similar to that observed under atmospheric and vacuum conditions at ambient temperature, maintaining the compressibility and regularity characteristics that distinguish this material.
However, pressure-strain and force-displacement curves present slightly lower regularity compared to previous cases, with small deviations from the perfectly smooth trend observed previously.
These irregularities, however minimal and noticeable only due to the exceptional quality of curves in other conditions, are attributable to ice formation on the piston surface due to exposure to cryogenic liquid nitrogen temperatures (-196°C).
Despite preventive vacuum pumping, residual system moisture condenses and solidifies on metal surfaces, introducing small perturbations in piston movement that are reflected in slight irregularities in acquired curves.
The relative density graph shows consistent increase, with values doubling between initial and final configuration, similarly to what observed in other conditions.
The absence of marked variations in final densification among the three experimental conditions indicates that, for fumed silica, temperature and air presence do not significantly influence the maximum degree of compaction achievable in the tested pressure range.
This behavior contrasts with what observed for other materials such as cryoperlite, where cryogenic temperature produced appreciable densification reduction, suggesting that the nanometric structure of fumed silica maintains its compressibility even at low temperatures.
A critical aspect emerged in cryogenic tests regarding the need to optimize compression speed to ensure adequate data acquisition.
As discussed in the general introduction on cryoperlite, rapid compression was adopted to reduce jumps due to porous structure collapse.
However, for fumed silica under cryogenic conditions, this rapid compression procedure resulted in recording a limited number of experimental points during acquisition.
This reduced number of data made Heckel equation application problematic: in four cryogenic experiments conducted, in two cases it was not possible to perform reliable analysis through Heckel, as acquired points were numerically insufficient to identify with certainty a linear region and to perform regression with robust statistical meaning.
The Kawakita equation instead always presented sufficient number of points distributed in the pressure range necessary to perform linear regression, allowing extraction of characteristic parameters even in experiments where Heckel was not applicable.
Yield pressure P_y calculated from the Kawakita equation is approximately 300 N, a value higher than the approximately 200 N obtained under atmospheric and vacuum conditions. This apparent yield pressure increase under cryogenic conditions could indicate effective material stiffening at low temperatures, or could be influenced by inferior quality of acquired data and limited number of points available for regression.
Given the uncertainty introduced by experimental difficulties in cryogenic tests, this value should be interpreted with caution and cannot be considered definitive without further experimental verification with optimized data acquisition.

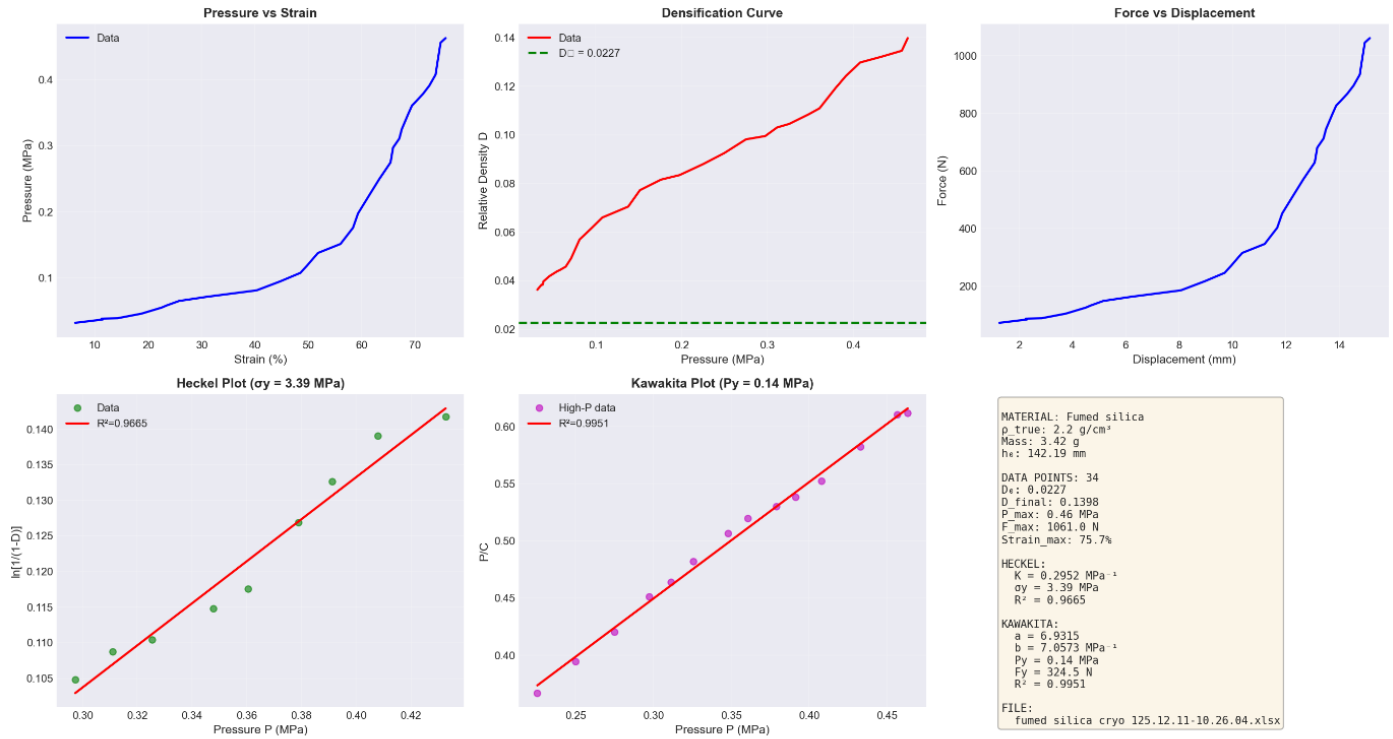

Figure 24: Graph Fumed silica Test 1 cryo-vacuum

Condition	N° test	D_0	Max strain %	σ_y (MPa)	P_y (MPa)	Force (N)
Atmospheric	3	0.0227	67.3±5.8	13.28±5.99	0.0925±0.0163	211.8±37.4
Vacuum	4	0.0227	62.8±14.4	18.97±17.44	0.0992±0.0365	227.2±83.5
Cryogenic	4	0.0227	82.4±5.1	2.41±1.39	0.1488±0.0413	340.7±94.6

Table 7: Fumed silica all experiment data

Data presented in the table were obtained from a selection of tests conducted under each experimental condition: atmospheric (tests 1, 2, 3, 4) and vacuum and cryogenic (all conducted tests).
For vacuum and cryogenic conditions, all experiments provided consistent and physically coherent results.
For atmospheric tests, test 0.1 was excluded from analysis, corresponding to the very first compression attempt ever performed with the apparatus.
This preliminary test presented laser system acquisition problems in the low-pressure region, compromising initial curve reliability.
High-pressure data from the same test are valid and were retained for curve development in the final compression phase.
Given the importance of the low-pressure region for application of Heckel and Kawakita equations, test 0.1 was excluded from characteristic parameter analysis.
Subsequent atmospheric tests (1, 2, 3, 4), conducted after laser system problem resolution, provided excellent and perfectly repeatable results, confirming that fumed silica represents the most suitable material among those tested for application of powder compression equations.

6.2 Comparison between materials

6.2.1 Mechanical behavior under atmospheric conditions

Comparative analysis of the four insulating materials under atmospheric conditions is presented in Figure 30 and Figure 29**Errore. L'origine riferimento non è stata trovata.**, which show respectively key parameters extracted from compression tests and fit quality obtained with Heckel and Kawakita equations through determination coefficients R^2.
The maximum strain parameter shows significant variability between materials: fumed silica presents the highest value (67.34%), followed by cryoperlite (65.42%), while filtered perlite (35.00%) and microspheres (42.03%) show lower values.
Strain is measured with good precision under atmospheric conditions for all materials, with the most unfavorable case represented by fumed silica which shows the greatest variability among repeated tests.
Final relative density shows different values among materials: filtered perlite reaches 0.11, cryoperlite 0.10, microspheres 0.08, and fumed silica 0.07.

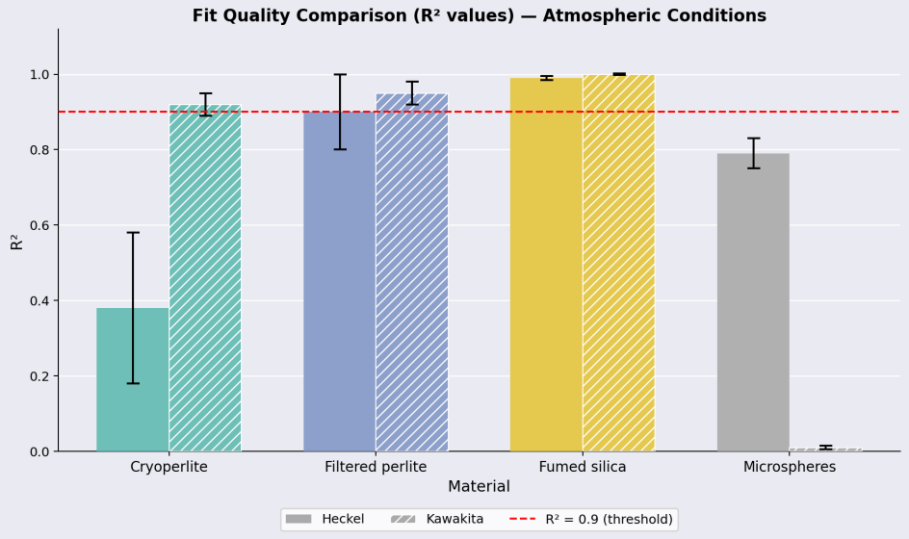

Figure 25: Fit quality atmospheric conditions

As expected, both final density and compression percentage vary significantly depending on the material under analysis.
Maximum pressure applied is substantially uniform among materials (0.45-0.48 MPa), with minimal variability between different experiments despite manual load application, confirming excellent experimental methodology repeatability.
Parameters extracted from theoretical equations show distinct behaviors.
Yield strength σ_y derived from the Heckel equation varies from 5.63 MPa (cryoperlite) to 15.22 MPa (filtered perlite), with fumed silica at 13.28 MPa and microspheres at 6.69 MPa.
Observing Figure 29, the Heckel equation shows excellent fit quality only for fumed silica ($R^2 \approx 0.99$), while for filtered perlite ($R^2 \approx 0.90$) it is at the acceptability threshold, and for cryoperlite ($R^2 \approx 0.38$) and microspheres ($R^2 \approx 0.79$) values are below the $R^2 = 0.9$ threshold.
Heckel parameter variability is significant for some materials, as evidenced by error bars.
Yield force and yield pressure P_y derived from the Kawakita equation show different patterns in terms of precision.
The Kawakita equation returns results with reduced error bars for fumed silica ($P_y \approx 0.09$ MPa, ~210 N), while for cryoperlite (~1100 N) and filtered perlite (~740 N) dispersion is greater.
Observing R^2 coefficients in Figure 29, the Kawakita equation returns R^2 values above 0.9 for all materials except microspheres (where the model is not applicable).
In particular, fumed silica ($R^2 \approx 1.00$), filtered perlite ($R^2 \approx 0.95$) and cryoperlite ($R^2 \approx 0.92$) present high linearity in the P/C vs P curve.
Direct comparison between the two models highlights that the Kawakita equation provides superior fit quality compared to the Heckel equation for most tested materials.
Yield force values extracted from Kawakita follow the order: fumed silica (~210 N) < filtered perlite (~740 N) < cryoperlite (~1100 N nominal).
For cryoperlite, strong dispersion of individual data (values between 600 and 1300 N in different tests) suggests an effective value probably around 900 N, as evidenced by analysis of result averaging discussed in paragraph 6.1.3.

In summary, under atmospheric conditions the Kawakita equation provides consistently higher R^2 coefficients compared to the Heckel equation for materials reaching plastic deformation, indicating better model adherence to experimental data.

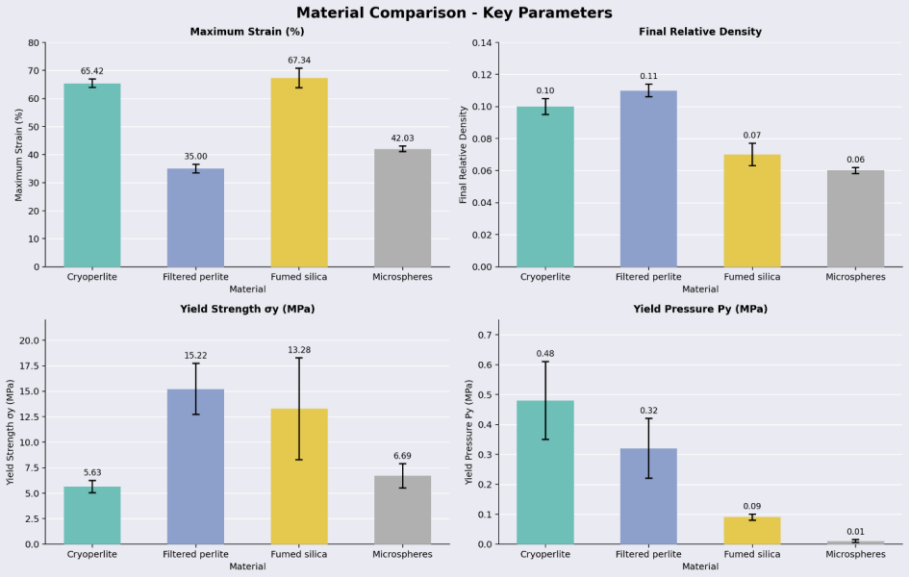

Figure 26: Comparison between materials at atmospheric conditions

6.2.2 Mechanical behavior under vacuum conditions

Comparative analysis of materials under vacuum conditions is presented in Figure 32 and Figure 31, which show respectively key parameters extracted from compression tests and fit quality through R^2 coefficients.

The maximum strain parameter shows the following order among materials: fumed silica presents the highest value (62.75%), followed by cryoperlite (58.96%) and microspheres (50.73%), while filtered perlite shows the lowest value (28.98%).

Strain is measured with good precision under vacuum conditions, with fumed silica presenting the greatest variability among repeated tests.

Final relative density shows significantly different values among materials: fumed silica reaches 0.11, filtered perlite 0.10, cryoperlite 0.08, and microspheres 0.07.

As expected, both final density and compression percentage vary significantly depending on the material under analysis.

Maximum pressure applied is substantially uniform among materials (0.43-0.45 MPa), with minimal variability between different experiments despite manual load application, confirming experimental methodology repeatability.

Parameters extracted from theoretical equations show distinct behaviors.

Yield strength σ_y derived from the Heckel equation presents very high values for filtered perlite (31.87 MPa) and fumed silica (18.97 MPa), with cryoperlite (7.57 MPa) and microspheres (5.75 MPa) at lower values.

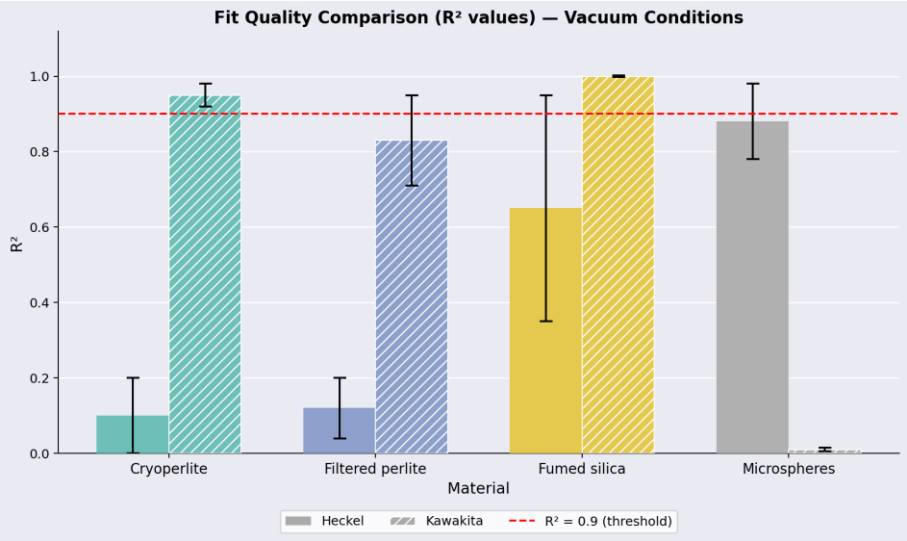

Figure 27: Fit quality vacuum conditions

Observing Figure 31, the Heckel equation shows acceptable fit quality only for microspheres ($R^2 \approx 0.90$), while for cryoperlite ($R^2 \approx 0.11$), filtered perlite ($R^2 \approx 0.12$) and fumed silica ($R^2 \approx 0.65$) R^2 values are below the acceptability threshold.
The Heckel equation returns highly variable values for fumed silica and filtered perlite, as evidenced by wide error bars.
Yield force and yield pressure P_y derived from the Kawakita equation show better precision, although error bars remain wide for some materials.
Values follow the order: fumed silica (≈227 N, 0.10 MPa) < filtered perlite (≈833 N, 0.36 MPa) < cryoperlite (≈1052 N, 0.46 MPa).
Figure 31 shows that the Kawakita equation returns R^2 values above 0.9 for fumed silica ($R^2 \approx 1.00$) and cryoperlite ($R^2 \approx 0.96$), while filtered perlite ($R^2 \approx 0.84$) presents lower fit quality but still better compared to the Heckel equation.

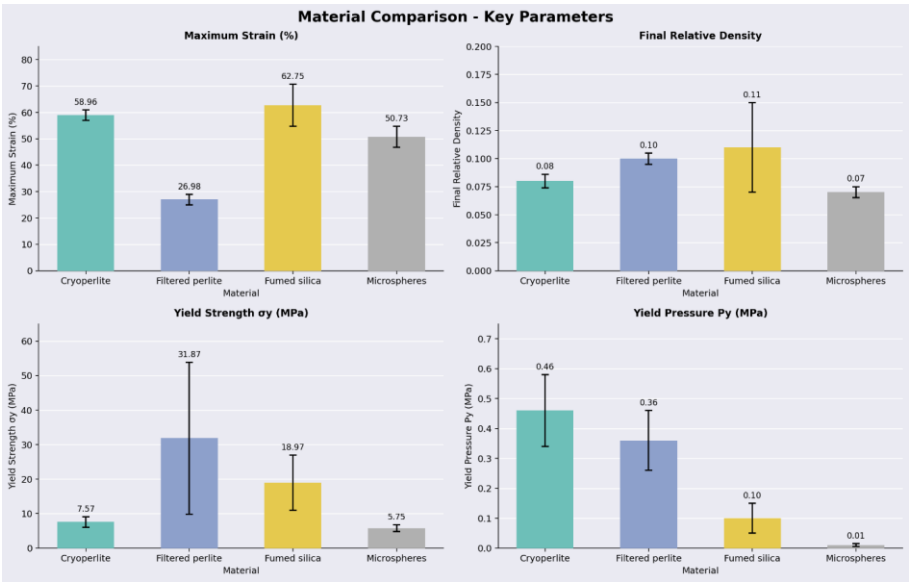

Figure 28: Comparison between materials at vacuum conditions

In summary, under vacuum conditions the Kawakita equation provides significantly superior fit quality compared to the Heckel equation for most tested materials, with R^2 coefficients indicating better model adherence to experimental data.

6.2.3 Mechanical behavior under cryogenic conditions

Comparative analysis of materials under cryogenic conditions is presented in Figure 34 and Figure 33, which show respectively key parameters extracted from compression tests under cryogenic vacuum and fit quality through R^2 coefficients.

The maximum strain parameter shows the following order among materials: fumed silica presents the highest value (82.38%), followed by cryoperlite (48.48%), filtered perlite (34.06%) and microspheres (22.55%).

Cryogenic conditions make strain measurements more stable, with generally reduced variability compared to other conditions.

However, variations remain quite wide for fumed silica, as evidenced by error bars.

Final relative density shows different values among materials: fumed silica reaches 0.20, filtered perlite 0.11, cryoperlite 0.07, and microspheres 0.04.

Fumed silica presents the greatest variability in this parameter, with significant error bars indicating dispersion in results between different tests.

Maximum pressure applied is substantially uniform among materials (0.44-0.47 MPa), with minimal variability between different experiments.

Once again, despite manual load application, pressure is similar and repeated in tests, confirming experimental methodology repeatability also under cryogenic conditions.

Parameters extracted from theoretical equations show distinct behaviors.

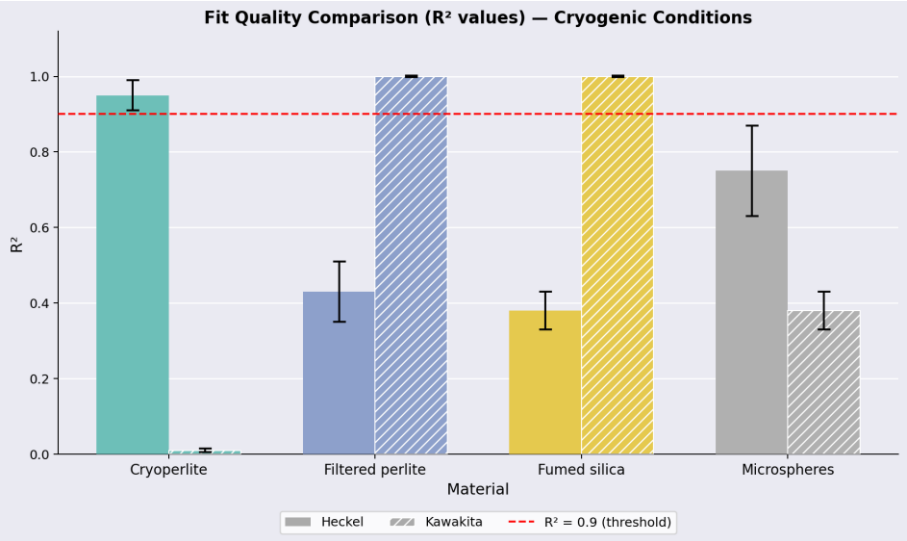

Figure 29: Fit quality cryo-vacuum conditions

Yield strength σ_y derived from the Heckel equation presents an extremely high value for microspheres (31.86 MPa), followed by filtered perlite (11.75 MPa), cryoperlite (9.04 MPa) and fumed silica (2.41 MPa).
Observing Figure 33, the Heckel equation shows more stable results compared to previous conditions: cryoperlite presents $R^2 \approx 0.95$, microspheres $R^2 \approx 0.75$, filtered perlite $R^2 \approx 0.44$, and fumed silica $R^2 \approx 0.37$.
Only cryoperlite exceeds the acceptability threshold of $R^2 = 0.9$, while other materials present values below this threshold.
Yield force and yield pressure P_y derived from the Kawakita equation are applicable only to two materials under cryogenic conditions.
Filtered perlite presents a value of approximately 486 N (0.21 MPa) and fumed silica approximately 341 N (0.15 MPa).
For microspheres, the extremely high value of approximately 4094 N (1.79 MPa) is caused by a single test where the Kawakita equation managed to perform regression on a curve with non-linear profile, making this result absolutely unreliable and to be ignored.
Figure 33 confirms this analysis: the Kawakita equation shows $R^2 \approx 1.00$ for filtered perlite and $R^2 \approx 1.00$ for fumed silica, indicating excellent fits for these two materials.
The $R^2 \approx 0.38$ value for microspheres confirms unreliability of the extracted parameter.
For cryoperlite, it was not possible to obtain parameters from the Kawakita equation, as indicated by the absent bar in the graph.
In summary, under cryogenic conditions both equations show limited applicability: the Heckel equation provides more stable results compared to previous conditions but with acceptable fit only for cryoperlite, while the Kawakita equation, although providing excellent fits where

applicable (filtered perlite and fumed silica), is inapplicable for cryoperlite and produces unreliable results for microspheres.

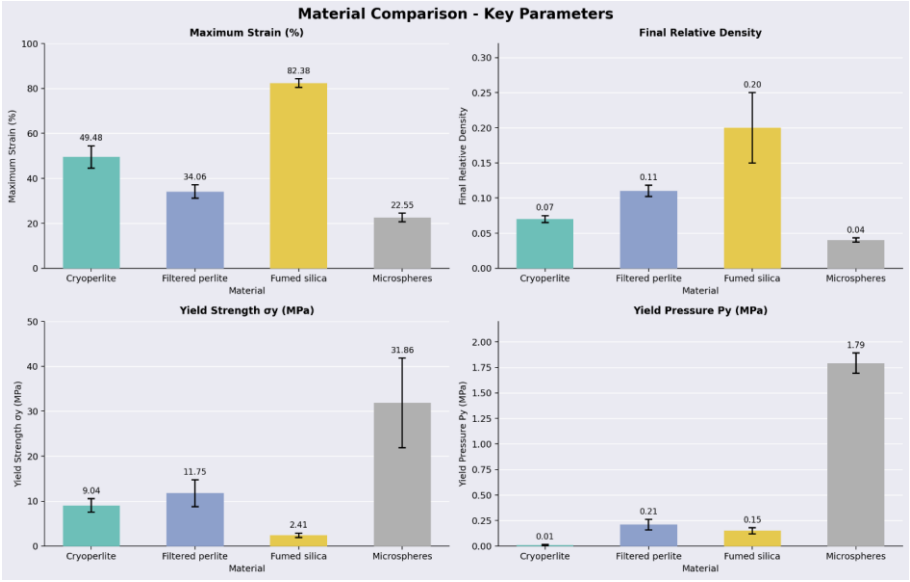

Figure 30: Comparison between materials at cryo vacuum conditions

6.3 Effect of environmental conditions

Systematic comparison between the three experimental conditions (atmospheric, vacuum, and cryovacuum) reveals the influence of temperature and air presence on densification mechanisms of insulating materials.
Figure 36 and Figure 35 present respectively the comparison of key parameters and fit quality for all tested conditions.

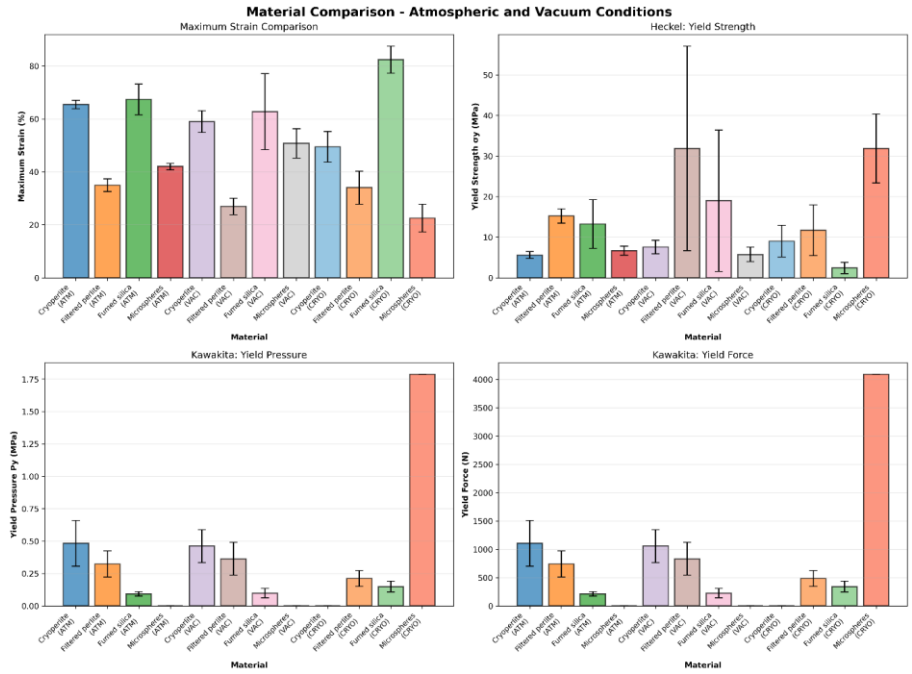

Figure 32: Results from the equations at all conditions for all materials

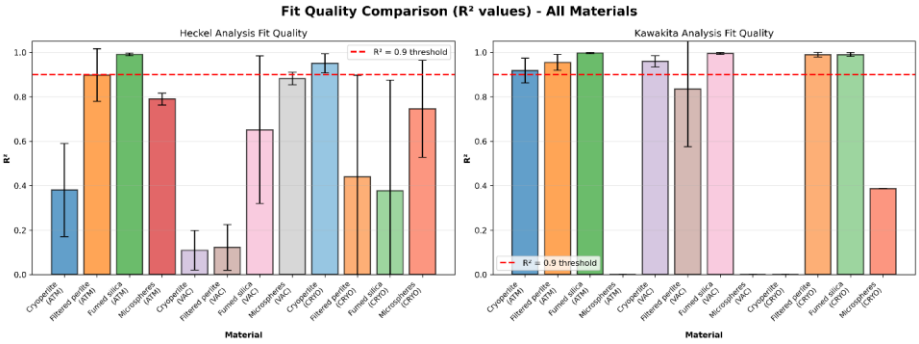

Figure 31: Equation quality fit for all material in all conditions

Maximum Strain

The maximum strain parameter shows different trends depending on the material.

For cryoperlite, a progressive reduction is observed moving from atmospheric (65.42%) to vacuum (58.96%) to cryogenic (48.48%) conditions.

For filtered perlite, strain decreases moving from atmospheric (35.00%) to vacuum (28.98%), with intermediate value under cryogenic conditions (34.06%).

Microspheres show an increase moving from atmospheric (42.03%) to vacuum (50.73%) with subsequent reduction in cryogenic (22.55%).
Fumed silica presents high values in atmospheric (67.34%) and vacuum (62.75%), with marked increase under cryogenic conditions (82.38%).

Heckel: Yield Strength
Yield strength values derived from the Heckel equation show significant variations between conditions.
Observing the fit quality graph (Figure 35), it emerges that the Heckel equation provides reliable results ($R^2 > 0.9$) only in few cases: fumed silica in atmospheric ($R^2 \approx 0.99$), filtered perlite in atmospheric ($R^2 \approx 0.90$), microspheres in vacuum ($R^2 \approx 0.90$), and cryoperlite in cryogenic ($R^2 \approx 0.95$).
For all other materials and conditions, R^2 values are below the acceptability threshold. In particular, a general deterioration of Heckel quality is noted moving from atmospheric to vacuum conditions for materials like fumed silica and filtered perlite, with partial recovery under cryogenic conditions for cryoperlite.

Kawakita: Yield Pressure and Yield Force
The Kawakita equation shows more consistent behaviors across different conditions.
For cryoperlite, yield force shows values of ~1100 N nominal (estimated ~900 N considering dispersion) in atmospheric and ~1052 N in vacuum, while it was not possible to extract parameters under cryogenic conditions.
For filtered perlite, an increase is observed moving from atmospheric (~740 N) to vacuum (~833 N), with subsequent reduction in cryogenic (~486 N). Fumed silica shows relatively stable values between atmospheric (~210 N) and vacuum (~227 N), with increase in cryogenic (~341 N).
The fit quality graph (Figure 35) shows that most materials maintain $R^2 > 0.9$ across different conditions, with excellent values ($R^2 \approx 1.00$) for fumed silica in all conditions and for filtered perlite in cryogenic.
Filtered perlite in vacuum shows $R^2 = 0.84$, slightly below ideal threshold.

Comparison of fit quality between conditions
Systematic comparison of R^2 coefficients (Figure 35) reveals distinct patterns for the two models.
For the Heckel equation, fit quality varies considerably between conditions: marked deterioration is observed moving from atmospheric to vacuum for fumed silica (from $R^2 \approx 0.99$ to $R^2 \approx 0.65$) and filtered perlite (from $R^2 \approx 0.90$ to $R^2 \approx 0.12$), while cryoperlite shows improvement in cryogenic ($R^2 \approx 0.95$).
For the Kawakita equation, R^2 coefficients remain generally high across different conditions for materials where the model is applicable. Fumed silica maintains $R^2 \approx 1.00$ in all conditions, filtered perlite presents $R^2 \approx 0.95$ in atmospheric, $R^2 \approx 0.84$ in vacuum and $R^2 \approx 1.00$ in cryogenic, while cryoperlite shows $R^2 \approx 0.92$ in atmospheric and $R^2 \approx 0.96$ in vacuum.

Repeatability considerations
Error bars show significant variability in extracted parameters for some materials and conditions.
Cryoperlite in atmospheric presents marked dispersion due to jumps in compression curves discussed in paragraph 6.1.3. Fumed silica shows excellent repeatability in atmospheric with reduced error bars, while in vacuum and cryogenic variability increases, partly due to limited number of acquired points with rapid compression in cryogenic.

Filtered perlite shows intermediate variability across different conditions.
In conclusion, comparative analysis between conditions shows that the Kawakita equation generally provides higher and more consistent R^2 coefficients compared to the Heckel equation across different environmental conditions.
The Heckel equation shows limited applicability strongly dependent on specific conditions, with reliable results only in selected cases.
Variations in yield force values extracted from Kawakita between different conditions reflect the effect of temperature and air presence on material densification mechanisms.

7. DISCUSSION

Commentato [GES1]: In 7.1 e 7.2 ci alcuni aspetti ripetuti più volte, cdi considerare una riorganizzazione delle sezioni e sottosezioni (magari accorciando un pochino) per rendere la lettura più fruibile. Se non riesce, va bene anche così

7.1 Interpretation of mechanical parameters and densification mechanisms

7.1.1 Applicability and validity of theoretical models

The comparative analysis of parameters extracted from the Heckel and Kawakita equations reveals substantial differences in the applicability of the two models to the tested cryogenic insulating powders.

The fit quality, quantified through determination coefficients R^2, constitutes the primary criterion for evaluating the validity of applying the models outside their theoretical development ranges.

The Kawakita equation demonstrates systematically superior applicability compared to the Heckel equation for the tested materials.

In cases where plastic deformation was achieved (fumed silica, perlites), Kawakita returns R^2 coefficients greater than 0.94 under atmospheric and vacuum conditions, reaching values close to 1.00 for fumed silica in all experimental conditions.

This superiority is attributable to the very nature of the Kawakita model, specifically developed for highly compressible powders ("fluffy powders") with high initial porosity, conditions that characterize all analyzed materials (initial porosity >90%, apparent densities 0.05-0.16 g/cm³).

The Heckel equation, conversely, presents limited applicability strongly dependent on experimental conditions.

R^2 values above the acceptability threshold (0.90) were obtained only in specific cases: fumed silica under atmospheric conditions ($R^2 \approx 0.99$), filtered perlite under atmospheric conditions ($R^2 \approx 0.90$ at the acceptability limit), microspheres under vacuum ($R^2 \approx 0.90$), and cryoperlite under cryogenic conditions ($R^2 \approx 0.95$).

This last result for cryoperlite is particularly interesting as it represents the only case where Heckel provides an excellent fit under cryogenic conditions, suggesting that the densification mechanism at low temperature for this material approaches more closely the assumptions of continuous plastic flow on which the model is based.

It is fundamental to emphasize that both models were applied outside their optimal theoretical ranges.

The experimental conditions (initial porosity >90%, maximum pressures <0.5 MPa) are located in a boundary region relative to traditional application fields: Kawakita is typically used for low pressures and high porosities, but not as extreme as those of cryogenic materials; Heckel requires sufficiently high pressures to induce significant plastic deformation, a condition not always achieved in the experimental setup.

Consequently, the extracted parameters must be interpreted primarily as comparative indicators between materials and experimental conditions, rather than as absolute values with rigorous physical meaning.

7.1.2 Fundamental limitations for glass microspheres

Glass microspheres represent the most critical case of experimental setup inadequacy.

The maximum applicable pressure (Pmax = 0.45 MPa) proved insufficient to characterize this material, as evidenced by comparison with data from Fesmire et al. (2008).

The experimental pressure range lies entirely within the elastic pre-fracture zone of the microspheres, well below the threshold necessary to induce rupture of the hollow spheres and consequent plastic densification of the material.

This limitation finds direct confirmation in physical observations: the material extracted from the compression chamber invariably maintains its fluid behavior in all tested conditions, without evidence of cluster formation or cohesive aggregates.
The relative density, although showing an increase up to almost doubling the initial value, remains confined to the particle rearrangement and elastic phase, without reaching the permanent deformation phase.
Consequently, for glass microspheres neither the Heckel nor the Kawakita equation are applicable in a physical sense.
The extracted parameters, when numerically obtainable, have no meaning as descriptors of the plastic behavior of the material and must be considered artifacts of mathematical fitting on a non-representative region.
Heckel curves present absence of identifiable linear region, while Kawakita profiles show anomalous trends (decreasing or with peaks) incompatible with the theoretical predictions of the model.
The real yield pressure of the microspheres therefore remains non-determinable in the available experimental range and would require a setup capable of applying significantly higher pressures, on the order of at least 1-2 MPa according to literature data.

7.1.3 Yield pressures and mechanical resistance

For materials in which plastic deformation was achieved, the yield pressures extracted from the Kawakita equation provide a quantitative scale of mechanical resistance to the formation of permanent bonds between particles.
The observed increasing order of mechanical resistance is: fumed silica (~0.092 MPaunder atmospheric and vacuum conditions) < filtered perlite (~0.323 MPa) < cryoperlite (~0.393–0.480 MPa nominal).
Fumed silica presents the lowest yield pressure among characterizable materials, with P_y values ≈ 0.092 MPa under atmospheric conditions and ≈ 0.099 MPa under vacuum.
This low resistance is consistent with the nanometric structure of the material (particles 2.5-50 nm) and with the experimental observation of formation of a solid disk with appreciable mechanical resistance at the end of compression.
The consistency of values between atmospheric and vacuum conditions (variation within experimental uncertainty) indicates that mechanical resistance is determined primarily by direct interactions between nanometric silica particles, rather than by the presence of interstitial air.
Filtered perlite shows an intermediate yield pressure (P_y ≈ 0.323 MPa under atmospheric conditions, ≈ 0.364 MPa under vacuum).
However, it is important to note that this value corresponds to formation of partially cohesive clusters rather than a complete solid disk.
The sample extracted from the compression chamber initially maintains the cylindrical shape impressed by the piston, but crumbles easily under minimal manual stress, highlighting that the material is in an intermediate condition between pure particle rearrangement and complete plastic densification.
This behavior suggests that the true yield pressure for formation of a completely consolidated disk would probably be higher than the 1000 N applicable by the setup.
Cryoperlite presents the highest yield pressure among characterizable materials (P_y ≈ 0.393–0.480 MPa nominal), with significant dispersion of individual values in atmospheric tests (range 0.262–0.568 MPa).
The average value of approximately 900 N appears physically sensible because: (a) it falls within the applied force range (900-1000 N), consistently with the observation that the yield

pressure must necessarily have been reached to allow disk formation; (b) it is compatible with analysis of curve morphology indicating transition toward the plastic regime beyond 500 N.
The extracted material effectively forms a consolidated disk, although fragile and easily crumbled, confirming achievement of a densification state superior to that of filtered perlite but with bonds between particles not yet completely stabilized.

7.1.4 Densification mechanisms and consolidation behavior

During uniaxial compression, the tested materials undergo distinct sequences of densification mechanisms that depend on their structural morphology.
In the initial phase, all materials undergo primarily particle rearrangement, with particles repositioning to occupy available void spaces.
For microspheres, characterized by perfect spherical geometry, the entire experimental range remains confined to this phase followed by elastic compression, with relative density almost doubling (from 0.0345 to ~0.07-0.08) without reaching permanent deformation. Fumed silica, owing to its nanometric structure (2.5-50 nm), shows gradual and continuous transition toward the formation of permanent bonds at relatively low pressures ($P_y \approx 0.092$ MPa), producing solid disks with appreciable mechanical resistance.
Porous materials (filtered perlite and cryoperlite) present more complex mechanisms dominated by collapse of internal hollow structures.
Filtered perlite (20 μm) shows exponential curves reflecting progressive yielding of thin walls, with formation of partially cohesive clusters at $P_y \approx 0.323–0.364$ MPa.
Cryoperlite (0.5 mm), with macroscopic granules, exhibits more dramatic and discontinuous collapses, manifested in marked jumps in atmospheric curves.
These discrete events are significantly reduced under vacuum (R^2 from 0.92 to 0.96 for Kawakita), confirming that part of the discontinuities derives from sudden expulsion of trapped air.
Despite the higher yield pressure ($P_y \approx 0.393–0.480$ MPa), cryoperlite forms consolidated but fragile disks, indicating that the larger granule size allows more complete collapse of internal structures, creating mechanical continuity through interlocking between fragments, although the bonds remain insufficient to sustain significant stresses.
The observed maximum deformation values (silica 67-82%, cryoperlite 48-65%, filtered perlite 27-35%, microspheres 22-51%) must be interpreted as limited to the tested experimental range, not as ultimate deformation of the materials.
Silica, despite starting from the lowest initial apparent density ($D_0 = 0.0227$), reaches higher final densities (0.10-0.20), highlighting exceptional densification capacity consistent with efficient rearrangement of the nanometric structure.
The coherence between quantitative parameters and qualitative observations is evident: materials with P_y well within the experimental range (silica ≈21% of maximum force) form robust structures; materials at the upper limit (filtered perlite ≈74-83%, cryoperlite ≈90-110%) produce partial or fragile consolidation; materials outside the range (microspheres) show no permanent deformation.

7.1.5 Effect of environmental conditions on mechanical parameters

The transition from atmospheric to vacuum conditions produces primarily qualitative improvement of experimental data rather than substantial variations in mechanical parameters. The elimination of interstitial air generates notably more regular curves, particularly evident for cryoperlite (R^2 from 0.92 to 0.96 for Kawakita), but yield pressures remain substantially unchanged: silica $P_y \approx 0.092–0.099$ MPa, cryoperlite ≈ 0.393–0.459 MPa, filtered perlite ≈ 0.323–0.364 MPa.

This invariance suggests that mechanical resistance is determined primarily by intrinsic material properties and particle-particle interactions, while air influences the mode of densification (continuous vs. discontinuous) rather than the threshold necessary to trigger it.
For fumed silica, the more pronounced increase in final density under vacuum indicates that residual air between nanometric particles occupied a non-negligible fraction of total volume, whereas for perlites the final density remains unchanged, suggesting that vibration already eliminates most accessible air and residual porosity is primarily structural (internal cavities within granules).
Cryogenic conditions introduce material-specific modifications revealing thermal embrittlement phenomena.
Filtered perlite shows significant reduction of P_y from ≈ 0.323–0.364 MPa to ≈ 0.212 MPa (34-42% decrease), accompanied by increase in Kawakita parameter 'a', indicative of thermal embrittlement of the glassy structure: at -196°C, reduced atomic mobility favors brittle fracture of hollow walls that yield at lower loads without local plastic deformation.
Fumed silica shows apparent increase in P_y to ≈ 0.149 MPa, but this data requires caution due to suboptimal acquisition quality (limited number of points, ice formation, impossibility to apply Heckel in 2/4 tests).
Cryoperlite presents completely anomalous behavior with "U"-shaped Kawakita profile (repeatable in 3/3 cryogenic tests), incompatible with the assumption of monotonic porosity reduction.
The most plausible interpretation involves extreme thermal embrittlement: initial catastrophic collapse with complete granule fragmentation (U descending branch, facilitating rearrangement), followed by increasing resistance of densely packed fragments (U ascending branch).
Significantly, Heckel maintains linear region ($R^2 \approx 0.95$) providing P_y consistent with vacuum, highlighting that Kawakita, assuming specific porosity reduction kinetics, is more sensitive to complex mechanisms operating at low temperature, while Heckel, focused on density-pressure relationship at high density, proves more robust.

7.1.6 Correlation between extracted parameters and experimental evidence

Validation of the interpretation of extracted parameters emerges from coherence with direct physical observations on post-compression samples.
Fumed silica and cryoperlite, forming consolidated solid disks (although with different resistance), present reliable yield pressures within the applied range.
Filtered perlite, producing only partially cohesive clusters, shows P_y at the upper limit of the range, suggesting that complete consolidation would require higher pressures.
Microspheres, without evidence of permanent deformation, confirm complete inadequacy of the experimental range.
Coherence between R^2 and curve regularity reinforces this validation: silica with $R^2 \approx 1.00$ and robust disk represents ideal applicability; cryoperlite with variable R^2 (0.92-0.96 in atmosphere/vacuum, inapplicable in cryogenic) and fragile disk indicates behavior at the limit; perlite with intermediate R^2 (0.84-1.00) and clusters suggests incomplete plastic transition; microspheres with low R^2 and absence of consolidation confirm inapplicability when plastic phase is not reached.
The integrated interpretation of mechanical parameters, densification mechanisms, and physical evidence provides robust characterization, confirming superiority of Kawakita for high-porosity materials, but always requires validation through final physical state and recognition of limitations in applying theoretical models to extreme conditions.

7.2 Study limitations and sources of uncertainty

7.2.1 Experimental setup limitations

The main limitation of the experimental setup is represented by the maximum applicable force (1000 N, ~0.45 MPa), insufficient to completely characterize glass microspheres and limiting filtered perlite to partial consolidation.
As demonstrated by comparison with Fesmire et al. (2008), complete characterization of microspheres would require pressures of 1-2 MPa to induce fracture of hollow spheres and access the plastic regime.
Manual load application, despite demonstrating good repeatability on maximum pressure (0.43-0.48 MPa, variability <10%), introduces variability in compression velocity requiring rapid compressions for some materials (cryoperlite) with consequent reduction in acquired points.
A motorized system would allow complete standardization of velocity and systematic studies on the effect of deformation rate.
The chamber geometry (filling height 30 mm over 54 mm total) introduces a relatively low height/diameter ratio that could influence stress distribution, particularly near lateral walls.

7.2.2 Experimental issues under cryogenic conditions

Cryogenic conditions introduced specific issues partially compromising data quality.
Ice formation represents the most significant problem: despite preventive pumping below 20 mbar, residual moisture condenses and solidifies on metallic surfaces at -196°C, particularly on the mobile piston where it introduces irregular friction resistances visible as segmentations in force-displacement curves.
Ice also forms on the external surface requiring manual removal before each test, but formation on the internal piston remains difficult to completely control.
Rapid compression adopted to reduce ice problems and curve jumps significantly reduced acquired points, problematic for Heckel which requires sufficient number in the linear region: for silica under cryogenic conditions, 2/4 tests did not allow Heckel application due to data insufficiency.
Thermal uniformity through the sample introduces further uncertainty: the cooling time (25 minutes) was determined with thermocouple in microspheres reaching -177°C, but direct verification was performed only for this material, not excluding residual thermal gradients in others, particularly for highly insulating materials like cryoperlite.

7.2.3 Application of models outside theoretical range

As discussed in 7.1.1, both equations were applied outside their optimal theoretical ranges, and the extracted parameters must be interpreted as comparative indicators rather than absolute values with rigorous physical meaning.
Beyond this general limitation, specific sources of uncertainty affect parameter reliability.
For the Heckel equation, the assumption of densification through continuous plastic flow is particularly problematic for materials that densify via porous structure collapse (perlites) or nanometric particle rearrangement (fumed silica), mechanisms fundamentally different from the plastic flow assumed by the model.
For the Kawakita equation, although specifically developed for compressible powders, application to porosities exceeding 90% and to complex mechanisms such as fracture and structural collapse introduces non-negligible uncertainties: parameter 'a' theoretically corresponds to initial porosity, but deviations are common due to difficulties in determining

V_0, extrapolation to infinite pressure, and changes in deformation mechanism during compression, as noted by Kawakita & Lüdde (1970).

7.2.4 Data quality and repeatability

Data quality shows marked dependence on material and conditions. Silica presents best repeatability under atmospheric conditions ($R^2 \approx 1.00$ for Kawakita), with increased variability under vacuum/cryogenic conditions due to operational problems but maintaining $R^2 > 0.99$.
Cryoperlite under atmospheric conditions shows maximum dispersion (P_y range 0.262–0.568 MPa, >100% relative to mean value) due to marked jumps from discontinuous collapse, requiring exclusion of 5/8 atmospheric tests producing values incompatible with physical evidence.
Rapid compression and vacuum significantly improve conditions (R^2 from 0.92 to 0.96).
Filtered perlite presents intermediate variability requiring exclusion of some tests (4/7 atmospheric, 1/4 vacuum) producing parameters outside physically acceptable range, probably due to variations in sample preparation.
Exclusion followed objective criteria: (a) P_y exceeding maximum applied force; (b) very low P_y implying consolidated disk in contradiction with observations; (c) very low R^2 (<0.5 Kawakita, <0.3 Heckel) indicating evident inapplicability.

7.2.5 Uncertainties in initial density determination

Determination of initial apparent density through vibration (1250 cycles) introduces systematic uncertainty influencing Kawakita parameter 'a'.
The standardized protocol produces final density dependent on flow properties, particle morphology, and air elimination capacity, varying significantly between materials.
For silica, residual air even after vibration is evidenced by final density increase under vacuum, indicating that air trapped between nanometric particles contributes significantly to apparent volume.
For perlites, final density unchanged between atmosphere and vacuum suggests vibration sufficient to eliminate inter-granular air, but internal porosity within granules remains inaccessible.
Ambiguity in defining "solid volume" for particles with macroscopic cavities introduces further uncertainty. Kawakita & Lüdde (1970) emphasize that deviations of 'a' from measured porosity are common due to fluctuations in V_0. Initial height measurement (±0.5 mm over 30 mm nominal) introduces ~1.7% uncertainty on volume, propagating into D_0 and derived parameters.

7.3 Implications for insulating system design

The experimental results obtained in the present study have direct implications for the insulation technologies currently employed in liquid hydrogen (LH2) storage tanks, including double-walled tanks with evacuated perlite powder in operation at the Kennedy Space Center and the Kawasaki HyTouch terminal, and emerging systems based on VIPs with glass microsphere, fumed silica, or perlite cores.
Regarding perlite, the historically dominant material in such systems, compression tests show that under the cryogenic and vacuum conditions representative of actual operating environments, the material undergoes significant volumetric reduction compared to atmospheric conditions.
This behavior is relevant because progressive compaction of the perlite bed in the tank annulus can generate localized voids, a phenomenon already documented at NASA's 3,200 m³ tank in

2001, which resulted in an increased boil-off rate, and reduce the long-term repeatability of insulation performance.
The parameters extracted from the Kawakita equation further indicate that cryoperlite, while exhibiting compressibility comparable to filtered perlite, reaches a higher degree of compaction, a factor to be considered in annulus design.
Hollow glass microspheres, the reference candidate for NASA's new 4,700 m^3 tank to replace perlite, exhibit a markedly stiffer mechanical response and significantly lower volumetric deformation under the same conditions.
This behavior provides greater dimensional stability and reduces void formation in the annulus during operation, supporting the advantages already documented in the literature in terms of a 46% reduction in boil-off rate compared to conventional perlite.
However, the pressure range investigated did not allow full characterization of the plastic behavior of microspheres, which represents a limitation in estimating compressive strength under more severe loading conditions.
For VIPs, in which fumed silica, perlite, and microspheres are used as core materials, the compressibility of the filler is a critical parameter: excessive deformation of the core compromises the maintenance of the internal vacuum, an indispensable requirement for thermal performance, and the dimensional stability of the panel.
The results indicate that fumed silica, which did not reach a plateau under any of the tested conditions due to instrumental limitations, exhibits the highest compressibility among the studied materials.
In cryogenic VIPs, this could translate into greater susceptibility to performance loss under load.

8. CONCLUSIONS AND FUTURE DEVELOPMENTS

The present study characterized the mechanical behavior of four insulating materials for cryogenic applications, glass microspheres, filtered perlite, cryoperlite, and fumed silica, by subjecting them to uniaxial compression under three environmental conditions: atmospheric, vacuum, and cryogenic.

The analysis was carried out by applying the Heckel and Kawakita equations, with the aim of extracting quantitative parameters comparable across materials and conditions, and of identifying the prevailing densification mechanisms in each case.

The Kawakita equation proved to be the most suitable tool for the tested materials, achieving R^2 coefficients above 0.94 in the majority of material-condition combinations where plastic deformation was attained.

This result is attributable to the nature of the model itself, specifically developed for highly compressible powders with high initial porosity, a characteristic shared by all analyzed materials (porosity >90%, apparent density 0.05–0.16 g/cm³).

The Heckel equation showed limited applicability, strongly dependent on experimental conditions, with acceptable R^2 (>0.90) only in specific cases.

Fumed silica confirmed itself as the most compressible material across all conditions, with maximum strains up to 82% under cryogenic conditions and consistently lower Kawakita yield pressures (≈0.09–0.15 MPa).

Filtered perlite and cryoperlite exhibit intermediate resistance (Py ≈ 0.32–0.48 MPa under atmospheric and vacuum conditions), with cryoperlite displaying anomalous behavior at cryogenic temperature, characterized by a "U"-shaped Kawakita profile interpretable as catastrophic collapse followed by recompacting of fragments.

Glass microspheres exhibited the mechanically stiffest behavior, with reduced strains and absence of permanent consolidation within the investigated pressure range, confirming the inadequacy of the experimental setup for their full characterization.

The transition from atmospheric to vacuum conditions produced primarily a qualitative improvement of experimental data, with more regular curves, without substantial variations in the extracted mechanical parameters.

This indicates that mechanical resistance is determined mainly by the intrinsic properties of the materials rather than by the presence of interstitial air.

Cryogenic conditions instead introduced material-specific modifications attributable to thermal embrittlement phenomena: reduction of the yield pressure of filtered perlite from ≈0.32 MPa to ≈0.21 MPa (–34–42%), anomalous behavior of cryoperlite not describable through the Kawakita model, and apparent increase of Py for fumed silica to ≈0.15 MPa, to be interpreted with caution due to the suboptimal quality of data acquired under such conditions.

Future research efforts should be devoted to the extension of the experimental pressure range.

A setup with a maximum load of at least 2–5 MPa, applied through a motorized system at controlled velocity, would allow full characterization of the plastic regime of glass microspheres and complete consolidation of perlite, overcoming the fundamental limitations identified in this study.

The adoption of a motorized loading system would also eliminate the variability introduced by manual application, enabling systematic studies on the effect of strain rate.

Regarding cryogenic conditions, resolving the technical issues that compromised the quality of data acquired at –196°C represents a priority.

Ice formation on measurement surfaces and the loss of data points during the loading phase, particularly critical for cryoperlite, limited the applicability of theoretical models.

The implementation of a preventive degassing procedure for samples and localized heating of measurement elements would allow data quality comparable to that obtained under atmospheric and vacuum conditions.
A natural extension of this work concerns the cyclic behavior of materials under repeated thermal and mechanical loads, more representative of the actual operating conditions of cryogenic tanks.
The results of this study provide a first-loading characterization, but the degradation of mechanical properties after successive filling and emptying cycles remains unquantified.

BIBLIOGRAPHY

[1] I. - International Energy Agency, «World Energy Outlook 2023», 2023. [Online]. Disponibile su: www.iea.org/terms

[2] J. E. Fesmire, J. P. Sass, Z. Nagy, S. J. Sojourner, D. L. Morris, e S. D. Augustynowicz, «Cost-efficient storage of cryogens», in *AIP Conference Proceedings*, 2008, pagg. 1383–1391. doi: 10.1063/1.2908498.

[3] J. E. Fesmire, A. M. Swanger, J. A. Jacobson, e W. U. Notardonato, «Energy Efficient Large-Scale Storage of Liquid Hydrogen».

[4] A. G. Krenn, R. C. Youngquist, e S. O. Starr, «ANNULAR AIR LEAKS IN A LIQUID HYDROGEN STORAGE TANK».

[5] A. E. Giannakopoulos, A. Zisis, A. D. Zervaki, C. D. Dimopoulos, E. Platypodis, e R. Eberwein, «Effective elastic moduli and failure mechanisms of a random assembly of thin walled glass microbubbles», *Int. J. Solids Struct.*, vol. 320, set. 2025, doi: 10.1016/j.ijsolstr.2025.113528.

[6] J. E. Fesmire, S. D. Augustynowicz, Z. F. Nagy, S. J. Sojourner, e D. L. Morris, «Vibration and thermal cycling effects on bulk-fill insulation materials for cryogenic tanks», in *AIP Conference Proceedings*, apr. 2006, pagg. 1359–1366. doi: 10.1063/1.2202556.

[7] J. P. Sass, W. W. S. Cyr, T. M. Barrett, R. G. Baumgartner, J. W. Lott, e J. E. Fesmire, «Glass bubbles insulation for liquid hydrogen storage tanks», in *AIP Conference Proceedings*, 2010, pagg. 772–779. doi: 10.1063/1.3422430.

[8] «NICOLHy-Novel Insulation Concepts for LH2 Storage Tanks Project deliverable D1.1 LH2 storage tank and insulation technologies, applications, and standards».

[9] J. P. Sass, J. E. Fesmire, Z. F. Nagy, S. J. Sojourner, D. L. Morris, e S. D. Augustynowicz, «Thermal performance comparison of glass microsphere and perlite insulation systems for liquid hydrogen storage tanks», in *AIP Conference Proceedings*, 2008, pagg. 1375–1382. doi: 10.1063/1.2908497.

[10] A. M. Rashad, «A synopsis about perlite as building material - A best practice guide for Civil Engineer», 15 settembre 2016, *Elsevier Ltd*. doi: 10.1016/j.conbuildmat.2016.06.001.

[11] P. M. Angelopoulos, «Insights in the Physicochemical and Mechanical Properties and Characterization Methodology of Perlites», *Minerals*, vol. 14, n. 1, gen. 2024, doi: 10.3390/min14010113.

[12] R. Baetens *et al.*, «Vacuum insulation panels for building applications: A review and beyond», febbraio 2010. doi: 10.1016/j.enbuild.2009.09.005.

[13] M. Gonçalves, N. Simões, C. Serra, e I. Flores-Colen, «A review of the challenges posed by the use of vacuum panels in external insulation finishing systems», 1 gennaio 2020, *Elsevier Ltd*. doi: 10.1016/j.apenergy.2019.114028.

[14] D. Božiček, J. Peterková, J. Zach, e M. Košir, «Vacuum insulation panels: An overview of research literature with an emphasis on environmental and economic studies for building applications», 1 gennaio 2024, *Elsevier Ltd*. doi: 10.1016/j.rser.2023.113849.

[15] «M.J. Adams, 1996, Micromechanical analyses of the pressure-volume relationships for powders under confined uniaxial compression».

[16] I. G. Watkins e M. Prado, «Mechanical Properties of Glass Microspheres», *Procedia Materials Science*, vol. 8, pagg. 1057–1065, 2015, doi: 10.1016/j.mspro.2015.04.168.

[17] B. Dillinger e V. Blacksburg, «Crush Strength Analysis of Hollow Glass Microspheres», 2016.

[18] M. L. Hentschel e N. W. Page, «Elastic properties of powders during compaction. Part 1: Pseudo-isotropic moduli», *J. Mater. Sci.*, vol. 42, n. 4, pagg. 1261–1268, feb. 2007, doi: 10.1007/s10853-006-1145-x.
[19] A. Thomas e J. Clayton, «Stress distribution in a powder column under uniaxial compression», *Powder Technol.*, vol. 408, ago. 2022, doi: 10.1016/j.powtec.2022.117768.
[20] R. W. Werlink, J. E. Fesmire, e J. P. Sass, «Vibration considerations for cryogenic tanks using glass bubbles insulation», in *AIP Conference Proceedings*, 2012, pagg. 55–65. doi: 10.1063/1.4706905.
[21] P. J. Denny, «Compaction equations: a comparison of the Heckel and Kawakita equations». [Online]. Disponibile su: www.elsevier.com/locate/powtec
[22] J. Nordström, I. Klevan, e G. Alderborn, «A protocol for the classification of powder compression characteristics», *European Journal of Pharmaceutics and Biopharmaceutics*, vol. 80, n. 1, pagg. 209–216, gen. 2012, doi: 10.1016/j.ejpb.2011.09.006.
[23] «Some Considerations on Powder Compression Equations Kimio Kawakita».

APPENDICES

A. Complete experimental data

This appendix presents the complete set of graphs obtained during the mechanical characterization campaigns conducted on the four insulating materials under investigation: glass microspheres, filtered perlite, cryoperlite, and fumed silica.
For each material, graphs relative to the three experimental conditions are reported: atmospheric, vacuum, and cryogenic.
Unlike what is presented in Chapter 6, where a single representative experiment was selected for each condition for the purpose of quantitative analysis using the Heckel and Kawakita equations, this appendix includes the totality of performed tests, including those that exhibited instrumental anomalies, measurement artifacts, or physically uninterpretable behaviors that rendered them unsuitable or unreliable for use in the main analysis.
The specific reasons for the exclusion of each problematic dataset are described in the relevant paragraphs of Chapters 6 and 7, to which the reader is referred for further details.
The inclusion of these data serves a dual purpose: on one hand, to ensure the transparency and reproducibility of the research by making the complete raw dataset available for potential future analyses; on the other, to document the experimental challenges encountered, particularly under vacuum and cryogenic conditions, which constitute in themselves a significant outcome with respect to the design of more adequate experimental setups for the characterization of these materials.
The graphs are organized by material and, within each material, by experimental condition, following the same structure adopted in Chapter 6.

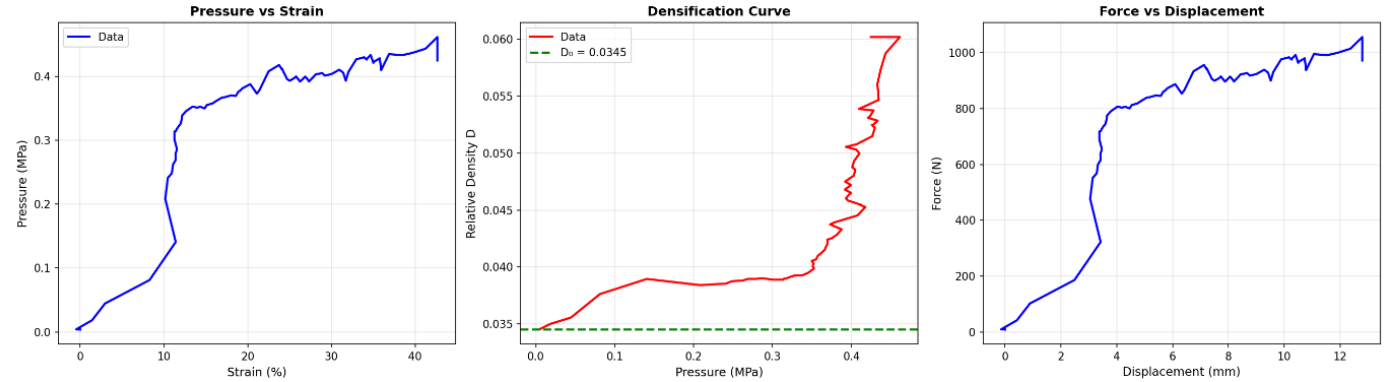

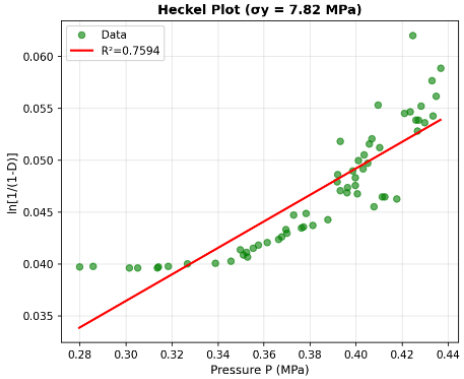

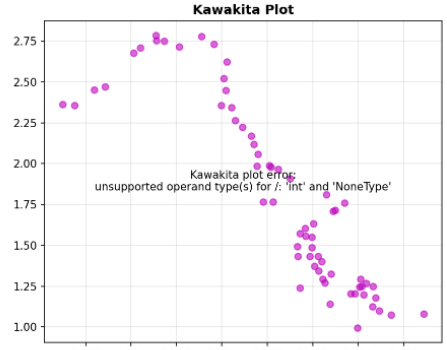


```
MATERIAL: Microspheres
ρ_true: 2.4 g/cm³
Mass: 5.69 g
h₀: 152.08 mm

DATA POINTS: 75
D₀: 0.0345
D_final: 0.0602
P_max: 0.46 MPa
F_max: 1056.5 N
Strain_max: 42.7%

HECKEL:
  K = 0.1279 MPa⁻¹
  σy = 7.82 MPa
  R² = 0.7594

KAWAKITA:
  Not available

FILE:
  microspheres atm 125.11.24-14.37.19.xlsx
```

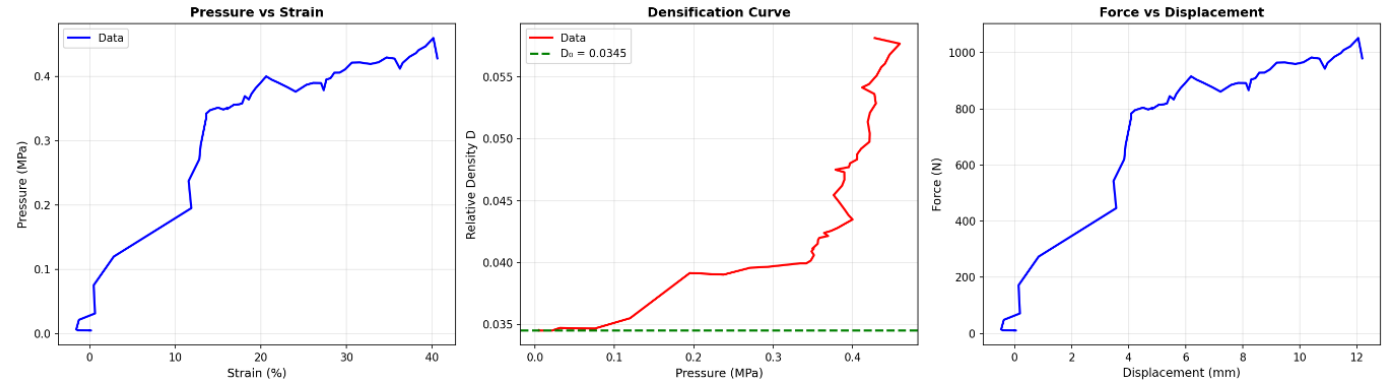

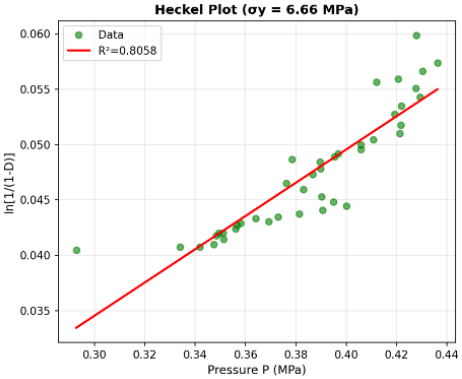

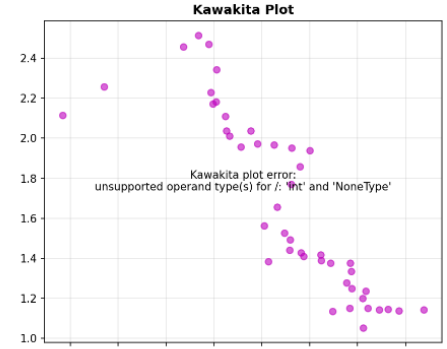


```
MATERIAL: Microspheres
ρ_true: 2.4 g/cm³
Mass: 5.69 g
h₀: 151.61 mm

DATA POINTS: 65
D₀: 0.0345
D_final: 0.0581
P_max: 0.46 MPa
F_max: 1052.6 N
Strain_max: 40.6%

HECKEL:
  K = 0.1501 MPa⁻¹
  σy = 6.66 MPa
  R² = 0.8058

KAWAKITA:
  Not available

FILE:
  microspheres atm 225.11.24-14.47.02.xlsx
```

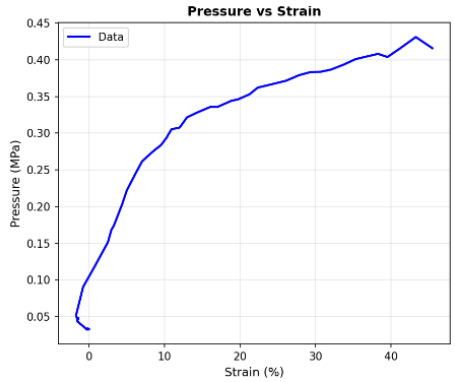

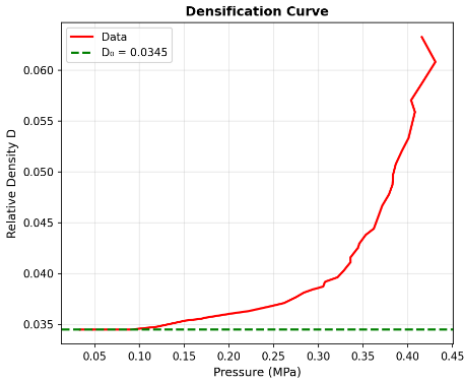

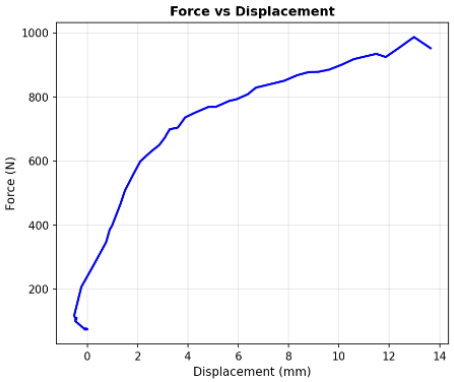

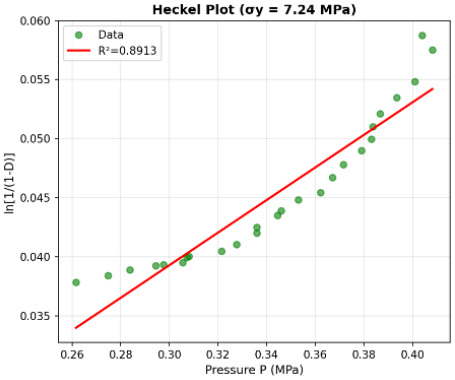

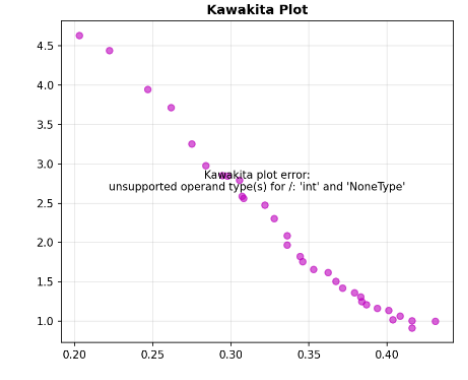


```
MATERIAL: Microspheres
ρ_true: 2.4 g/cm³
Mass: 5.69 g
h₀: 151.23 mm

DATA POINTS: 64
D₀: 0.0345
D_final: 0.0633
P_max: 0.43 MPa
F_max: 987.0 N
Strain_max: 45.5%

HECKEL:
  K = 0.1381 MPa⁻¹
  σy = 7.24 MPa
  R² = 0.8913

KAWAKITA:
  Not available

FILE:
  microsphere vacuum 125.12.01-10.45.38.xlsx
```

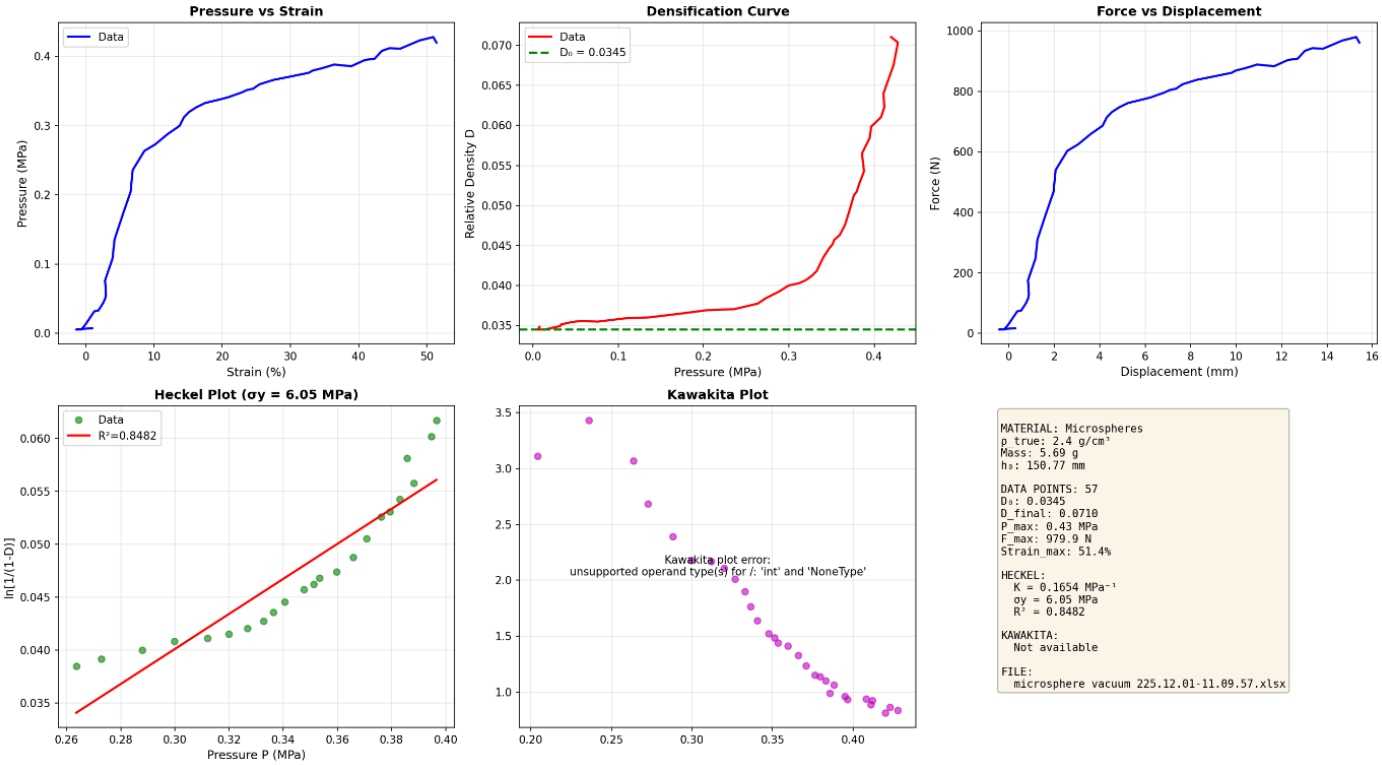


```
MATERIAL: Microspheres
ρ_true: 2.4 g/cm³
Mass: 5.69 g
h₀: 150.77 mm

DATA POINTS: 57
D₀: 0.0345
D_final: 0.0710
P_max: 0.43 MPa
F_max: 979.9 N
Strain_max: 51.4%

HECKEL:
  K = 0.1654 MPa⁻¹
  σy = 6.05 MPa
  R² = 0.8482

KAWAKITA:
  Not available

FILE:
  microsphere vacuum 225.12.01-11.09.57.xlsx
```

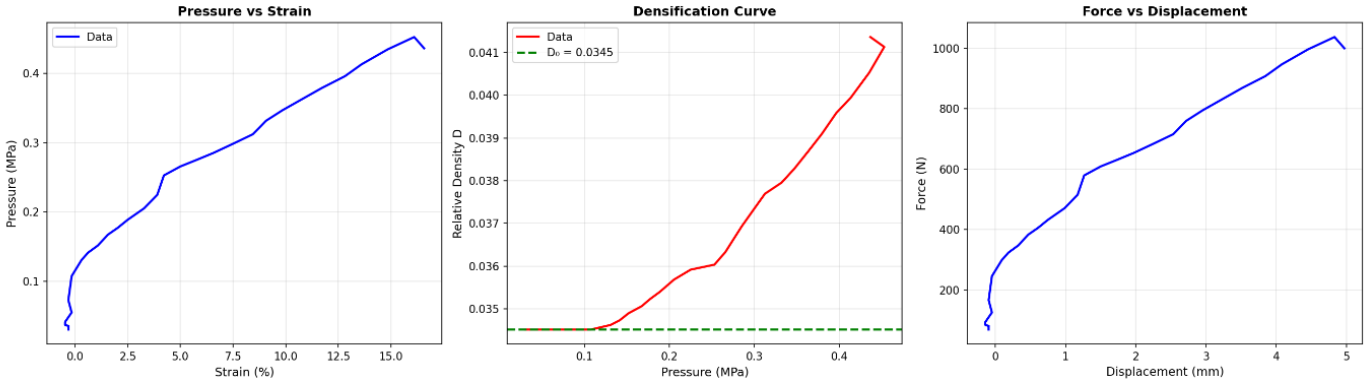


```
MATERIAL: Microspheres
ρ_true: 2.4 g/cm³
Mass: 5.69 g
h₀: 150.11 mm

DATA POINTS: 31
D₀: 0.0345
D_final: 0.0414
P_max: 0.45 MPa
F_max: 1037.0 N
Strain_max: 16.6%

HECKEL:
  K = 0.0243 MPa⁻¹
  σy = 41.21 MPa
  R² = 0.9956

KAWAKITA:
  Not available

FILE:
  microsphere cryo 225.12.12-14.45.37.xlsx
```

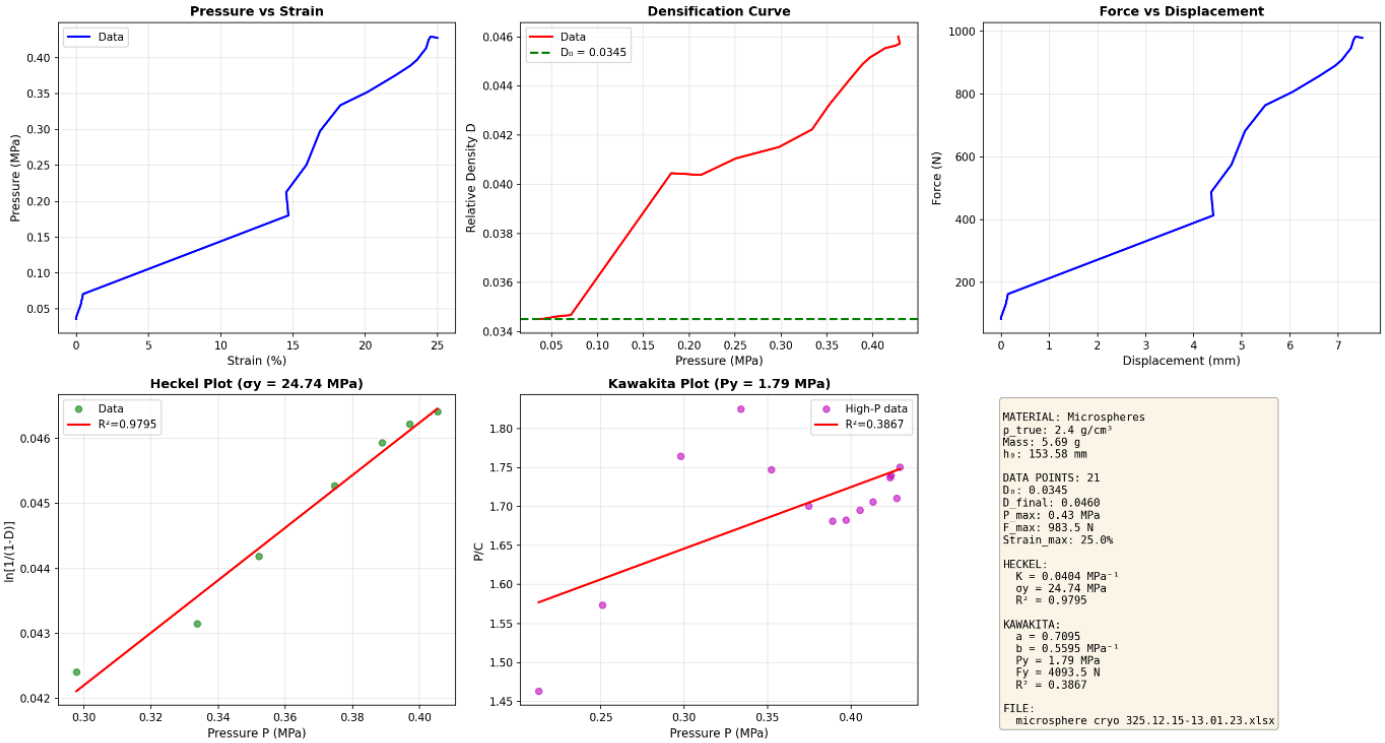


```
MATERIAL: Microspheres
ρ_true: 2.4 g/cm³
Mass: 5.69 g
h₀: 153.58 mm

DATA POINTS: 21
D₀: 0.0345
D_final: 0.0460
P_max: 0.43 MPa
F_max: 983.5 N
Strain_max: 25.0%

HECKEL:
  K = 0.0404 MPa⁻¹
  σy = 24.74 MPa
  R² = 0.9795

KAWAKITA:
  a = 0.7095
  b = 0.5595 MPa⁻¹
  Py = 1.79 MPa
  Fy = 4093.5 N
  R² = 0.3867

FILE:
  microsphere cryo 325.12.15-13.01.23.xlsx
```

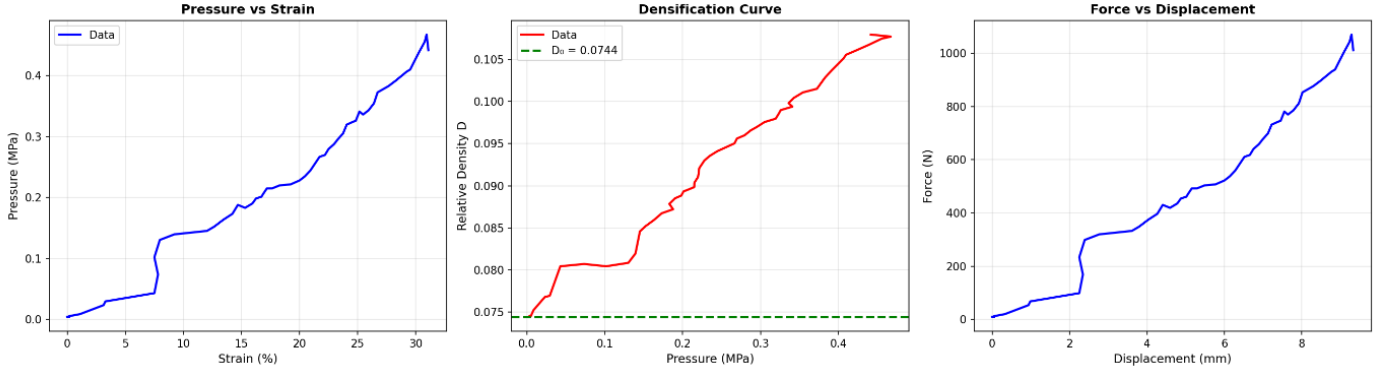

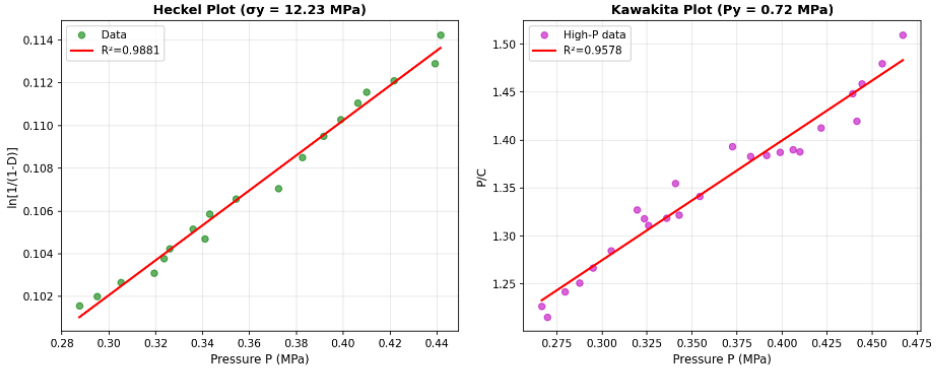


```
MATERIAL: Filtered perlite
ρ_true: 2.2 g/cm³
Mass: 11.25 g
h₀: 147.06 mm

DATA POINTS: 85
D₀: 0.0744
D_final: 0.1080
P_max: 0.47 MPa
F_max: 1069.8 N
Strain_max: 31.1%

HECKEL:
  K = 0.0817 MPa⁻¹
  σy = 12.23 MPa
  R² = 0.9881

KAWAKITA:
  a = 1.1106
  b = 1.3859 MPa⁻¹
  Py = 0.72 MPa
  Fy = 1652.5 N
  R² = 0.9578

FILE:
  filterperlite atm 225.11.25-12.12.35.xlsx
```

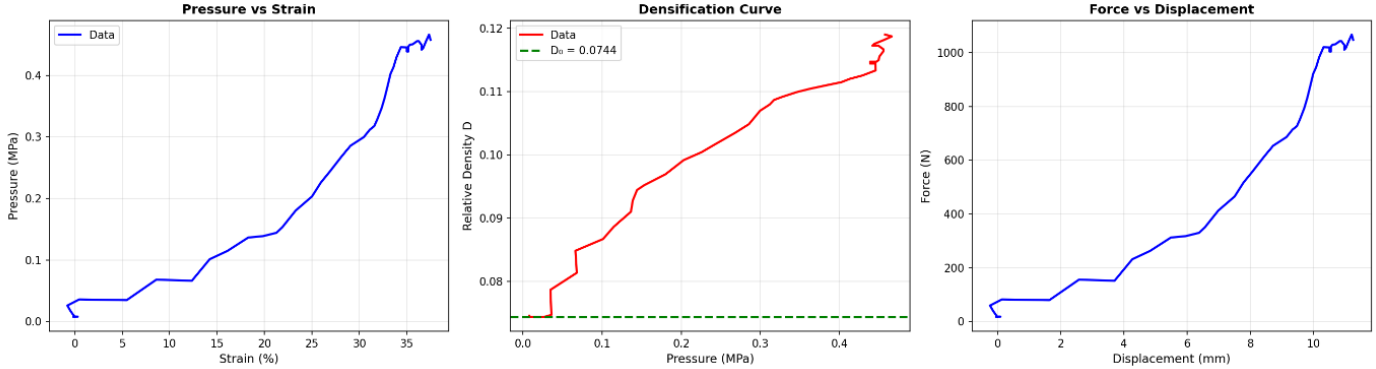

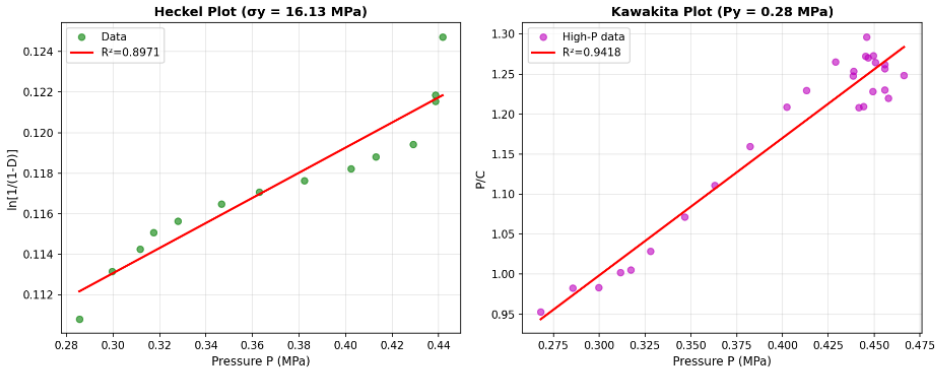


```
MATERIAL: Filtered perlite
ρ_true: 2.2 g/cm³
Mass: 11.25 g
h₀: 147.77 mm

DATA POINTS: 60
D₀: 0.0744
D_final: 0.1190
P_max: 0.47 MPa
F_max: 1067.6 N
Strain_max: 37.5%

HECKEL:
  K = 0.0620 MPa⁻¹
  σy = 16.13 MPa
  R² = 0.8971

KAWAKITA:
  a = 2.0685
  b = 3.5511 MPa⁻¹
  Py = 0.28 MPa
  Fy = 644.9 N
  R² = 0.9418

FILE:
  filterperlite atm 325.11.24-15.47.43.xlsx
```

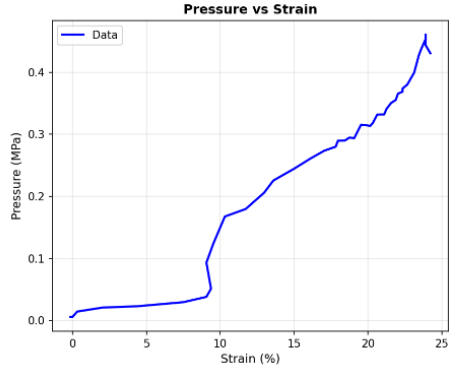

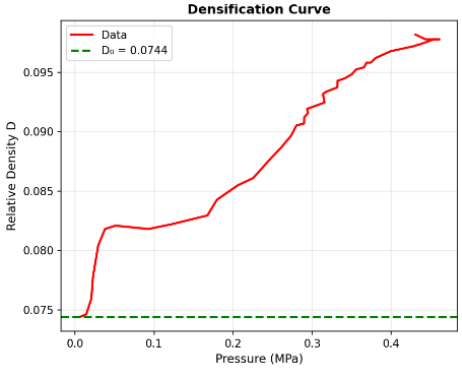

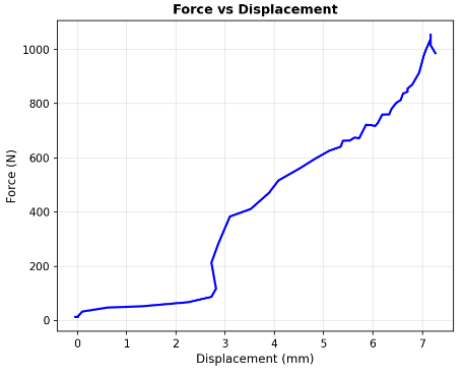

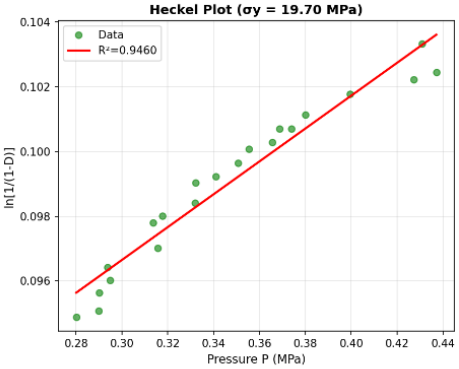

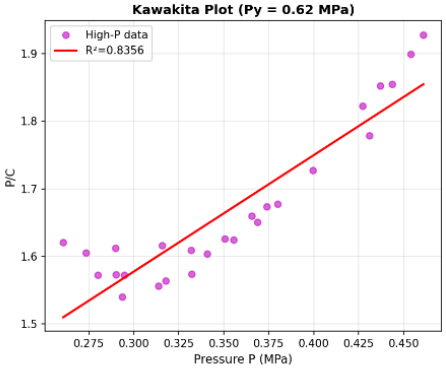


```
MATERIAL: Filtered perlite
ρ_true: 2.2 g/cm³
Mass: 11.25 g
h₀: 145.52 mm

DATA POINTS: 59
D₀: 0.0744
D_final: 0.0982
P_max: 0.46 MPa
F_max: 1055.6 N
Strain_max: 24.2%

HECKEL:
  K = 0.0508 MPa⁻¹
  σy = 19.70 MPa
  R² = 0.9460

KAWAKITA:
  a = 0.9428
  b = 1.6243 MPa⁻¹
  Py = 0.62 MPa
  Fy = 1409.9 N
  R² = 0.8356

FILE:
  filterperlite atm 425.11.25-14.05.59.xlsx
```

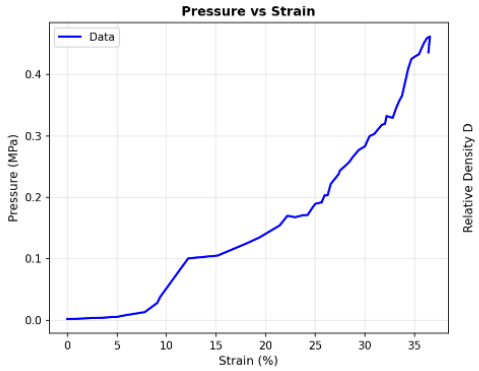

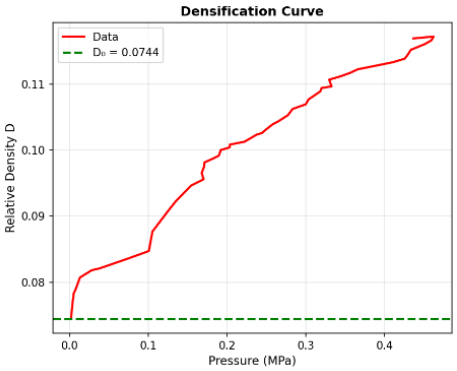

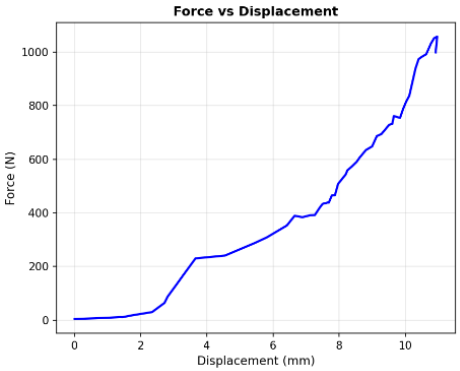

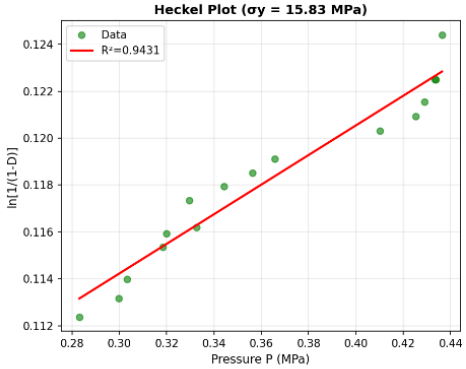

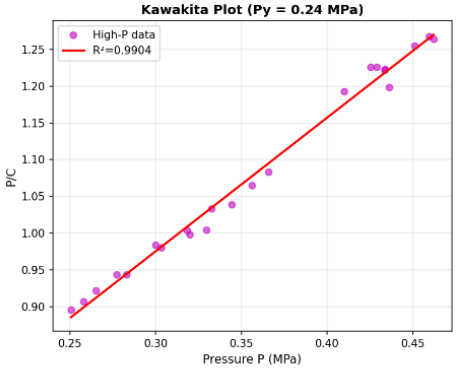


```
MATERIAL: Filtered perlite
ρ_true: 2.2 g/cm³
Mass: 11.25 g
h₀: 147.95 mm

DATA POINTS: 51
D₀: 0.0744
D_final: 0.1173
P_max: 0.46 MPa
F_max: 1058.2 N
Strain_max: 36.6%

HECKEL:
  K = 0.0632 MPa⁻¹
  σy = 15.83 MPa
  R² = 0.9431

KAWAKITA:
  a = 2.3232
  b = 4.2210 MPa⁻¹
  Py = 0.24 MPa
  Fy = 542.6 N
  R² = 0.9904

FILE:
  filterperlite atm 525.11.25-14.17.31.xlsx
```

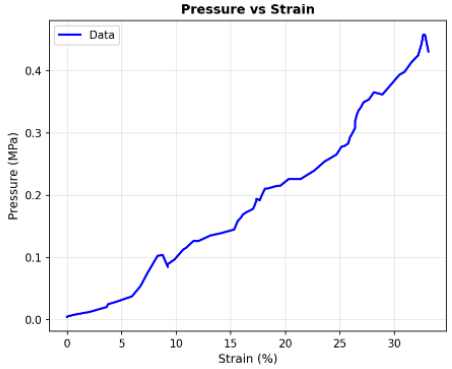

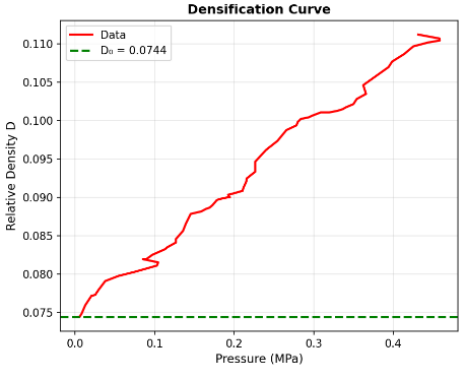

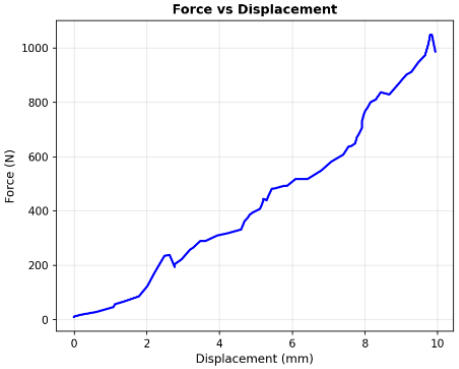

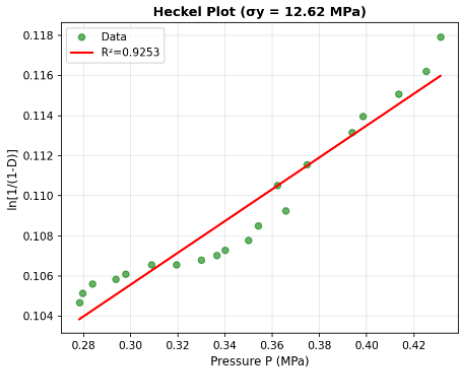

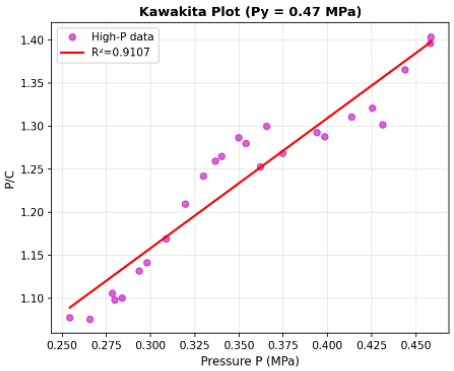


```
MATERIAL: Filtered perlite
ρ_true: 2.2 g/cm³
Mass: 11.25 g
h₀: 178.42 mm

DATA POINTS: 82
D₀: 0.0744
D_final: 0.1112
P_max: 0.46 MPa
F_max: 1049.8 N
Strain_max: 33.1%

HECKEL:
  K = 0.0793 MPa⁻¹
  σy = 12.62 MPa
  R² = 0.9253

KAWAKITA:
  a = 1.4189
  b = 2.1441 MPa⁻¹
  Py = 0.47 MPa
  Fy = 1068.2 N
  R² = 0.9107

FILE:
  filterperlite atm 625.11.25-13.47.12.xlsx
```

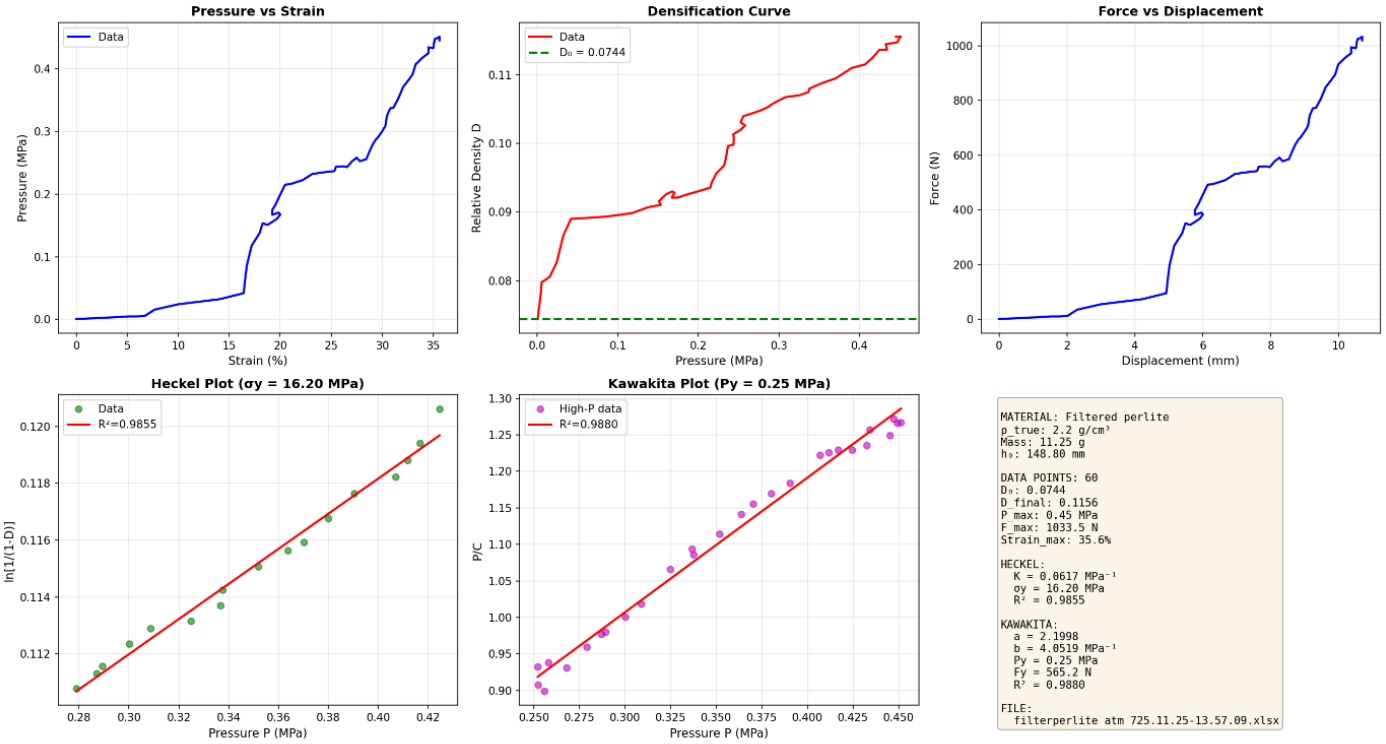
Pressure vs Strain
Data
Pressure (MPa)
Strain (%)
Densification Curve
Data
D₀ = 0.0744
Relative Density D
Pressure (MPa)
Force vs Displacement
Force (N)
Displacement (mm)
Heckel Plot (σy = 16.20 MPa)
Data
R²=0.9855
ln[1/(1-D)]
Pressure P (MPa)
Kawakita Plot (Py = 0.25 MPa)
High-P data
R²=0.9880
P/C
Pressure P (MPa)
MATERIAL: Filtered perlite
ρ_true: 2.2 g/cm³
Mass: 11.25 g
h₀: 148.80 mm
DATA POINTS: 60
D₀: 0.0744
D_final: 0.1156
P max: 0.45 MPa
F_max: 1033.5 N
Strain_max: 35.6%
HECKEL:
K = 0.0617 MPa⁻¹
σy = 16.20 MPa
R² = 0.9855
KAWAKITA:
a = 2.1998
b = 4.0519 MPa⁻¹
Py = 0.25 MPa
Fy = 565.2 N
R² = 0.9880
FILE:
filterperlite atm 725.11.25-13.57.09.xlsx

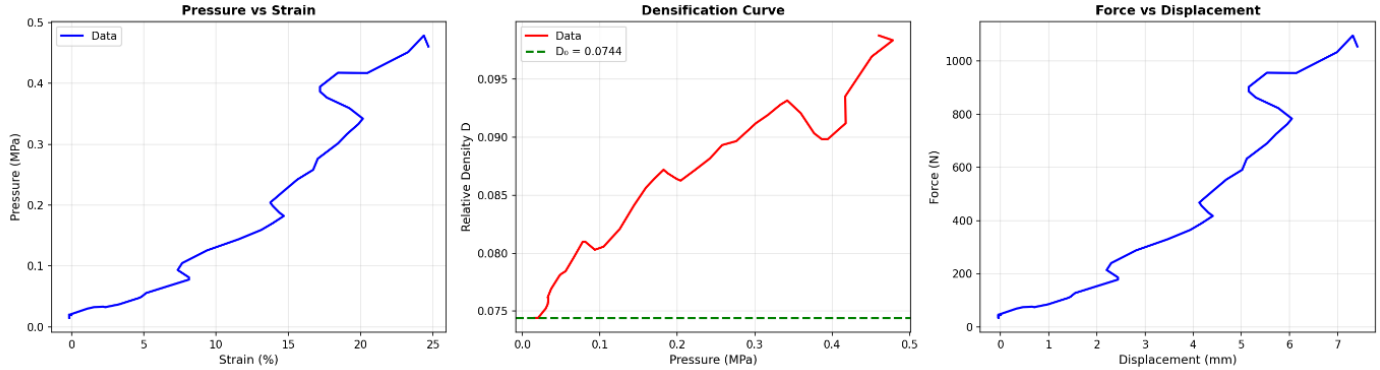

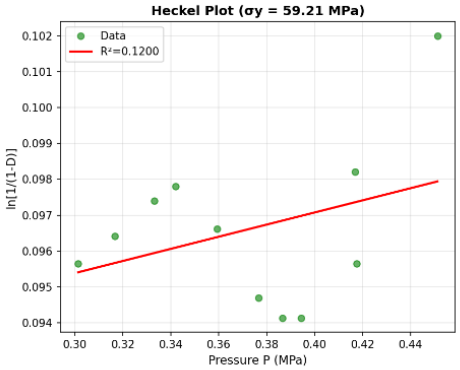

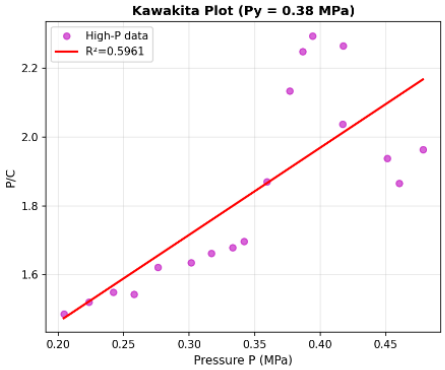


```
MATERIAL: Filtered perlite
ρ_true: 2.2 g/cm³
Mass: 11.25 g
h₀: 143.73 mm

DATA POINTS: 62
D₀: 0.0744
D_final: 0.0988
P_max: 0.48 MPa
F_max: 1095.8 N
Strain_max: 24.7%

HECKEL:
  K = 0.0169 MPa⁻¹
  σy = 59.21 MPa
  R² = 0.1200

KAWAKITA:
  a = 1.0451
  b = 2.6438 MPa⁻¹
  Py = 0.38 MPa
  Fy = 866.3 N
  R² = 0.5961

FILE:
  filterperlite vacuum 225.11.28-10.07.57.xlsx
```

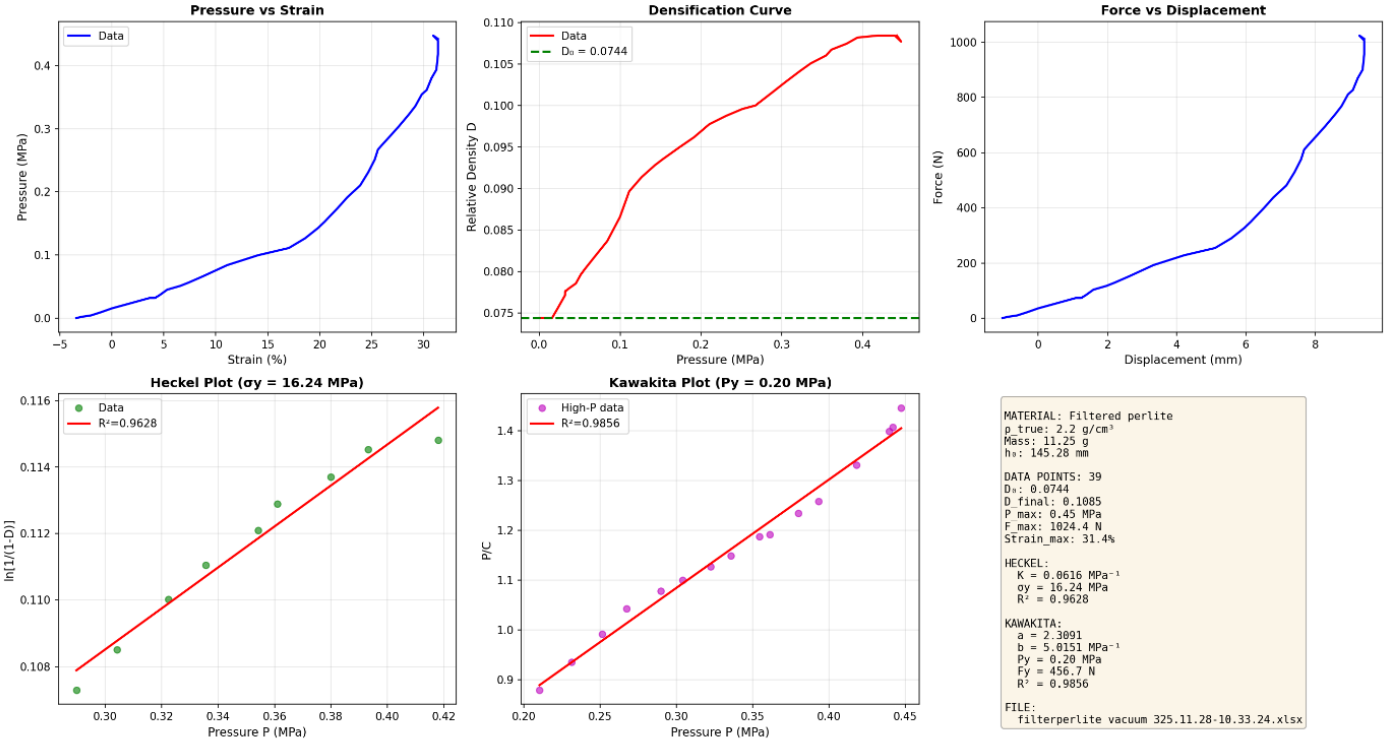
Pressure vs Strain
Data
Pressure (MPa)
Strain (%)
Densification Curve
Data
D₀ = 0.0744
Relative Density D
Pressure (MPa)
Force vs Displacement
Force (N)
Displacement (mm)
Heckel Plot (σy = 16.24 MPa)
Data
R²=0.9628
ln[1/(1-D)]
Pressure P (MPa)
Kawakita Plot (Py = 0.20 MPa)
High-P data
R²=0.9856
P/C
Pressure P (MPa)
MATERIAL: Filtered perlite
ρ_true: 2.2 g/cm³
Mass: 11.25 g
h₀: 145.28 mm
DATA POINTS: 39
D₀: 0.0744
D_final: 0.1085
P_max: 0.45 MPa
F_max: 1024.4 N
Strain_max: 31.4%
HECKEL:
K = 0.0616 MPa⁻¹
σy = 16.24 MPa
R² = 0.9628
KAWAKITA:
a = 2.3091
b = 5.0151 MPa⁻¹
Py = 0.20 MPa
Fy = 456.7 N
R² = 0.9856
FILE:
filterperlite vacuum 325.11.28-10.33.24.xlsx

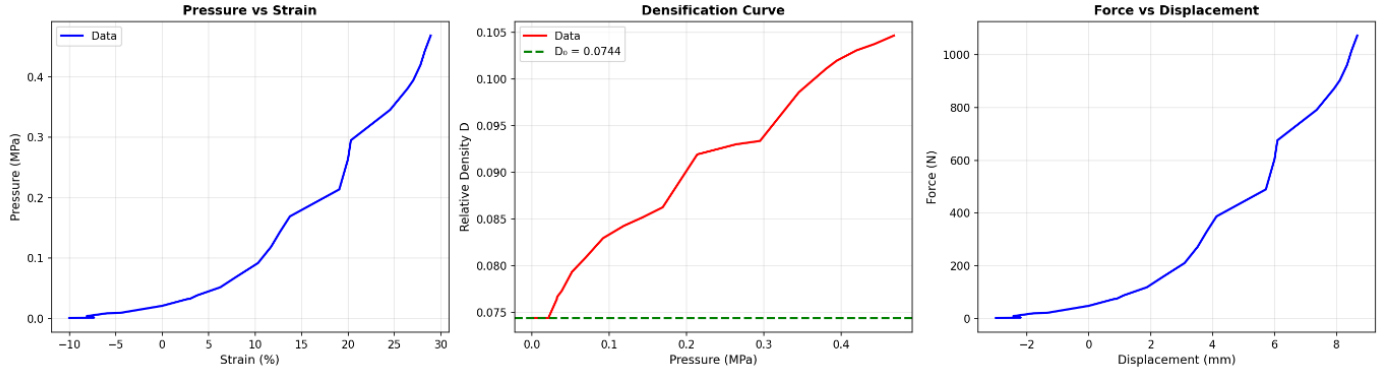


```
MATERIAL: Filtered perlite
ρ_true: 2.2 g/cm³
Mass: 11.25 g
h₀: 144.81 mm

DATA POINTS: 24
D₀: 0.0744
D_final: 0.1046
P_max: 0.47 MPa
F_max: 1072.9 N
Strain_max: 28.9%

HECKEL:
  K = 0.0782 MPa⁻¹
  σy = 12.79 MPa
  R² = 0.9543

KAWAKITA:
  a = 1.1503
  b = 1.8105 MPa⁻¹
  Py = 0.55 MPa
  Fy = 1265.0 N
  R² = 0.8549

FILE:
  filterperlite vacuum 425.12.01-12.08.31.xlsx
```

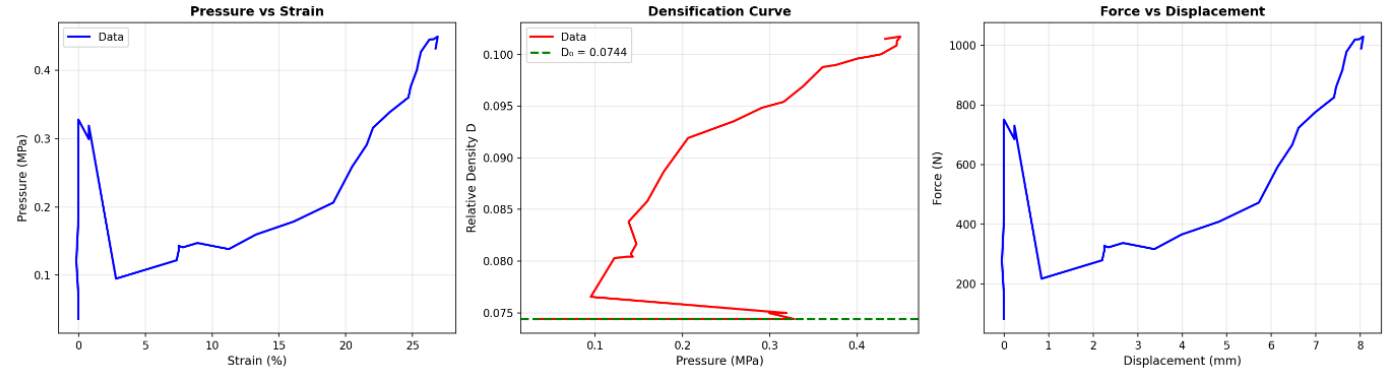

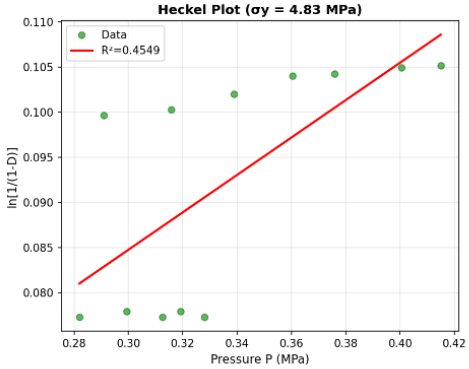

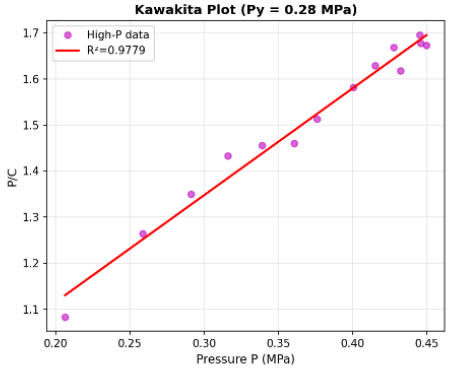


```
MATERIAL: Filtered perlite
ρ_true: 2.2 g/cm³
Mass: 11.25 g
h₀: 146.03 mm

DATA POINTS: 35
D₀: 0.0744
D_final: 0.1017
P_max: 0.45 MPa
F_max: 1029.8 N
Strain_max: 26.9%

HECKEL:
  K = 0.2071 MPa⁻¹
  σy = 4.83 MPa
  R² = 0.4549

KAWAKITA:
  a = 1.5345
  b = 3.5606 MPa⁻¹
  Py = 0.28 MPa
  Fy = 643.2 N
  R² = 0.9779

FILE:
  filterperlite cryo 225.12.12-13.00.31.xlsx
```

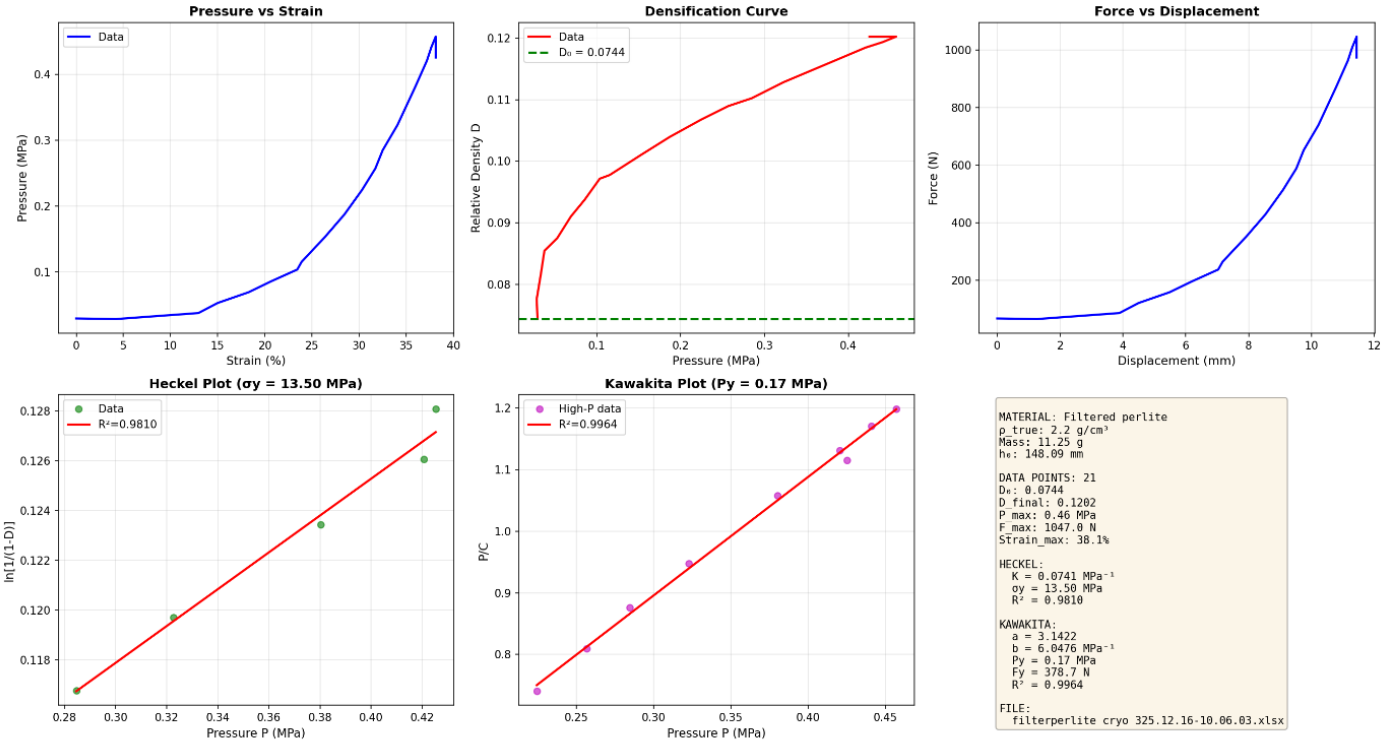


```
MATERIAL: Filtered perlite
ρ_true: 2.2 g/cm³
Mass: 11.25 g
h₀: 148.09 mm

DATA POINTS: 21
D₀: 0.0744
D_final: 0.1202
P_max: 0.46 MPa
F_max: 1047.0 N
Strain_max: 38.1%

HECKEL:
  K = 0.0741 MPa⁻¹
  σy = 13.50 MPa
  R² = 0.9810

KAWAKITA:
  a = 3.1422
  b = 6.0476 MPa⁻¹
  Py = 0.17 MPa
  Fy = 378.7 N
  R² = 0.9964

FILE:
  filterperlite cryo 325.12.16-10.06.03.xlsx
```

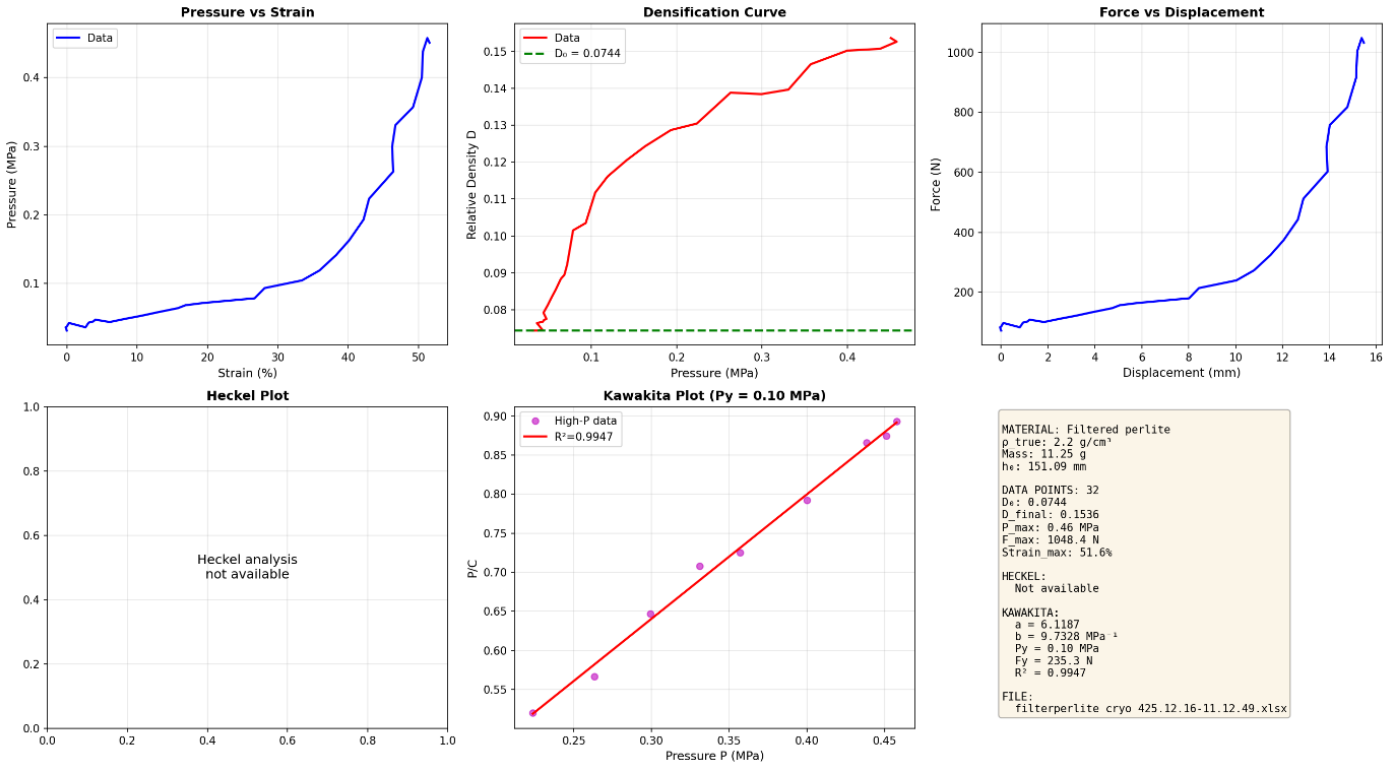


```
MATERIAL: Filtered perlite
ρ_true: 2.2 g/cm³
Mass: 11.25 g
h₀: 151.09 mm

DATA POINTS: 32
D₀: 0.0744
D_final: 0.1536
P_max: 0.46 MPa
F_max: 1048.4 N
Strain_max: 51.6%

HECKEL:
  Not available

KAWAKITA:
  a = 6.1187
  b = 9.7328 MPa⁻¹
  Py = 0.10 MPa
  Fy = 235.3 N
  R² = 0.9947

FILE:
  filterperlite cryo 425.12.16-11.12.49.xlsx
```

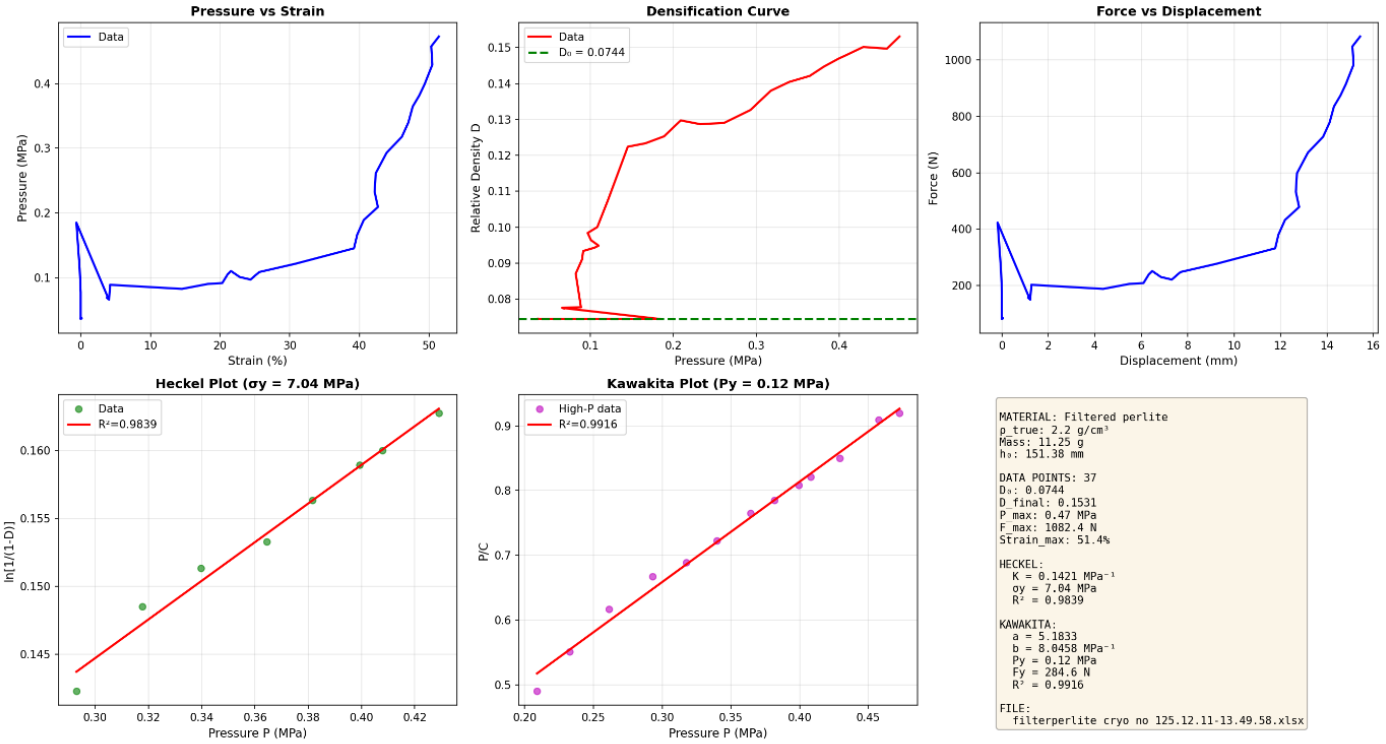
Pressure vs Strain
Data
Pressure (MPa)
Strain (%)
Densification Curve
Data
D₀ = 0.0744
Relative Density D
Pressure (MPa)
Force vs Displacement
Force (N)
Displacement (mm)
Heckel Plot (σy = 7.04 MPa)
Data
R²=0.9839
ln[1/(1-D)]
Pressure P (MPa)
Kawakita Plot (Py = 0.12 MPa)
High-P data
R²=0.9916
P/C
Pressure P (MPa)
MATERIAL: Filtered perlite
ρ_true: 2.2 g/cm³
Mass: 11.25 g
h₀: 151.38 mm
DATA POINTS: 37
D₀: 0.0744
D_final: 0.1531
P_max: 0.47 MPa
F_max: 1082.4 N
Strain_max: 51.4%
HECKEL:
K = 0.1421 MPa⁻¹
σy = 7.04 MPa
R² = 0.9839
KAWAKITA:
a = 5.1833
b = 8.0458 MPa⁻¹
Py = 0.12 MPa
Fy = 284.6 N
R² = 0.9916
FILE:
filterperlite cryo no 125.12.11-13.49.58.xlsx

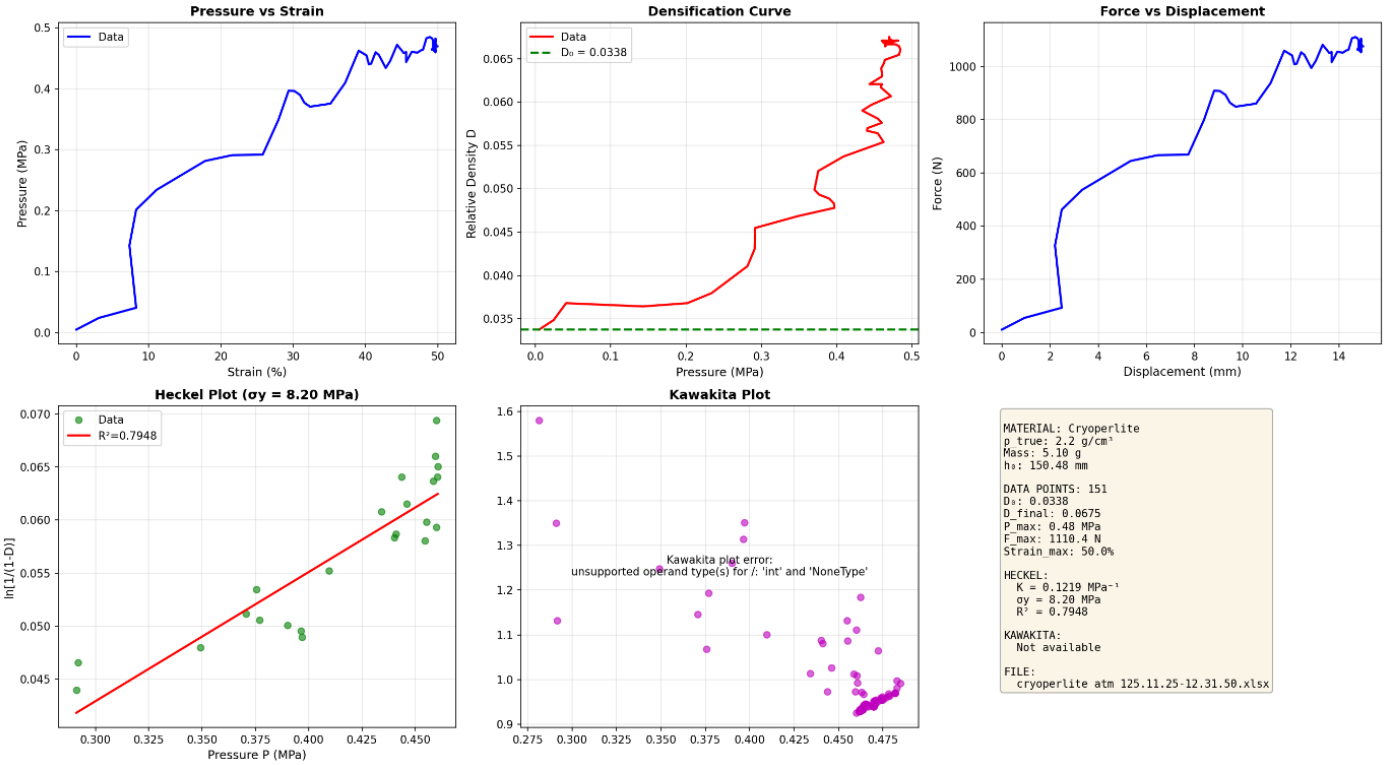


```
MATERIAL: Cryoperlite
ρ_true: 2.2 g/cm³
Mass: 5.10 g
h₀: 150.48 mm

DATA POINTS: 151
D₀: 0.0338
D_final: 0.0675
P_max: 0.48 MPa
F_max: 1110.4 N
Strain_max: 50.0%

HECKEL:
  K = 0.1219 MPa⁻¹
  σy = 8.20 MPa
  R² = 0.7948

KAWAKITA:
  Not available

FILE:
  cryoperlite atm 125.11.25-12.31.50.xlsx
```

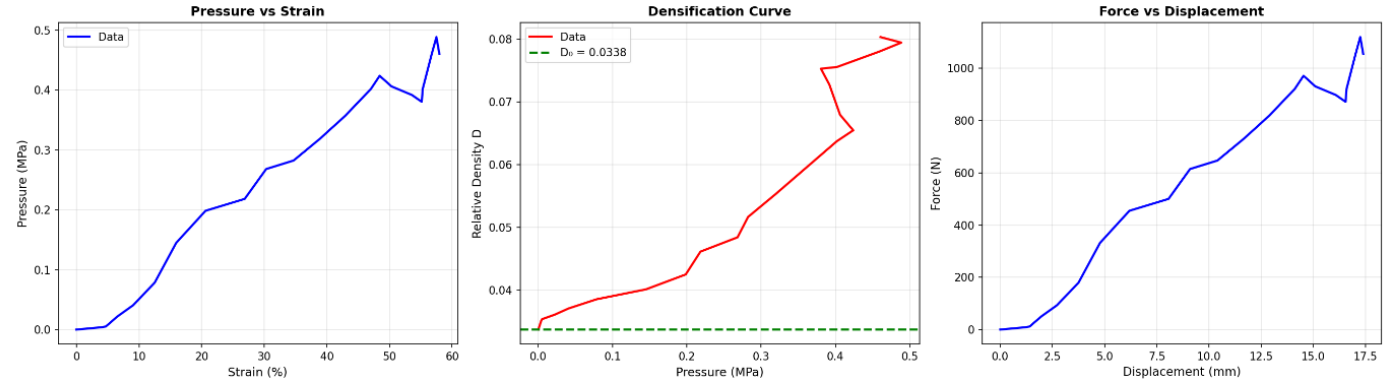

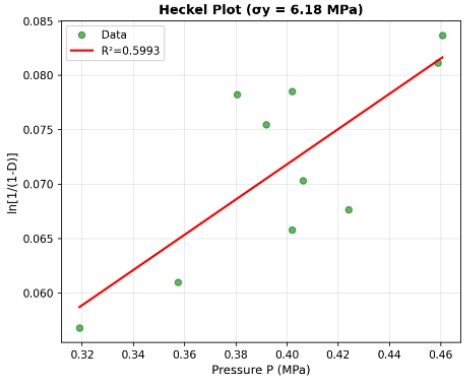

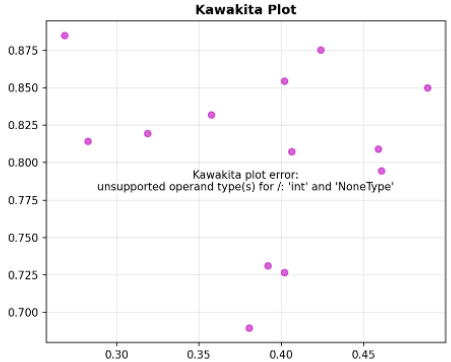


```
MATERIAL: Cryoperlite
ρ_true: 2.2 g/cm³
Mass: 5.10 g
h₀: 152.22 mm

DATA POINTS: 22
D₀: 0.0338
D_final: 0.0803
P_max: 0.49 MPa
F_max: 1119.1 N
Strain_max: 58.0%

HECKEL:
  K = 0.1618 MPa⁻¹
  σy = 6.18 MPa
  R² = 0.5993

KAWAKITA:
  Not available

FILE:
  cryoperlite atm 225.11.25-15.10.16.xlsx
```

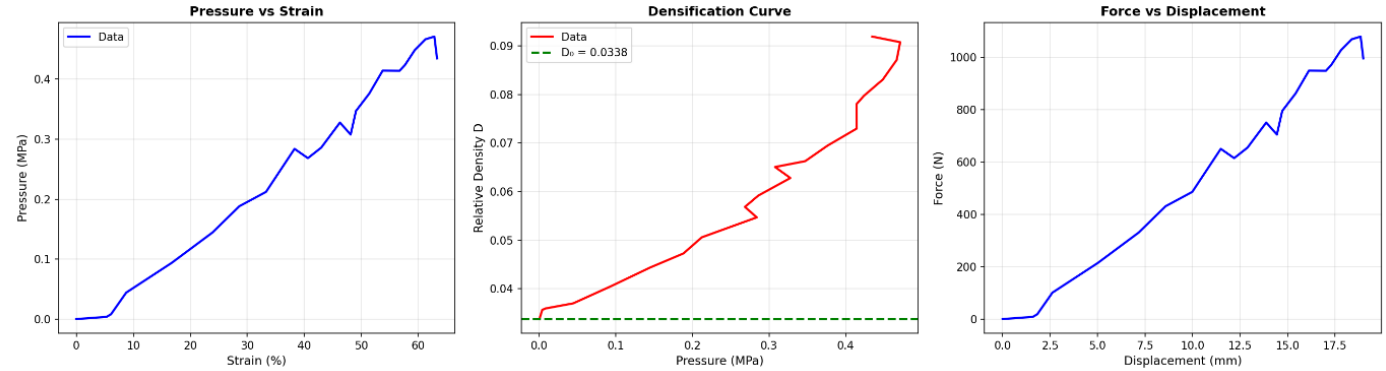

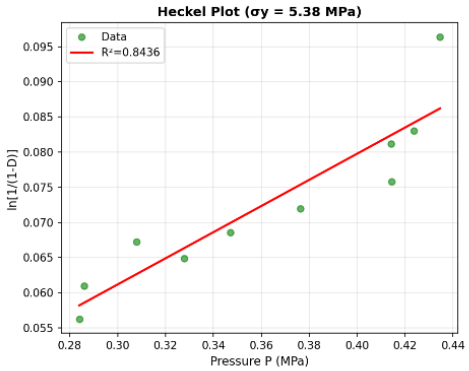

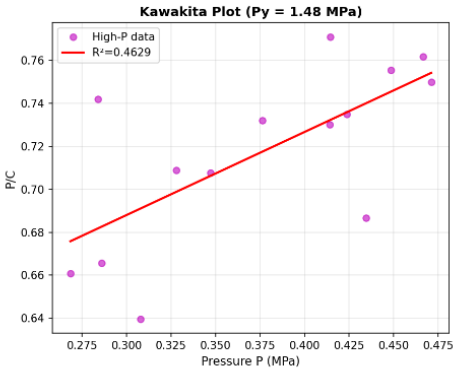


```
MATERIAL: Cryoperlite
ρ_true: 2.2 g/cm³
Mass: 5.10 g
h₀: 152.59 mm

DATA POINTS: 22
D₀: 0.0338
D_final: 0.0919
P_max: 0.47 MPa
F_max: 1078.8 N
Strain_max: 63.3%

HECKEL:
  K = 0.1860 MPa⁻¹
  σy = 5.38 MPa
  R² = 0.8436

KAWAKITA:
  a = 1.7481
  b = 0.6756 MPa⁻¹
  Py = 1.48 MPa
  Fy = 3389.9 N
  R² = 0.4629

FILE:
  cryoperlite atm 325.11.25-15.23.08.xlsx
```

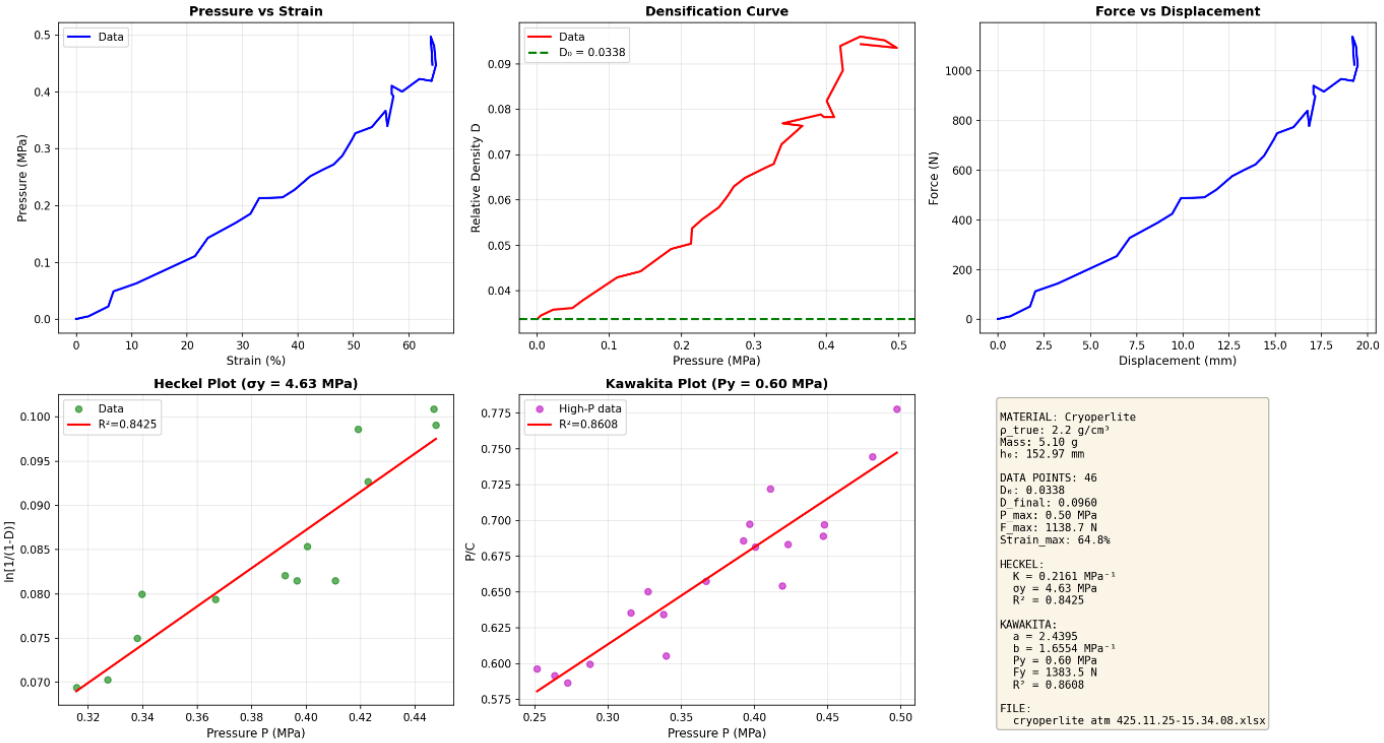


```
MATERIAL: Cryoperlite
ρ_true: 2.2 g/cm³
Mass: 5.10 g
h₀: 152.97 mm

DATA POINTS: 46
D₀: 0.0338
D_final: 0.0960
P_max: 0.50 MPa
F_max: 1138.7 N
Strain_max: 64.8%

HECKEL:
  K = 0.2161 MPa⁻¹
  σy = 4.63 MPa
  R² = 0.8425

KAWAKITA:
  a = 2.4395
  b = 1.6554 MPa⁻¹
  Py = 0.60 MPa
  Fy = 1383.5 N
  R² = 0.8608

FILE:
  cryoperlite atm 425.11.25-15.34.08.xlsx
```

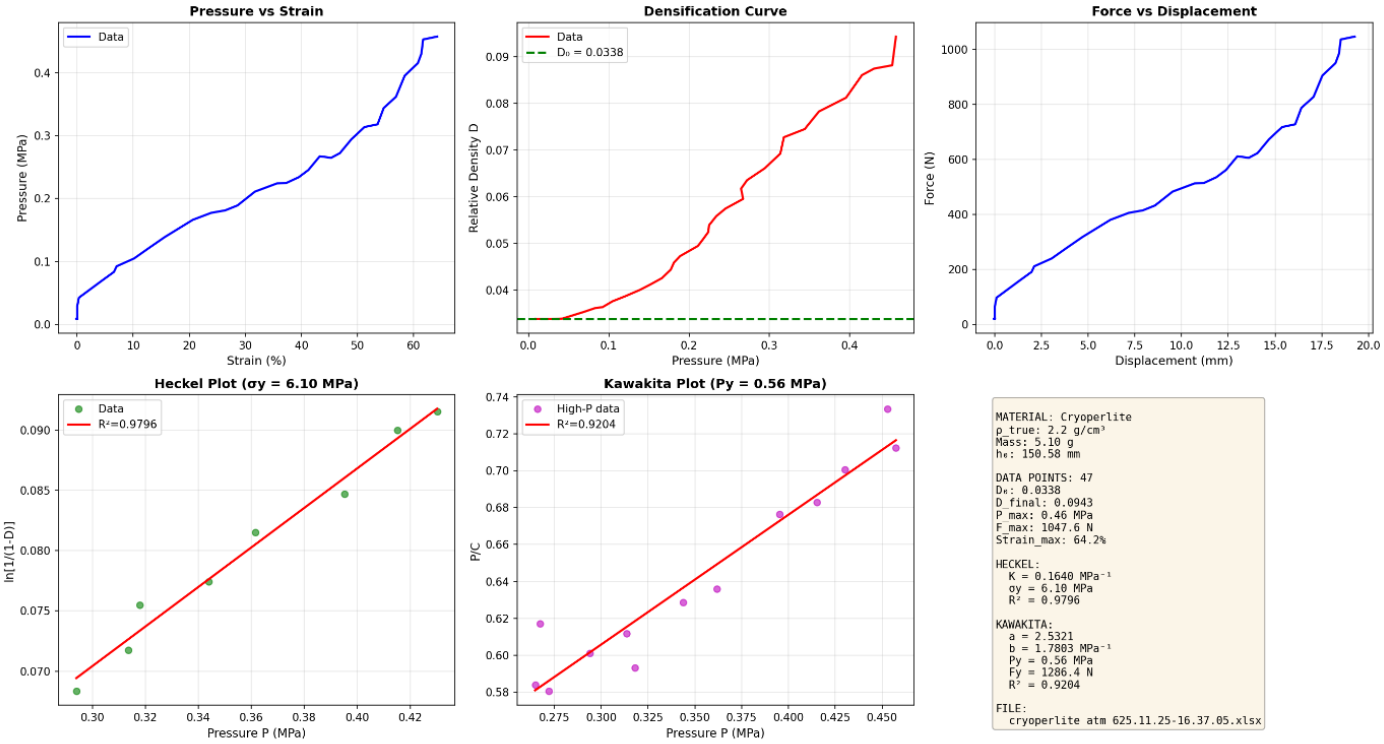
Pressure vs Strain
Data
Pressure (MPa)
Strain (%)
Densification Curve
Data
Dₕ = 0.0338
Relative Density D
Pressure (MPa)
Force vs Displacement
Force (N)
Displacement (mm)
Heckel Plot (σy = 6.10 MPa)
Data
R²=0.9796
ln[1/(1-D)]
Pressure P (MPa)
Kawakita Plot (Py = 0.56 MPa)
High-P data
R²=0.9204
P/C
Pressure P (MPa)
MATERIAL: Cryoperlite
ρ_true: 2.2 g/cm³
Mass: 5.10 g
hₑ: 150.58 mm
DATA POINTS: 47
Dᵢ: 0.0338
D_final: 0.0943
P_max: 0.46 MPa
F_max: 1047.6 N
Strain_max: 64.2%
HECKEL:
K = 0.1640 MPa⁻¹
σy = 6.10 MPa
R² = 0.9796
KAWAKITA:
a = 2.5321
b = 1.7803 MPa⁻¹
Py = 0.56 MPa
Fy = 1286.4 N
R² = 0.9204
FILE:
cryoperlite atm 625.11.25-16.37.05.xlsx

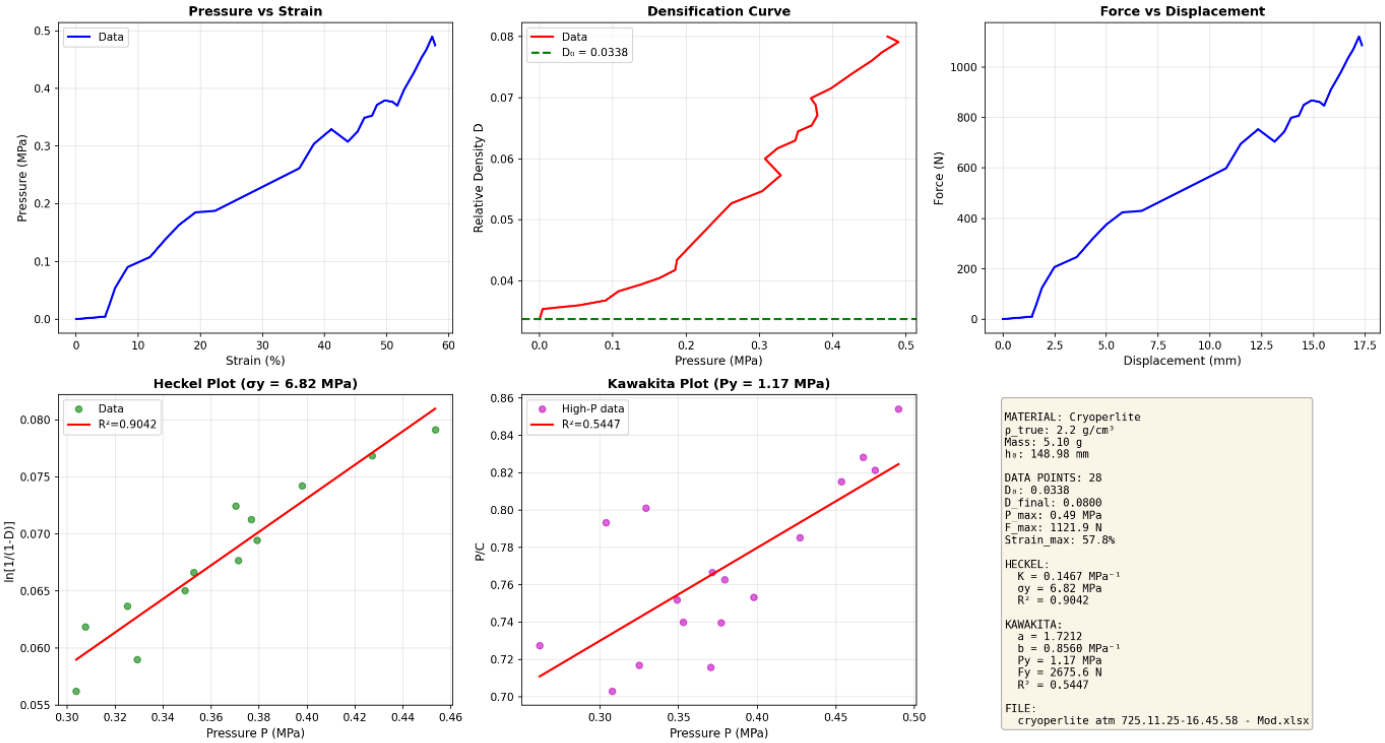
Pressure vs Strain
Data
Pressure (MPa)
Strain (%)
Densification Curve
Data
D₀ = 0.0338
Relative Density D
Pressure (MPa)
Force vs Displacement
Force (N)
Displacement (mm)
Heckel Plot (σy = 6.82 MPa)
Data
R²=0.9042
ln[1/(1-D)]
Pressure P (MPa)
Kawakita Plot (Py = 1.17 MPa)
High-P data
R²=0.5447
P/C
Pressure P (MPa)
MATERIAL: Cryoperlite
ρ_true: 2.2 g/cm³
Mass: 5.10 g
h₀: 148.98 mm
DATA POINTS: 28
D₀: 0.0338
D_final: 0.0800
P_max: 0.49 MPa
F_max: 1121.9 N
Strain_max: 57.8%
HECKEL:
K = 0.1467 MPa⁻¹
σy = 6.82 MPa
R² = 0.9042
KAWAKITA:
a = 1.7212
b = 0.8560 MPa⁻¹
Py = 1.17 MPa
Fy = 2675.6 N
R² = 0.5447
FILE:
cryoperlite atm 725.11.25-16.45.58 - Mod.xlsx

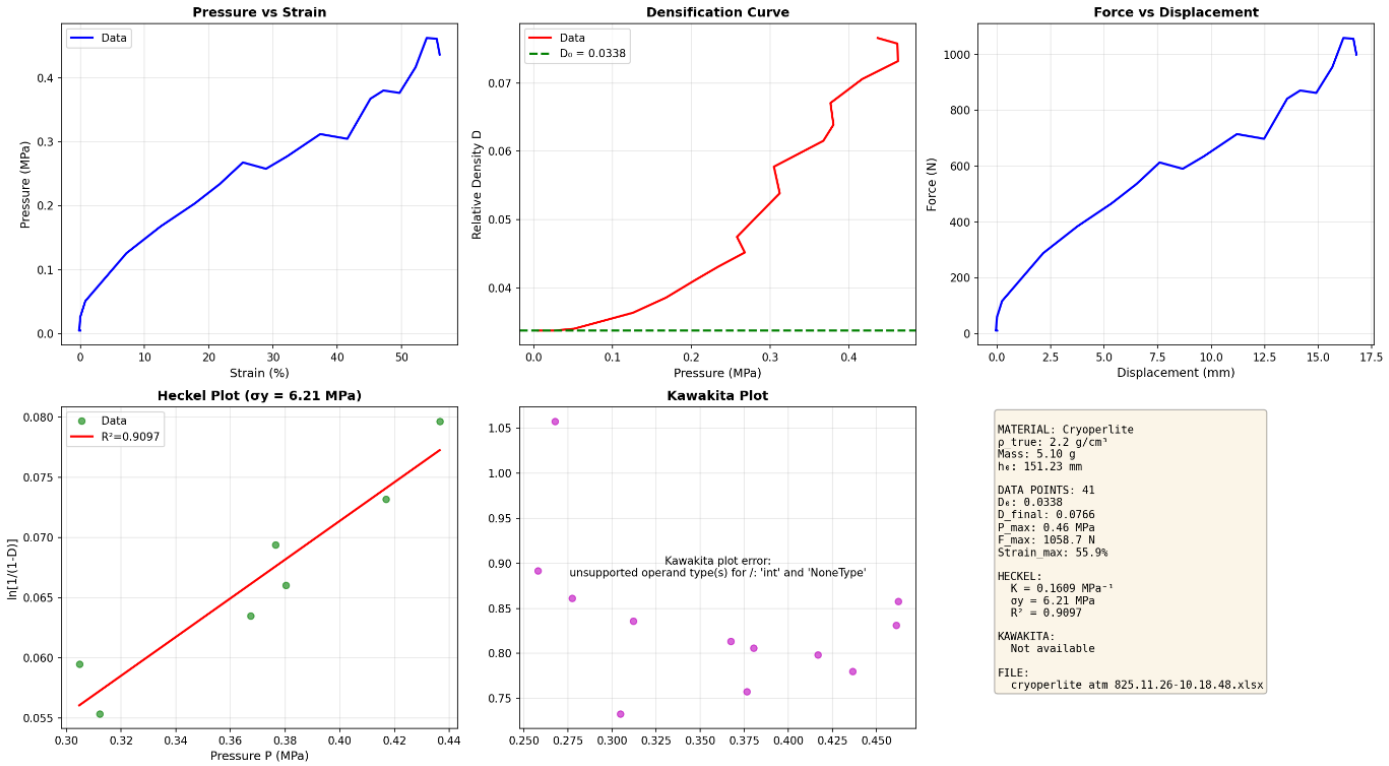
Pressure vs Strain
Data
Pressure (MPa)
Strain (%)
Densification Curve
Data
D₀ = 0.0338
Relative Density D
Pressure (MPa)
Force vs Displacement
Force (N)
Displacement (mm)
Heckel Plot (σy = 6.21 MPa)
Data
R²=0.9097
ln[1/(1-D)]
Pressure P (MPa)
Kawakita Plot
Kawakita plot error:
unsupported operand type(s) for /: 'int' and 'NoneType'
MATERIAL: Cryoperlite
ρ true: 2.2 g/cm³
Mass: 5.10 g
hₑ: 151.23 mm
DATA POINTS: 41
Dₑ: 0.0338
D_final: 0.0766
P_max: 0.46 MPa
F_max: 1058.7 N
Strain_max: 55.9%
HECKEL:
K = 0.1609 MPa⁻¹
σy = 6.21 MPa
R² = 0.9097
KAWAKITA:
Not available
FILE:
cryoperlite atm 825.11.26-10.18.48.xlsx

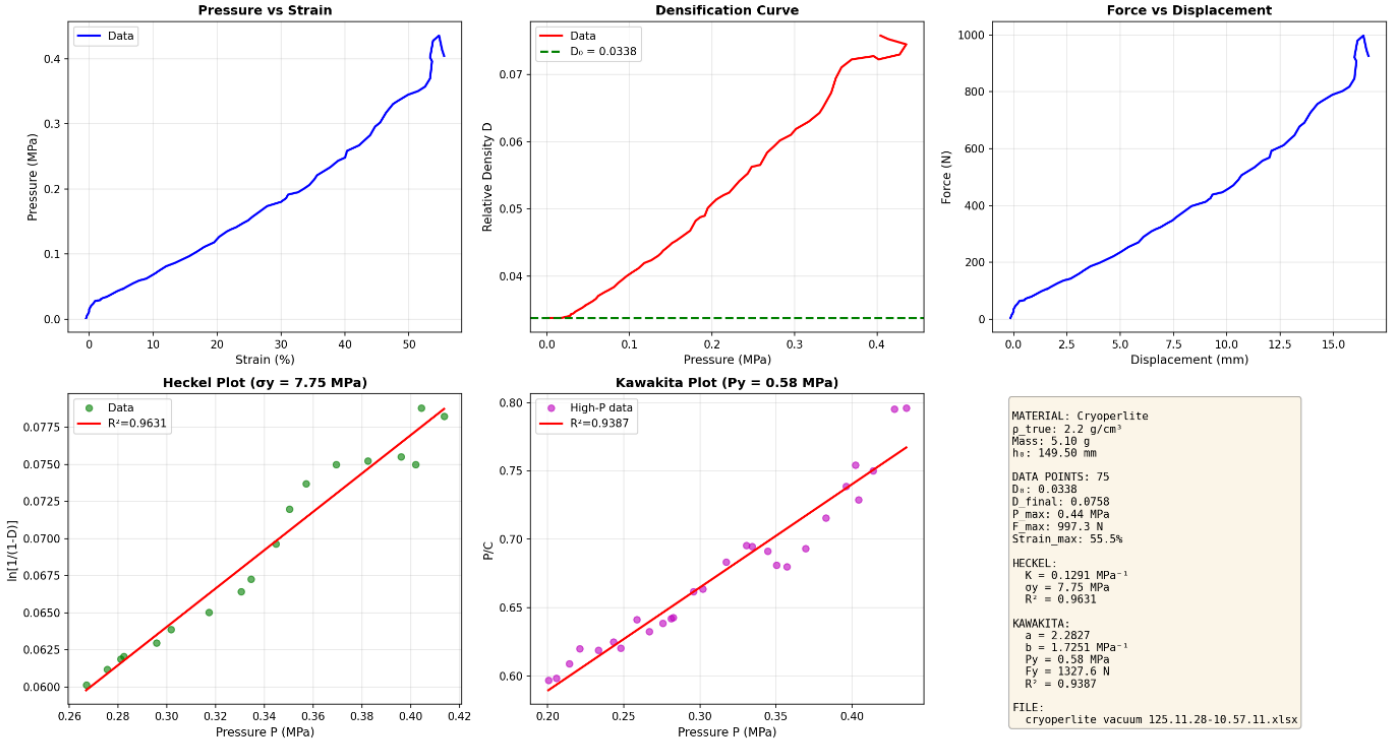


```
MATERIAL: Cryoperlite
ρ_true: 2.2 g/cm³
Mass: 5.10 g
h₀: 149.50 mm

DATA POINTS: 75
D₀: 0.0338
D_final: 0.0758
P_max: 0.44 MPa
F_max: 997.3 N
Strain_max: 55.5%

HECKEL:
  K = 0.1291 MPa⁻¹
  σy = 7.75 MPa
  R² = 0.9631

KAWAKITA:
  a = 2.2827
  b = 1.7251 MPa⁻¹
  Py = 0.58 MPa
  Fy = 1327.6 N
  R² = 0.9387

FILE:
  cryoperlite vacuum 125.11.28-10.57.11.xlsx
```

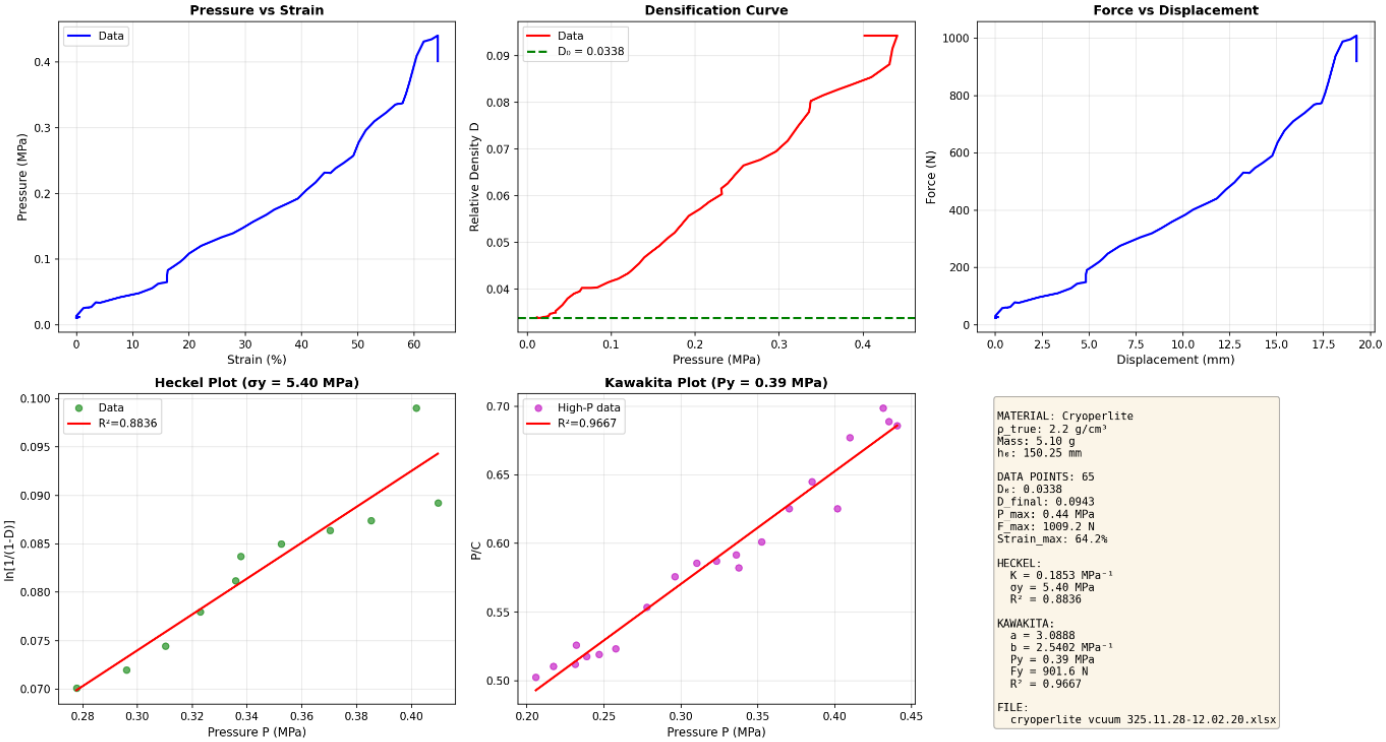
Pressure vs Strain
Data
Pressure (MPa)
Strain (%)
Densification Curve
Data
D₀ = 0.0338
Relative Density D
Pressure (MPa)
Force vs Displacement
Force (N)
Displacement (mm)
Heckel Plot (σy = 5.40 MPa)
Data
R²=0.8836
ln[1/(1-D)]
Pressure P (MPa)
Kawakita Plot (Py = 0.39 MPa)
High-P data
R²=0.9667
P/C
Pressure P (MPa)
MATERIAL: Cryoperlite
ρ_true: 2.2 g/cm³
Mass: 5.10 g
h₀: 150.25 mm
DATA POINTS: 65
D₀: 0.0338
D_final: 0.0943
P_max: 0.44 MPa
F_max: 1009.2 N
Strain_max: 64.2%
HECKEL:
K = 0.1853 MPa⁻¹
σy = 5.40 MPa
R² = 0.8836
KAWAKITA:
a = 3.0888
b = 2.5402 MPa⁻¹
Py = 0.39 MPa
Fy = 901.6 N
R² = 0.9667
FILE:
cryoperlite vcuum 325.11.28-12.02.20.xlsx

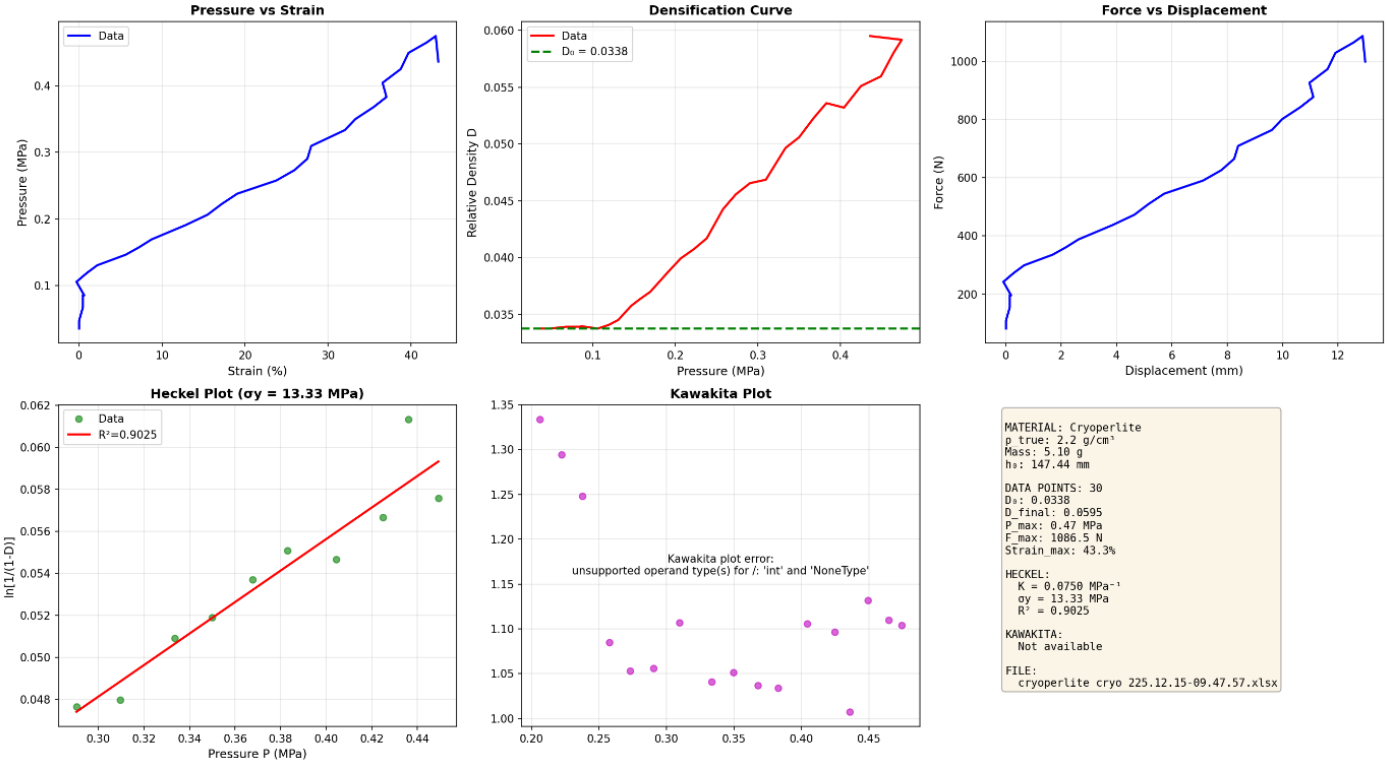


```
MATERIAL: Cryoperlite
ρ_true: 2.2 g/cm³
Mass: 5.10 g
h₀: 147.44 mm

DATA POINTS: 30
D₀: 0.0338
D_final: 0.0595
P_max: 0.47 MPa
F_max: 1086.5 N
Strain_max: 43.3%

HECKEL:
  K = 0.0750 MPa⁻¹
  σy = 13.33 MPa
  R² = 0.9025

KAWAKITA:
  Not available

FILE:
  cryoperlite cryo 225.12.15-09.47.57.xlsx
```

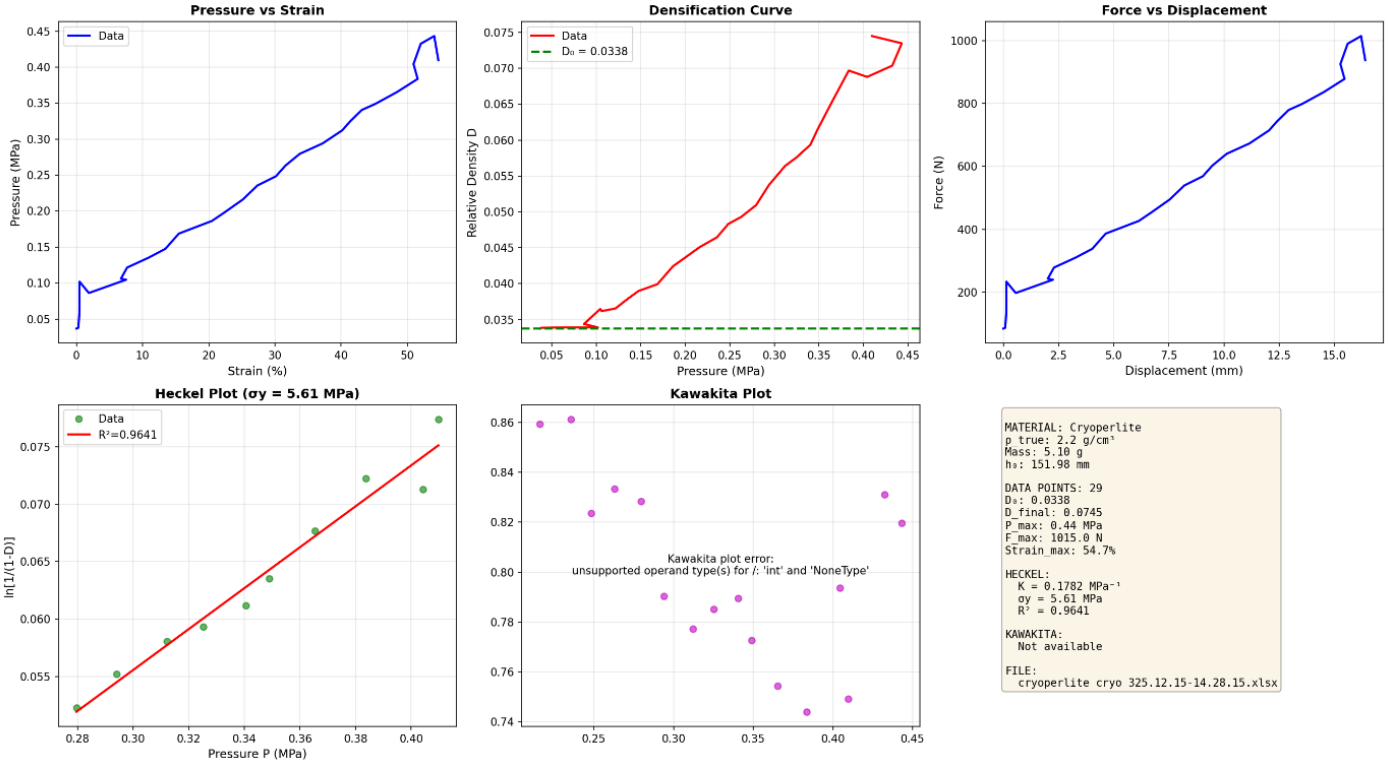


```
MATERIAL: Cryoperlite
ρ_true: 2.2 g/cm³
Mass: 5.10 g
h₀: 151.98 mm

DATA POINTS: 29
D₀: 0.0338
D_final: 0.0745
P_max: 0.44 MPa
F_max: 1015.0 N
Strain_max: 54.7%

HECKEL:
  K = 0.1782 MPa⁻¹
  σy = 5.61 MPa
  R² = 0.9641

KAWAKITA:
  Not available

FILE:
  cryoperlite cryo 325.12.15-14.28.15.xlsx
```

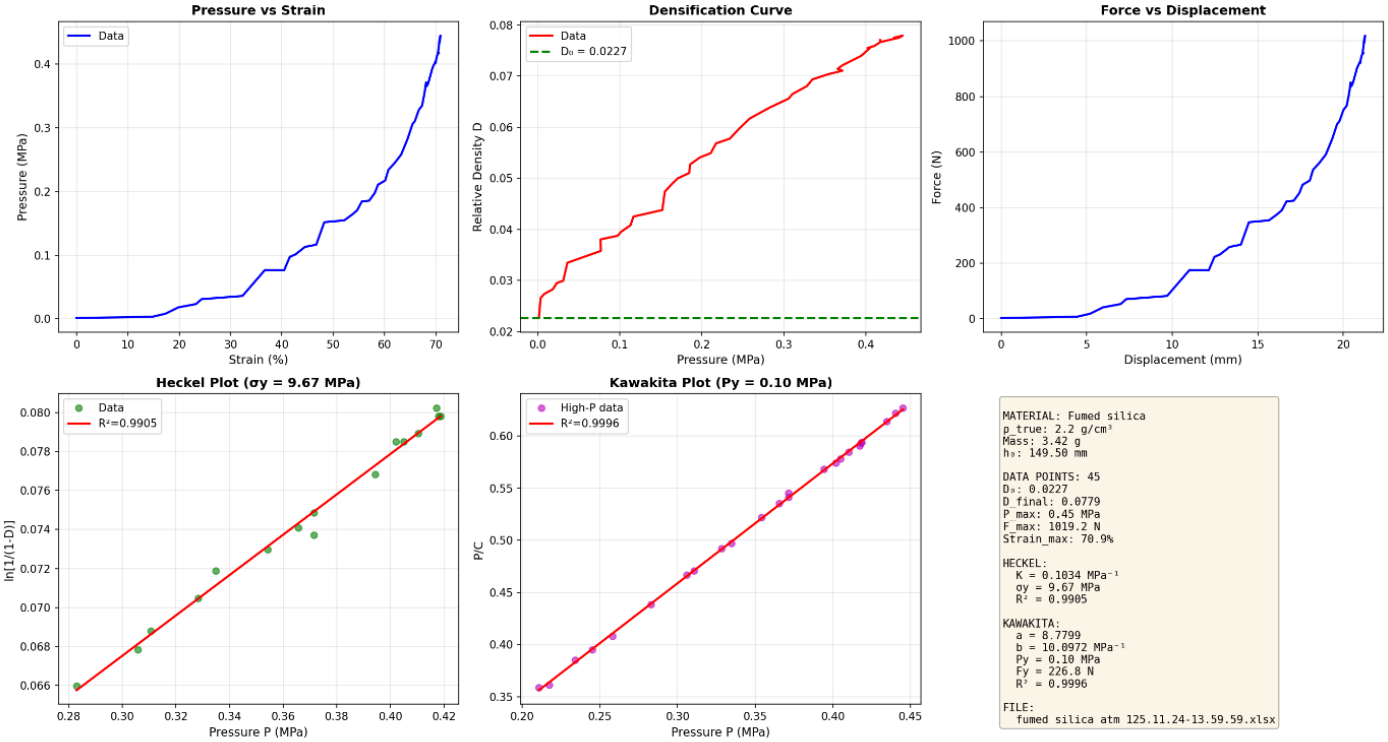


```
MATERIAL: Fumed silica
ρ_true: 2.2 g/cm³
Mass: 3.42 g
h₀: 149.50 mm

DATA POINTS: 45
D₀: 0.0227
D_final: 0.0779
P_max: 0.45 MPa
F_max: 1019.2 N
Strain_max: 70.9%

HECKEL:
  K = 0.1034 MPa⁻¹
  σy = 9.67 MPa
  R² = 0.9905

KAWAKITA:
  a = 8.7799
  b = 10.0972 MPa⁻¹
  Py = 0.10 MPa
  Fy = 226.8 N
  R² = 0.9996

FILE:
  fumed silica atm 125.11.24-13.59.59.xlsx
```

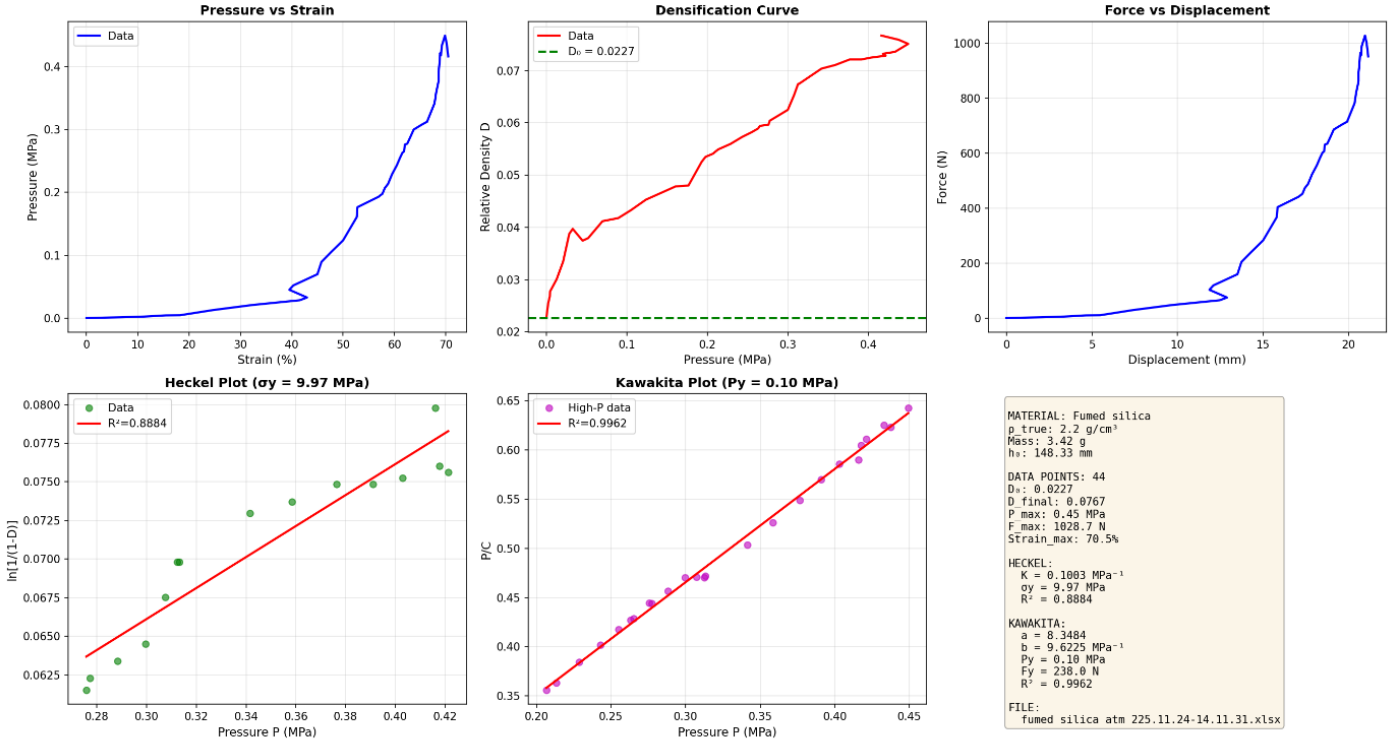


```
MATERIAL: Fumed silica
ρ_true: 2.2 g/cm³
Mass: 3.42 g
h₀: 148.33 mm

DATA POINTS: 44
D₀: 0.0227
D_final: 0.0767
P_max: 0.45 MPa
F_max: 1028.7 N
Strain_max: 70.5%

HECKEL:
  K = 0.1003 MPa⁻¹
  σy = 9.97 MPa
  R² = 0.8884

KAWAKITA:
  a = 8.3484
  b = 9.6225 MPa⁻¹
  Py = 0.10 MPa
  Fy = 238.0 N
  R² = 0.9962

FILE:
  fumed silica atm 225.11.24-14.11.31.xlsx
```

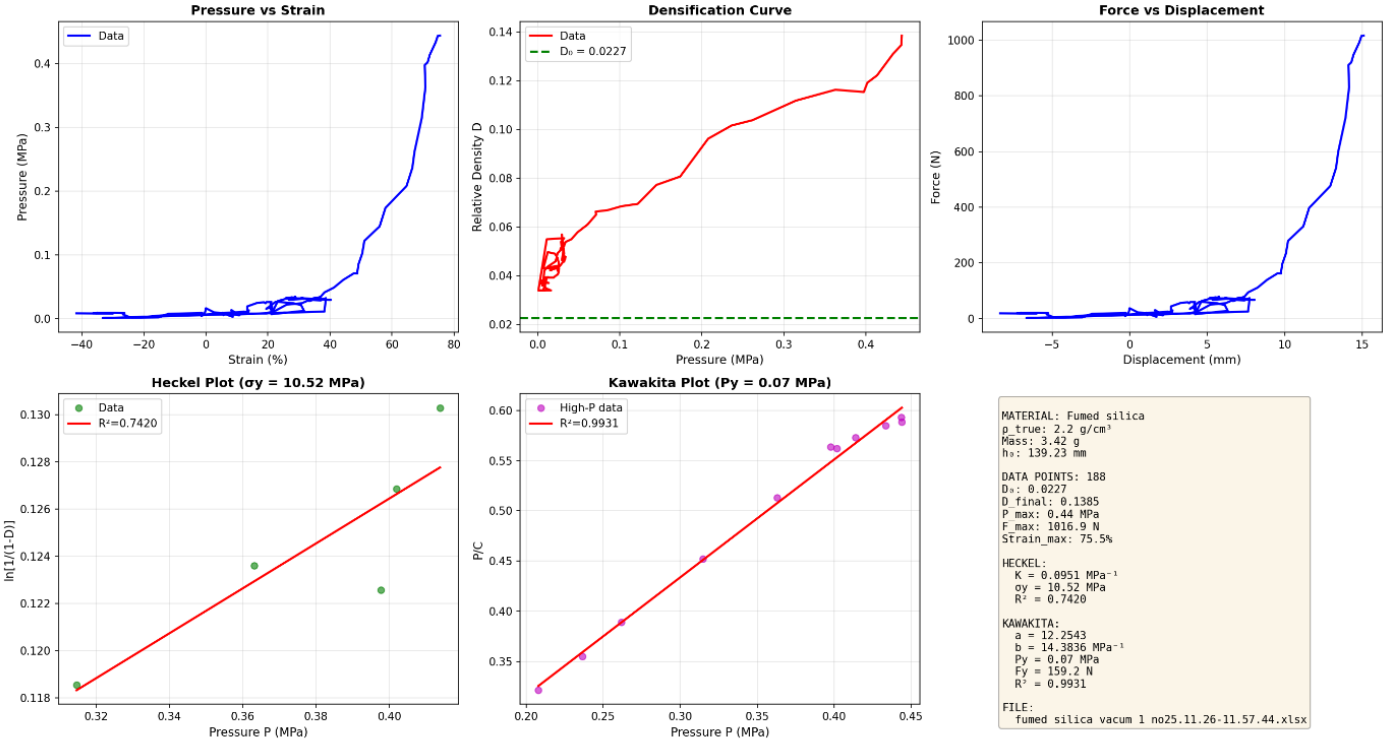


```
MATERIAL: Fumed silica
ρ_true: 2.2 g/cm³
Mass: 3.42 g
h₀: 139.23 mm

DATA POINTS: 188
D₀: 0.0227
D_final: 0.1385
P max: 0.44 MPa
F_max: 1016.9 N
Strain_max: 75.5%

HECKEL:
  K = 0.0951 MPa⁻¹
  σy = 10.52 MPa
  R² = 0.7420

KAWAKITA:
  a = 12.2543
  b = 14.3836 MPa⁻¹
  Py = 0.07 MPa
  Fy = 159.2 N
  R² = 0.9931

FILE:
  fumed silica vacum 1 no25.11.26-11.57.44.xlsx
```

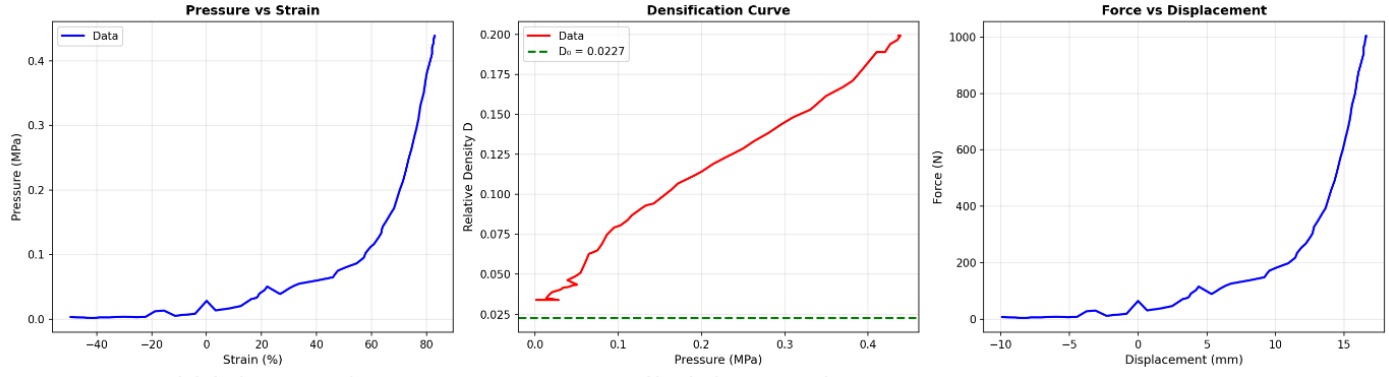


```
MATERIAL: Fumed silica
ρ_true: 2.2 g/cm³
Mass: 3.42 g
h₀: 140.83 mm

DATA POINTS: 66
D₀: 0.0227
D_final: 0.1995
P_max: 0.44 MPa
F_max: 1005.3 N
Strain_max: 83.0%

HECKEL:
  K = 0.4344 MPa⁻¹
  σy = 2.30 MPa
  R² = 0.9775

KAWAKITA:
  a = 11.8458
  b = 12.0657 MPa⁻¹
  Py = 0.08 MPa
  Fy = 189.8 N
  R² = 0.9992

FILE:
  fumed silica vacuum 125.11.26-13.36.28.xlsx
```

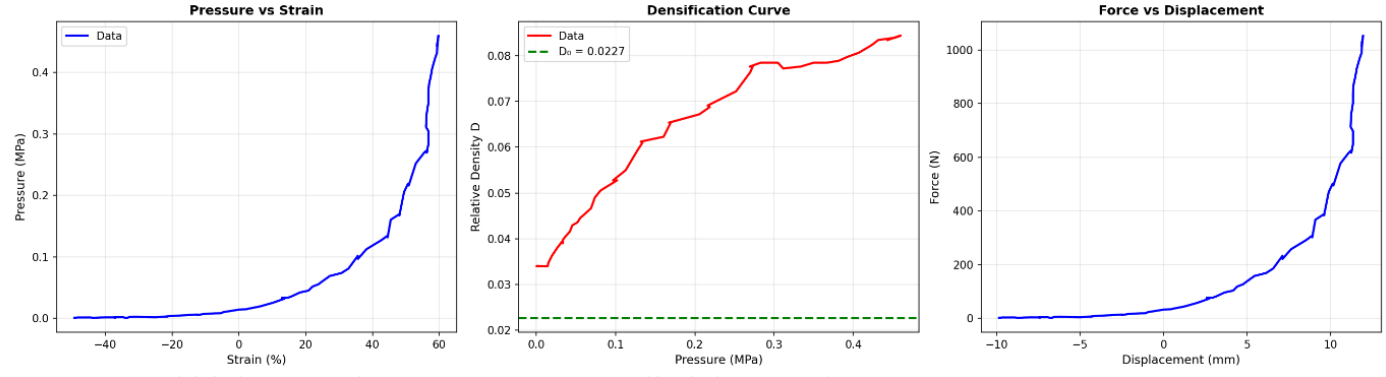

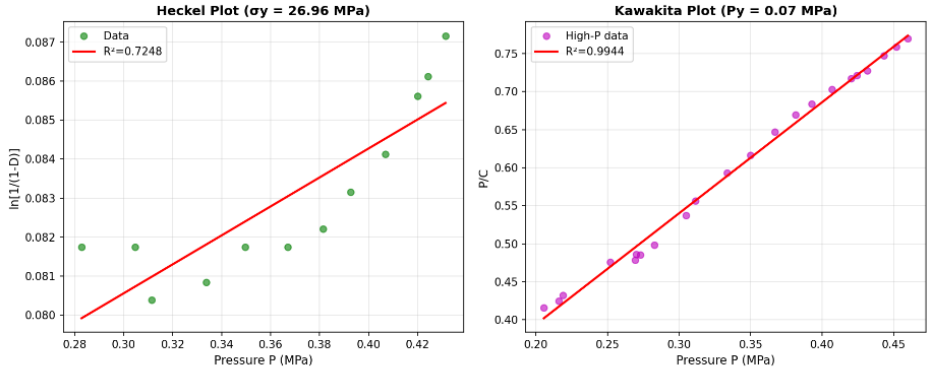


```
MATERIAL: Fumed silica
ρ_true: 2.2 g/cm³
Mass: 3.42 g
h₀: 136.75 mm

DATA POINTS: 89
D₀: 0.0227
D_final: 0.0844
P_max: 0.46 MPa
F_max: 1053.1 N
Strain_max: 59.8%

HECKEL:
  K = 0.0371 MPa⁻¹
  σy = 26.96 MPa
  R² = 0.7248

KAWAKITA:
  a = 9.8071
  b = 14.3205 MPa⁻¹
  Py = 0.07 MPa
  Fy = 159.9 N
  R² = 0.9944

FILE:
  fumed silica vacuum 225.11.26-14.12.45.xlsx
```

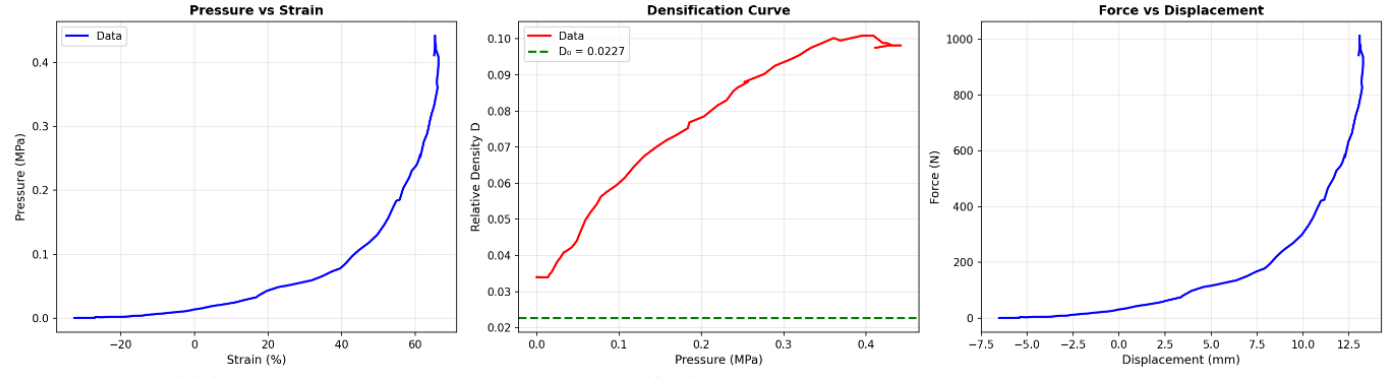

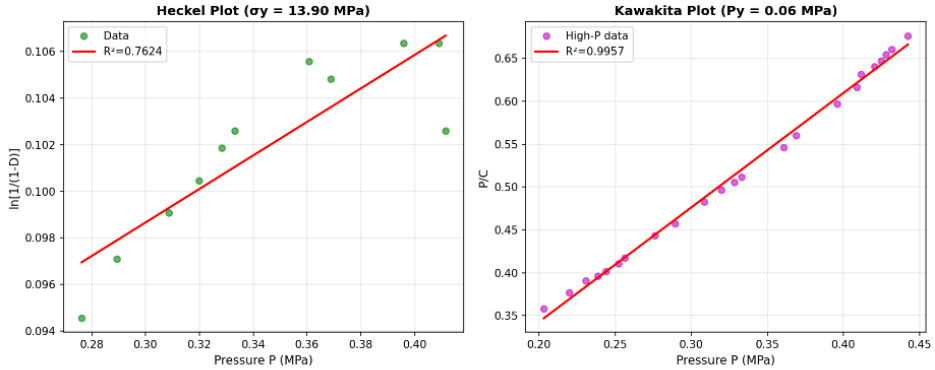


```
MATERIAL: Fumed silica
ρ_true: 2.2 g/cm³
Mass: 3.42 g
h₀: 138.58 mm

DATA POINTS: 76
D₀: 0.0227
D_final: 0.1009
P_max: 0.44 MPa
F_max: 1013.0 N
Strain_max: 66.3%

HECKEL:
  K = 0.0719 MPa⁻¹
  σy = 13.90 MPa
  R² = 0.7624

KAWAKITA:
  a = 13.1745
  b = 17.5780 MPa⁻¹
  Py = 0.06 MPa
  Fy = 130.3 N
  R² = 0.9957

FILE:
  fumed silica vacuum 425.11.26-15.16.44.xlsx
```

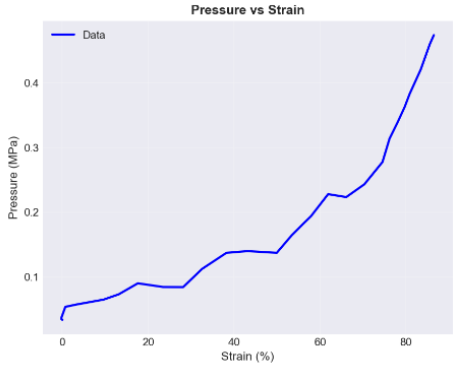

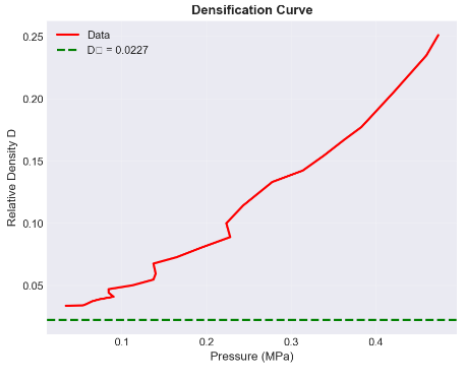

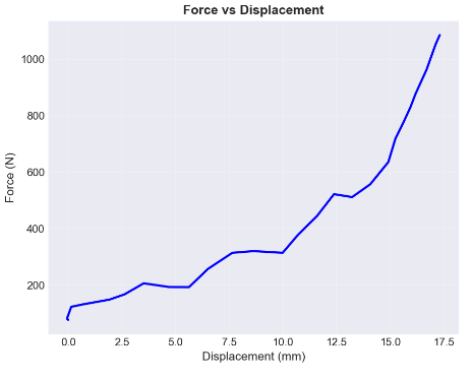

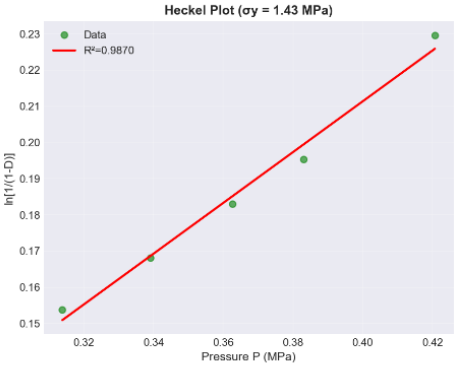

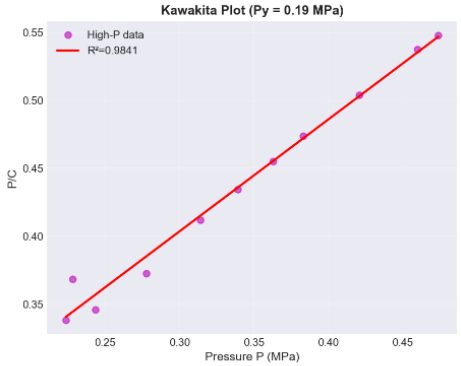


```
MATERIAL: Fumed silica
ρ_true: 2.2 g/cm³
Mass: 3.42 g
hₑ: 146.31 mm

DATA POINTS: 27
Dₑ: 0.0227
D_final: 0.2514
P_max: 0.47 MPa
F_max: 1085.3 N
Strain_max: 86.5%

HECKEL:
  K = 0.7016 MPa⁻¹
  σy = 1.43 MPa
  R² = 0.9870

KAWAKITA:
  a = 6.4022
  b = 5.2794 MPa⁻¹
  Py = 0.19 MPa
  Fy = 433.8 N
  R² = 0.9841

FILE:
  fumed silica cryo 225.12.12-11.05.42.xlsx
```

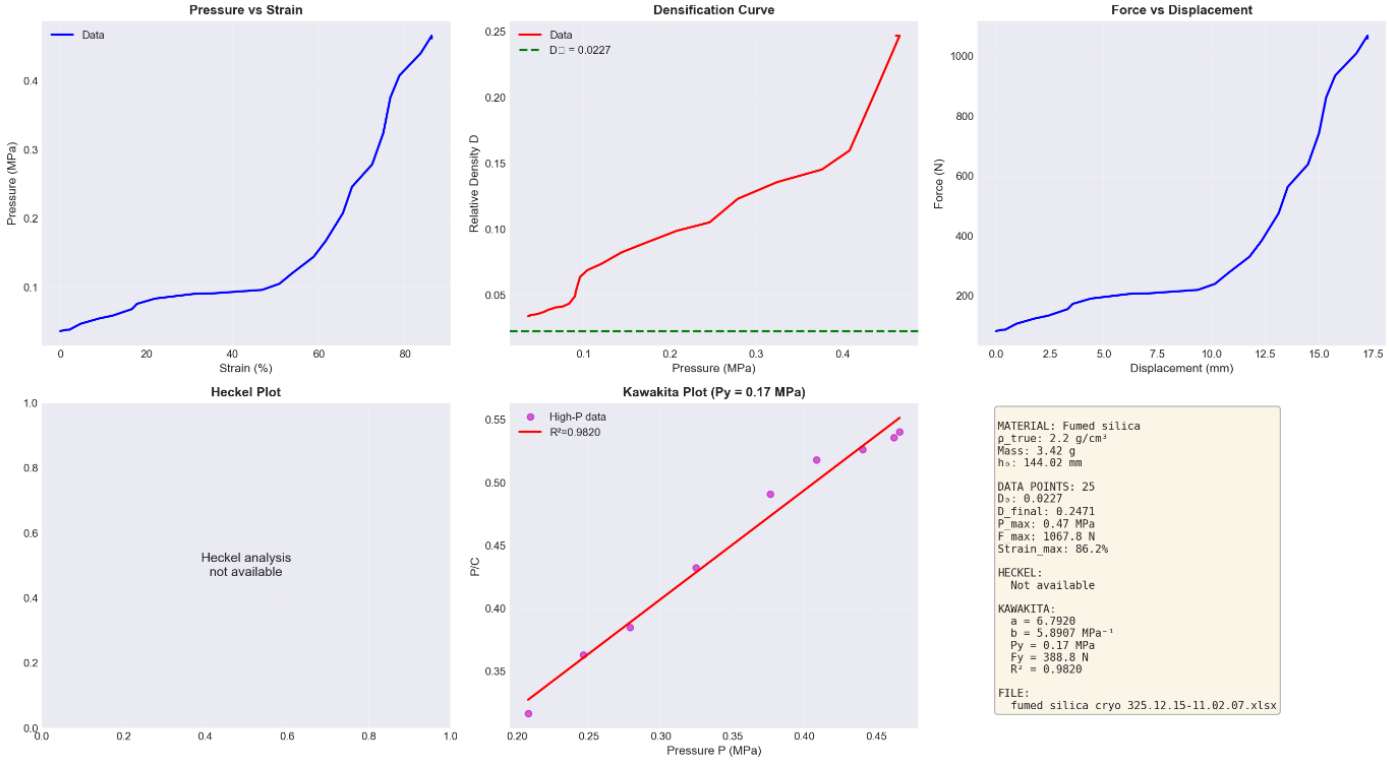
Pressure vs Strain
Data
Pressure (MPa)
Strain (%)
Densification Curve
Data
D□ = 0.0227
Relative Density D
Pressure (MPa)
Force vs Displacement
Force (N)
Displacement (mm)
Heckel Plot
Heckel analysis
not available
Kawakita Plot (Py = 0.17 MPa)
High-P data
R²=0.9820
P/C
Pressure P (MPa)
MATERIAL: Fumed silica
ρ_true: 2.2 g/cm³
Mass: 3.42 g
h₀: 144.02 mm
DATA POINTS: 25
D₀: 0.0227
D_final: 0.2471
P_max: 0.47 MPa
F_max: 1067.8 N
Strain_max: 86.2%
HECKEL:
Not available
KAWAKITA:
a = 6.7920
b = 5.8907 MPa⁻¹
Py = 0.17 MPa
Fy = 388.8 N
R² = 0.9820
FILE:
fumed silica cryo 325.12.15-11.02.07.xlsx

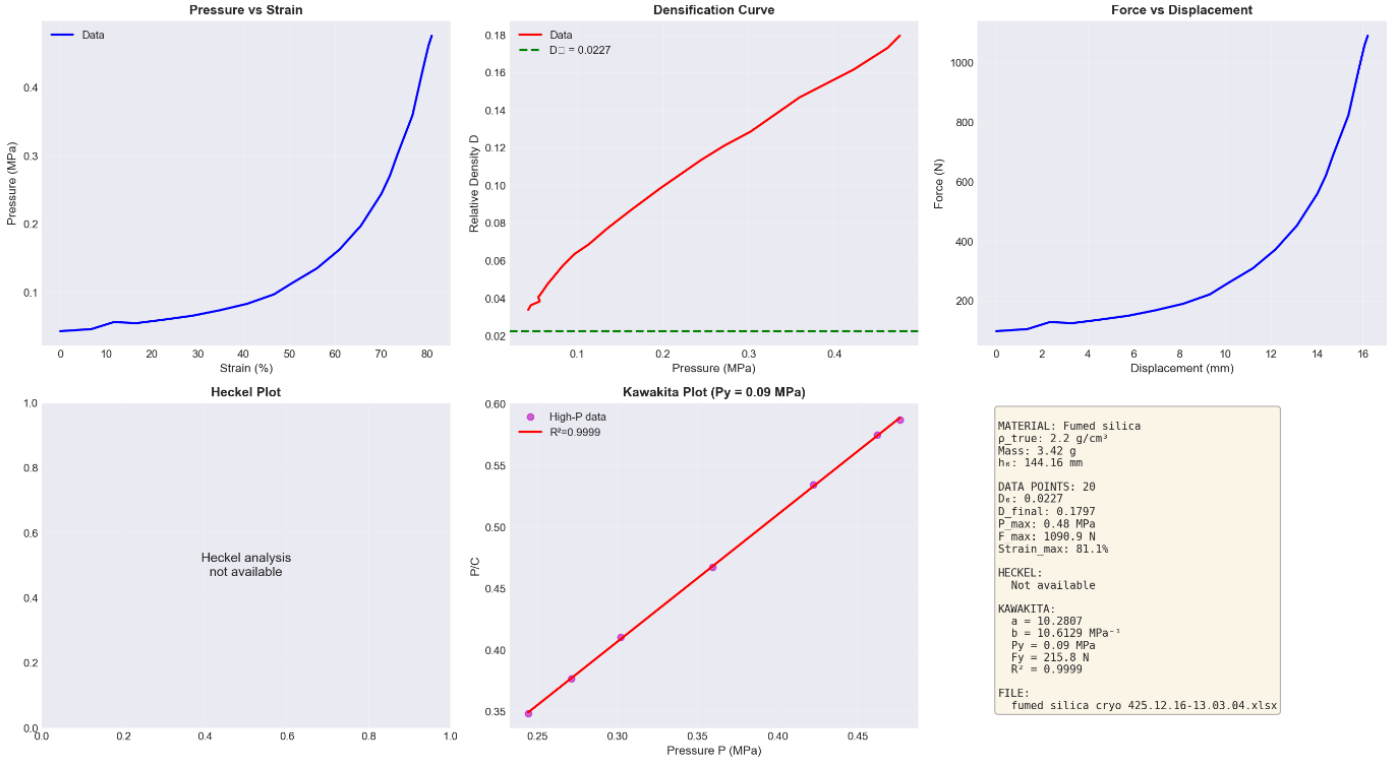
Pressure vs Strain
Data
Pressure (MPa)
Strain (%)
Densification Curve
Data
D□ = 0.0227
Relative Density D
Pressure (MPa)
Force vs Displacement
Force (N)
Displacement (mm)
Heckel Plot
Heckel analysis
not available
Kawakita Plot (Py = 0.09 MPa)
High-P data
R²=0.9999
P/C
Pressure P (MPa)
MATERIAL: Fumed silica
ρ_true: 2.2 g/cm³
Mass: 3.42 g
h_ε: 144.16 mm
DATA POINTS: 20
D_ε: 0.0227
D_final: 0.1797
P_max: 0.48 MPa
F_max: 1090.9 N
Strain_max: 81.1%
HECKEL:
Not available
KAWAKITA:
a = 10.2807
b = 10.6129 MPa⁻¹
Py = 0.09 MPa
Fy = 215.8 N
R² = 0.9999
FILE:
fumed silica cryo 425.12.16-13.03.04.xlsx

B. Python analysis scripts

This appendix contains the two Python scripts developed for the processing and analysis of experimental compression data collected during this study.
The scripts were used to perform all data filtering operations, unit conversions, and the application of the Heckel and Kawakita equations to the raw force-displacement datasets acquired from the experimental setup.
The two scripts are differentiated by experimental condition: the first handles atmospheric tests, while the second manages vacuum and cryogenic vacuum tests.
This distinction reflects the different data processing requirements associated with each condition, particularly regarding the handling of the preliminary vacuum pumping phase and the thermal stabilization period present in cryogenic acquisitions.
All graphical outputs presented throughout the thesis, including pressure-strain curves, relative density plots, force-displacement profiles, and Heckel and Kawakita linearization curves, were generated using these scripts.
They are provided in their entirety to ensure full reproducibility of the results and to facilitate potential extensions of this work to additional materials or experimental conditions.

Atmospheric script:

```
import pandas as pd
import numpy as np
import matplotlib.pyplot as plt
from scipy.signal import savgol_filter
from scipy.stats import linregress
import warnings
import datetime
import os
warnings.filterwarnings('ignore')

#
==========
# MATERIAL DATABASE WITH TAP DENSITY
#
==========

MATERIALS = {
    1: {
        'name': 'Filtered perlite',
        'density': 2.2,
        'tap_density': 0.163683,
    },
    2: {
        'name': 'Cryoperlite',
        'density': 2.2,
        'tap_density': 0.074255,
    },
    3: {
        'name': 'Microspheres',
        'density': 2.4,
        'tap_density': 0.082837,
    },
    4: {
        'name': 'Fumed silica',
        'density': 2.2,
        'tap_density': 0.049834,
    }
}

#
==========
# CONFIGURATION PARAMETERS
#
==========
```

```
SHEET_NAME = "AMR WinControl"
COL_FORCE = "10.0.0 - Load cell"
COL_POSITION = "80.1 - Laser sensor"
PISTON_DIAMETER = 54  # mm
powder_initial_height = 30  # mm
VOLUME_CM3 = 68.7  # ml

SMOOTH_WINDOW = 21
SMOOTH_ORDER = 3

ENABLE_DATA_CLEANING = True
MAX_DISPLACEMENT_JUMP = 15.0
MAX_TOTAL_DISPLACEMENT = 55.0
ENABLE_SMOOTHING = False

#
==========================================================================
==========
# HECKEL/KAWAKITA PARAMETERS
#
==========================================================================
==========

HECKEL_MIN_FRACTION = 0.6
HECKEL_MAX_FRACTION = 0.95
MIN_COMPRESSION = 0.01
KAWAKITA_PRESSURE_THRESHOLD = 0.25  # Default: 0.20 MPa

#
==========================================================================
==========
# BATCH RESULTS EXPORT FUNCTION (SIMPLIFIED)
#
==========================================================================
==========

def save_batch_results(filepath, material_name, rho_theoretical, powder_mass, h0_actual,
h0_found,
                       P_all, strain_all, D_all, D0, heckel_data, kawakita_data,
                       n_points_heckel, n_points_kawakita, warnings_log,
                       results_file="batch_analysis_results.txt"):

    import os

    file_exists = os.path.exists(results_file)

    with open(results_file, 'a', encoding='utf-8') as f:
        if not file_exists:
            f.write("="*110 + "\n")
```

```
        f.write("BATCH COMPRESSION ANALYSIS RESULTS - SINGLE CYCLE\n")
        f.write(f"Generated: {datetime.datetime.now().strftime('%Y-%m-%d
%H:%M:%S')}\n")
        f.write("="*110 + "\n\n")

    f.write("\n" + "="*110 + "\n")
    f.write(f"FILE: {os.path.basename(filepath)}\n")
    f.write(f"Analysis time: {datetime.datetime.now().strftime('%Y-%m-%d
%H:%M:%S')}\n")
    f.write("="*110 + "\n\n")

    # Material info
    f.write("MATERIAL INFORMATION:\n")
    f.write(f"  Material: {material_name}\n")
    f.write(f"  ρ_true: {rho_theoretical} g/cm³\n")
    f.write(f"  Powder mass: {powder_mass:.2f} g\n")
    f.write(f"  Initial height h0 (configured): {h0_actual} mm\n")
    f.write(f"  h0 laser_current (found in Excel): {h0_found:.2f} mm\n")
    f.write(f"  Piston diameter: {PISTON_DIAMETER} mm\n")
    f.write(f"  Volume: {VOLUME_CM3} ml\n\n")

    # Experimental results
    # Calculate displacement range (always available, even if Kawakita fails)
    disp_corrected = np.maximum(strain_all * powder_initial_height, 0.0)

    f.write("EXPERIMENTAL RESULTS:\n")
    f.write(f"  D₀ (initial relative density): {D0:.6f}\n")
    f.write(f"  D_final (final relative density): {D_all.max():.6f}\n")
    f.write(f"  Max pressure: {P_all.max():.4f} MPa\n")
    f.write(f"  Max strain: {strain_all.max()*100:.2f}%\n")
    f.write(f"  Displacement range: {disp_corrected.min():.2f}-{disp_corrected.max():.2f}
mm\n")
    f.write(f"  Total data points analyzed: {len(P_all)}\n")
    f.write(f"  Positive strain points: {np.sum(strain_all > 0)}\n\n")

    # Heckel results
    f.write("HECKEL ANALYSIS:\n")
    if heckel_data and len(heckel_data) > 2 and heckel_data[2] is not None:
        K_h, A_h, sigma_y, r2_h = heckel_data[2], heckel_data[3], heckel_data[4],
heckel_data[5]
        D_A = 1 - np.exp(-A_h)
        f.write(f"  ✓ Analysis successful\n")
        f.write(f"  Points in fit: {n_points_heckel}\n")
        f.write(f"  K (slope): {K_h:.6f} MPa⁻¹\n")
        f.write(f"  A (intercept): {A_h:.6f}\n")
        f.write(f"  σy (yield strength): {sigma_y:.4f} MPa\n")
        f.write(f"  DA (density after rearrangement): {D_A:.6f}\n")
        f.write(f"  R² (fit quality): {r2_h:.6f}\n\n")
    else:
        f.write(f"  ✗ Not available (insufficient data)\n\n")
```

```
        # Kawakita results
        f.write("KAWAKITA ANALYSIS:\n")
        if kawakita_data[2] is not None:
            a, b, P_y, r2_k = kawakita_data[2], kawakita_data[3], kawakita_data[4], kawakita_data[5]
            f.write(f"  ✓ Analysis successful\n")
            f.write(f"  Points in HIGH-PRESSURE fit: {n_points_kawakita['high_p']}\n")
            f.write(f"  Displacement range: {disp_corrected.min():.2f}-{disp_corrected.max():.2f} mm\n")
            f.write(f"  Points in ALL-DATA fit: {n_points_kawakita['all_data']}\n")
            f.write(f"\n  --- High-Pressure Region Fit (RECOMMENDED) ---\n")
            f.write(f"  a (max compression): {a:.6f}\n")
            f.write(f"  b (compressibility): {b:.6f} MPa⁻¹\n")
            f.write(f"   Py (yield pressure): {P_y:.4f} MPa | Yield Force: {P_y * (np.pi * (PISTON_DIAMETER/2)**2):.2f} N ← ROBUST ESTIMATE\n")
            f.write(f"  R² (fit quality): {r2_k:.6f}\n")

            if kawakita_data and len(kawakita_data) > 6 and kawakita_data[6] is not None:
                a_all = kawakita_data[6]
                b_all = kawakita_data[7]
                P_y_all = kawakita_data[8]
                r2_k_all = kawakita_data[9]
                f.write(f"\n  --- All-Data Fit (for comparison) ---\n")
                f.write(f"  a (max compression): {a_all:.6f}\n")
                f.write(f"  b (compressibility): {b_all:.6f} MPa⁻¹\n")
                f.write(f"  Py (yield pressure): {P_y_all:.4f} MPa | Yield Force: {P_y_all * (np.pi * (PISTON_DIAMETER/2)**2):.2f} N\n")
                f.write(f"  R² (fit quality): {r2_k_all:.6f}\n\n")
        else:
            f.write(f"  ✗ Not available (insufficient data)\n\n")

        # Warnings
        if warnings_log:
            f.write("WARNINGS:\n")
            for w in warnings_log:
                f.write(f"  ⚠ {w}\n")
            f.write("\n")

        f.write("-"*110 + "\n")

#
# ============================================================================
# MATERIAL SELECTION
#
# ============================================================================

def select_material():
```

```
    """Interactive material selection."""
    print("\nAvailable materials:")
    for key, mat in MATERIALS.items():
        print(f"  [{key}] {mat['name']}")
        print(f"      Bulk density: {mat['density']} g/cm³")
        print(f"      Tap density (measured): {mat['tap_density']:.4f}")

    while True:
        try:
            choice = int(input("Select material (1-4): "))
            if choice in MATERIALS:
                selected = MATERIALS[choice]
                density_tap = selected['tap_density']
                powder_mass = VOLUME_CM3 * density_tap

                print(f"\n✓ Selected: {selected['name']}")
                print(f"  ρ_true = {selected['density']} g/cm³")
                print(f"  ρ_tap = {density_tap:.4f} g/cm³")
                print(f"  Calculated mass = {powder_mass:.2f} g")

                return selected['tap_density'], selected['density'], selected['name'], powder_mass
            else:
                print("Invalid choice. Enter a number between 1 and 4.")
        except ValueError:
            print("Invalid input. Enter a number.")

#
==========
# DATA LOADING (SIMPLIFIED FOR SINGLE CYCLE)
#
==========

def load_data(filepath, sheet_name, force_col, laser_current_col):
    """Load data from Excel file - simplified for single monotonic loading."""
    print(f"\nLoading data from {filepath}...")
    df = pd.read_excel(filepath, sheet_name=sheet_name)

    force_raw = df[force_col].values
    laser_current = df[laser_current_col].values

    # FIND h0: First point where force becomes positive
    first_positive_idx = np.where(force_raw > 0)[0]
    if len(first_positive_idx) > 0:
        h0_idx = first_positive_idx[0]
        laser_initial = laser_current[h0_idx]
        print(f"\n✓ Found first positive force at index {h0_idx}")
        print(f"  Force: {force_raw[h0_idx]:.1f} N | Position: {laser_initial:.2f} mm")
    else:
```

```
        h0_idx = 0
        laser_initial = laser_current[0]
        print(f"\n⚠ No positive force found! Using first data point")

    displacement = laser_initial - laser_current

    # Extract only positive force region (single monotonic loading)
    positive_mask = force_raw > 0
    force = force_raw[positive_mask]
    displacement = displacement[positive_mask]

    print(f"✓ Loaded {len(force_raw)} total data points")
    print(f"✓ Extracted {len(force)} positive force points (single loading cycle)")
    print(f"  h0 Position: {laser_initial:.2f} mm")
    print(f"  Force range: {force.min():.1f} to {force.max():.1f} N")
    print(f"  Displacement range: {displacement.min():.2f} to {displacement.max():.2f} mm")

    return force, displacement, force_raw, laser_current, h0_idx, laser_initial

#
================================================================================
==========
# DATA CLEANING
#
================================================================================
==========

def clean_data(force, displacement):
    """Clean data by removing outliers."""
    if not ENABLE_DATA_CLEANING or len(force) == 0:
        return force, displacement

    print("\n--- Data Cleaning ---")
    n_original = len(force)
    valid_mask = np.ones(len(force), dtype=bool)

    # Remove extreme displacement outliers
    displacement_outliers = displacement > MAX_TOTAL_DISPLACEMENT
    valid_mask &= ~displacement_outliers
    if np.sum(displacement_outliers) > 0:
        print(f"  Removed {np.sum(displacement_outliers)} displacement outliers (>
{MAX_TOTAL_DISPLACEMENT} mm)")

    # Remove severe negative displacement (noise/vibration)
    negative_disp = displacement < -10
    valid_mask &= ~negative_disp
    if np.sum(negative_disp) > 0:
        print(f"  Removed {np.sum(negative_disp)} severe negative displacement points")

    # Remove displacement jumps
```

```
    if len(displacement) > 1:
        displacement_diff = np.abs(np.diff(displacement))
        jump_mask = np.zeros(len(force), dtype=bool)
        jump_mask[1:] = displacement_diff > MAX_DISPLACEMENT_JUMP
        valid_mask &= ~jump_mask
        if np.sum(jump_mask) > 0:
            print(f"  Removed {np.sum(jump_mask)} displacement jump points (> {MAX_DISPLACEMENT_JUMP} mm)")

    # Remove force jumps
    if len(force) > 1:
        force_diff = np.abs(np.diff(force))
        force_jump_mask = np.zeros(len(force), dtype=bool)
        force_jump_mask[1:] = force_diff > 700
        valid_mask &= ~force_jump_mask
        if np.sum(force_jump_mask) > 0:
            print(f"  Removed {np.sum(force_jump_mask)} force jump points (> 700 N)")

    force_clean = force[valid_mask]
    displacement_clean = displacement[valid_mask]

    n_removed = n_original - len(force_clean)
    print(f"  Total removed: {n_removed}/{n_original} ({100*n_removed/n_original:.1f}%)")
    print(f"  Remaining: {len(force_clean)} points")

    return force_clean, displacement_clean

#
# DATA SMOOTHING
#

def smooth_data(force, displacement):
    """Apply Savitzky-Golay smoothing."""
    if not ENABLE_SMOOTHING or len(force) < SMOOTH_WINDOW:
        return force, displacement

    print("\n--- Data Smoothing ---")

    try:
        force_smooth = savgol_filter(force, SMOOTH_WINDOW, SMOOTH_ORDER)
        displacement_smooth = savgol_filter(displacement, SMOOTH_WINDOW, SMOOTH_ORDER)

        force_rms = np.sqrt(np.mean((force - force_smooth)**2))
        disp_rms = np.sqrt(np.mean((displacement - displacement_smooth)**2))
```

```
        print(f"✓ Applied Savitzky-Golay filter (window={SMOOTH_WINDOW},
order={SMOOTH_ORDER})")
        print(f"  Force RMS change: {force_rms:.2f} N")
        print(f"  Displacement RMS change: {disp_rms:.3f} mm")

        return force_smooth, displacement_smooth

    except Exception as e:
        print(f"  ⚠ Smoothing failed: {e}")
        return force, displacement
def remove_unloading_phase(force, displacement, min_force_fraction=0.90):
    """Remove points after force drops below a fraction of maximum."""
    if len(force) < 3:
        return force, displacement

    print("\n--- Checking for unloading phase ---")

    max_force = force.max()
    threshold = max_force * min_force_fraction

    max_idx = np.argmax(force)

    cut_idx = len(force)
    for i in range(max_idx, len(force)):
        if force[i] < threshold:
            cut_idx = i
            print(f"  Force dropped below {min_force_fraction*100:.0f}% of max at index {i}")
            print(f"  Max force: {max_force:.1f} N, Current: {force[i]:.1f} N")
            break

    if cut_idx < len(force):
        removed = len(force) - cut_idx
        print(f"  Removing {removed} unloading points")
        return force[:cut_idx], displacement[:cut_idx]

    print("  No unloading phase detected")
    return force, displacement
#
==========================================================================
==========
# PARAMETER CALCULATION
#
==========================================================================
==========

def calculate_basic_parameters(force, displacement, d_piston, h0, tap_density, rho_theo,
powder_mass):
    """Calculate pressure, strain and relative density."""

    if len(force) == 0 or len(displacement) == 0:
```

```
        print("\n⚠ ERROR: Empty arrays!")
        return None, None, None, None, None

    A = np.pi * (d_piston/2)**2
    P = force / A
    strain = displacement / powder_initial_height
    D0 = tap_density / rho_theo

    # Handle negative displacement (clamp to 0 for density calculation)
    print(f"\n--- Displacement Analysis ---")
    print(f"  Raw displacement range: {displacement.min():.3f} to {displacement.max():.3f} mm")
    print(f"  Negative displacement points: {np.sum(displacement < 0)}/{len(displacement)}")

    displacement_corrected = np.maximum(displacement, 0.0)

    if np.any(displacement < 0):
        print(f"  ⚠ WARNING: {np.sum(displacement < 0)} negative displacement values detected!")
        print(f"  These indicate laser reading > h0 (vibrations/noise)")
        print(f"  Clamping to 0 for density calculation")

    h_current = powder_initial_height - displacement_corrected
    h_current = np.maximum(h_current, 0.1)  # Avoid zero/negative heights

    apparent_density = powder_mass / (A * h_current * 1e-3)
    D = apparent_density / rho_theo

    if np.any(D > 1.0):
        print(f"\n⚠ WARNING: Relative density exceeds 1.0! Max D = {D.max():.3f}")
        print(f"  This suggests measurement errors or incorrect parameters")

    if np.any(D < D0):
        n_below = np.sum(D < D0)
        print(f"\n⚠ WARNING: {n_below} points have D < D0!")
        print(f"  D range: {D.min():.6f} to {D.max():.6f}")
        print(f"  D0: {D0:.6f}")

    print(f"\n--- Basic Parameters ---")
    print(f"Piston area: {A:.2f} mm²")
    print(f"Powder mass: {powder_mass:.2f} g")
    print(f"Initial height h0: {h0} mm")
    print(f"Initial relative density D₀: {D0:.4f}")
    print(f"Final relative density D: {D.max():.3f}")
    print(f"Maximum pressure: {P.max():.2f} MPa")
    print(f"Maximum strain: {strain.max():.3f} ({strain.max()*100:.1f}%)")
    print(f"Data points: {len(force)}")

    return P, strain, D, D0, A
```

```
#
==========
# HECKEL ANALYSIS
#
==========

def heckel_analysis(P, D, min_frac=0.6, max_frac=0.95):
    """Apply Heckel equation."""

    warnings_list = []

    print(f"\n=== HECKEL ANALYSIS ===")
    print(f'Input data:")
    print(f"  Total points: {len(P)}")
    print(f"  D range: {D.min():.6f} to {D.max():.6f}")
    print(f"  P range: {P.min():.4f} to {P.max():.4f} MPa")

    D_min = D.min() * 0.5
    D_max = D.max() * 1.1

    print(f"\n✓ Using ADAPTIVE filtering:")
    print(f"  D_min threshold: {D_min:.6f}")
    print(f"  D_max threshold: {D_max:.6f}")

    valid_mask = (D >= D_min) & (D <= D_max)
    P_valid = P[valid_mask]
    D_valid = D[valid_mask]

    print(f"  Points after filter: {len(D_valid)}")

    if len(P_valid) < 10:
        msg = "Not enough valid points for Heckel analysis (< 10 points)"
        print(f"\n⚠ WARNING: {msg}")
        warnings_list.append(msg)
        return None, None, None, None, None, None, 0, warnings_list

    y_heckel = np.log(1.0 / (1.0 - D_valid))

    print(f"\nCalculating Heckel variable:")
    print(f"  y_heckel = ln[1/(1-D)]")
    print(f"  y_heckel range: {y_heckel.min():.6f} to {y_heckel.max():.6f}")

    print(f"\nIdentifying linear region:")
    P_max = P_valid.max()
    P_min_linear = min_frac * P_max
    P_max_linear = max_frac * P_max
```

```
    print(f"  P_max: {P_max:.4f} MPa")
    print(f"  Linear region: {P_min_linear:.4f} to {P_max_linear:.4f} MPa")
    print(f"  Fraction range: {min_frac} to {max_frac}")

    linear_mask = (P_valid >= P_min_linear) & (P_valid <= P_max_linear)
    P_linear = P_valid[linear_mask]
    y_linear = y_heckel[linear_mask]

    print(f"  Points in linear region: {len(P_linear)}")

    if len(P_linear) < 5:
        msg = f"Insufficient linear region points ({len(P_linear)} < 5)"
        print(f"\n⚠ WARNING: {msg}")
        warnings_list.append(msg)
        return None, None, None, None, None, None, 0, warnings_list

    slope, intercept, r_value, _, _ = linregress(P_linear, y_linear)
    K = slope
    A = intercept
    sigma_y = 1 / K if K > 0 else None
    r2 = r_value**2

    print(f"\n✓ Heckel fit successful:")
    print(f"  K (slope): {K:.6f} MPa⁻¹")
    print(f"  A (intercept): {A:.6f}")
    if sigma_y:
        print(f"  σy (yield strength): {sigma_y:.4f} MPa")
    print(f"  R²: {r2:.6f}")

    if r2 < 0.9:
        msg = f"Poor fit quality (R² = {r2:.3f} < 0.9)"
        print(f"  ⚠ WARNING: {msg}")
        warnings_list.append(msg)

    return P_linear, y_linear, K, A, sigma_y, r2, len(P_linear), warnings_list

#
================================================================================
==========
# KAWAKITA ANALYSIS
#
================================================================================
==========

def kawakita_analysis(P, strain, min_compression=0.01, pressure_threshold=None):
    """Apply Kawakita equation with configurable pressure threshold."""

    # Use global parameter if not specified
    if pressure_threshold is None:
        pressure_threshold = KAWAKITA_PRESSURE_THRESHOLD
```

```
    warnings_list = []

    print(f"\n=== KAWAKITA ANALYSIS ===")
    print(f"Input data:")
    print(f"  Total points: {len(P)}")
    print(f"  Strain range: {strain.min():.6f} to {strain.max():.6f}")
    print(f"  P range: {P.min():.4f} to {P.max():.4f} MPa")

    # Filter positive compression only
    valid_mask = strain >= min_compression
    P_valid = P[valid_mask]
    C_valid = strain[valid_mask]

    print(f"\n✓ Filtered data (strain >= {min_compression}):")
    print(f"  Valid points: {len(P_valid)}")

    if len(P_valid) < 3:
        msg = f"Insufficient data points ({len(P_valid)} < 5)"
        print(f"\n⚠ WARNING: {msg}")
        warnings_list.append(msg)
        return None, None, None, None, None, None, None, None, None, None, 0, 0,
warnings_list

    # FIXED PRESSURE THRESHOLD
    if P_valid.max() < pressure_threshold:
        msg = f"Max pressure {P_valid.max():.3f} MPa < threshold {pressure_threshold} MPa"
        print(f"\n⚠ WARNING: {msg}")
        warnings_list.append(msg)

        high_p_mask = np.ones(len(P_valid), dtype=bool)
    else:
        high_p_mask = P_valid >= pressure_threshold

    P_high_p = P_valid[high_p_mask]
    C_high_p = C_valid[high_p_mask]

    print(f"\nHigh-pressure region (P >= {pressure_threshold:.2f} MPa):")
    print(f"  Points: {len(P_high_p)}")
    print(f"  Pressure range: {P_high_p.min():.3f} - {P_high_p.max():.3f} MPa")
    print(f"  Strain range: {C_high_p.min()*100:.1f}% - {C_high_p.max()*100:.1f}%")

    if len(P_high_p) >= 3:
        y_kawakita_high = P_high_p / C_high_p

        slope_high, intercept_high, r_value_high, _, _ = linregress(P_high_p, y_kawakita_high)

        # Check for valid fit
        if intercept_high == 0 or slope_high < 0:
            msg = "Invalid Kawakita fit parameters"
```

```
        print(f"\n⚠ WARNING: {msg}")
        warnings_list.append(msg)
        a_high = b_high = P_y_high = r2_high = None
    else:
        a_high = 1 / intercept_high
        b_high = slope_high / intercept_high
        P_y_high = 1 / b_high if b_high != 0 else None
        r2_high = r_value_high**2

        print(f"\n✓ High-pressure fit successful:")
        print(f"  a (max compression): {a_high:.6f}")
        print(f"  b (compressibility): {b_high:.6f} MPa⁻¹")
        if P_y_high:
            print(f"  Py (yield pressure): {P_y_high:.4f} MPa")
        print(f"  R²: {r2_high:.6f}")

        if r2_high < 0.95:
            msg = f"Moderate fit quality (R² = {r2_high:.3f} < 0.95)"
            print(f"  ⚠ WARNING: {msg}")
            warnings_list.append(msg)
else:
    print(f"  ⚠ Insufficient high-pressure points")
    a_high = b_high = P_y_high = r2_high = None

# All-data fit (for comparison)
y_kawakita_all = P_valid / C_valid

try:
    slope_all, intercept_all, r_value_all, _, _ = linregress(P_valid, y_kawakita_all)

    if intercept_all != 0:
        a_all = 1 / intercept_all
        b_all = slope_all / intercept_all
        P_y_all = 1 / b_all if b_all != 0 else None
        r2_all = r_value_all**2
    else:
        a_all = b_all = P_y_all = r2_all = None
except:
    a_all = b_all = P_y_all = r2_all = None

print(f"\n✓ All-data fit:")
if a_all:
    print(f"  a (max compression): {a_all:.6f}")
    print(f"  b (compressibility): {b_all:.6f} MPa⁻¹")
    if P_y_all:
        print(f"  Py (yield pressure): {P_y_all:.4f} MPa")
    print(f"  R²: {r2_all:.6f}")
else:
    print(f"  Fit failed")
```

```
    return (P_high_p, y_kawakita_high, a_high, b_high, P_y_high, r2_high,
            a_all, b_all, P_y_all, r2_all, len(P_high_p), len(P_valid), warnings_list)

#
==========
# PLOTTING
#
==========

def plot_results(P_all, strain_all, D_all, P_mono, strain_mono, heckel_data, kawakita_data,
                 material_name, rho_theoretical, D0, powder_mass, force_raw, laser_current,
h0_actual,
                 filename=None, output_folder=None):
    """Plot comprehensive results - 2x3 layout."""

    import os

    fig = plt.figure(figsize=(18, 10))

    # 1. Pressure vs Strain
    ax1 = plt.subplot(2, 3, 1)
    ax1.plot(strain_all*100, P_all, 'b-', linewidth=2, label='Data')
    ax1.set_xlabel('Strain (%)', fontsize=11)
    ax1.set_ylabel('Pressure (MPa)', fontsize=11)
    ax1.set_title('Pressure vs Strain', fontsize=12, fontweight='bold')
    ax1.grid(True, alpha=0.3)
    ax1.legend()

    # 2. Relative Density vs Pressure
    ax2 = plt.subplot(2, 3, 2)
    ax2.plot(P_all, D_all, 'r-', linewidth=2, label='Data')
    ax2.axhline(y=D0, color='g', linestyle='--', linewidth=2, label=f'D₀ = {D0:.4f}')
    ax2.set_xlabel('Pressure (MPa)', fontsize=11)
    ax2.set_ylabel('Relative Density D', fontsize=11)
    ax2.set_title('Densification Curve', fontsize=12, fontweight='bold')
    ax2.grid(True, alpha=0.3)
    ax2.legend()

    # 3. Force vs Displacement
    ax3 = plt.subplot(2, 3, 3)
    disp_all = strain_all * powder_initial_height
    ax3.plot(disp_all, P_all * (np.pi * (PISTON_DIAMETER/2)**2), 'b-', linewidth=2)
    ax3.set_xlabel('Displacement (mm)', fontsize=11)
    ax3.set_ylabel('Force (N)', fontsize=11)
    ax3.set_title('Force vs Displacement', fontsize=12, fontweight='bold')
    ax3.grid(True, alpha=0.3)
```

```
# 4. Heckel Plot
ax4 = plt.subplot(2, 3, 4)
try:
    if heckel_data and heckel_data[0] is not None:
        P_heckel, y_heckel, K, A, sigma_y, r2 = heckel_data
        ax4.plot(P_heckel, y_heckel, 'go', markersize=6, label='Data', alpha=0.6)

        P_fit = np.linspace(P_heckel.min(), P_heckel.max(), 100)
        y_fit = K * P_fit + A
        ax4.plot(P_fit, y_fit, 'r-', linewidth=2, label=f'R²={r2:.4f}')

        ax4.set_xlabel('Pressure P (MPa)', fontsize=11)
        ax4.set_ylabel('ln[1/(1-D)]', fontsize=11)
        ax4.set_title(f'Heckel Plot (σy = {sigma_y:.2f} MPa)', fontsize=12, fontweight='bold')
        ax4.legend()
    else:
        ax4.text(0.5, 0.5, 'Heckel analysis\nnot available',
                 ha='center', va='center', transform=ax4.transAxes, fontsize=12)
        ax4.set_title('Heckel Plot', fontsize=12, fontweight='bold')
except Exception as e:
    ax4.text(0.5, 0.5, f'Heckel plot error:\n{str(e)}',
             ha='center', va='center', transform=ax4.transAxes, fontsize=10)
    ax4.set_title('Heckel Plot', fontsize=12, fontweight='bold')
ax4.grid(True, alpha=0.3)

# 5. Kawakita Plot
ax5 = plt.subplot(2, 3, 5)
try:
    if kawakita_data and kawakita_data[0] is not None:
        P_kaw, y_kaw, a, b, P_y, r2 = kawakita_data[:6]
        ax5.plot(P_kaw, y_kaw, 'mo', markersize=6, label='High-P data', alpha=0.6)

        P_fit = np.linspace(P_kaw.min(), P_kaw.max(), 100)
        slope = b * (1/a)
        intercept = 1/a
        y_fit = slope * P_fit + intercept
        ax5.plot(P_fit, y_fit, 'r-', linewidth=2, label=f'R²={r2:.4f}')

        ax5.set_xlabel('Pressure P (MPa)', fontsize=11)
        ax5.set_ylabel('P/C', fontsize=11)
        ax5.set_title(f'Kawakita Plot (Py = {P_y:.2f} MPa)', fontsize=12, fontweight='bold')
        ax5.legend()
    else:
        ax5.text(0.5, 0.5, 'Kawakita analysis\nnot available',
                 ha='center', va='center', transform=ax5.transAxes, fontsize=12)
        ax5.set_title('Kawakita Plot', fontsize=12, fontweight='bold')
except Exception as e:
    ax5.text(0.5, 0.5, f'Kawakita plot error:\n{str(e)}',
             ha='center', va='center', transform=ax5.transAxes, fontsize=10)
    ax5.set_title('Kawakita Plot', fontsize=12, fontweight='bold')
```

```
    ax5.grid(True, alpha=0.3)

    # 6. Summary text
    ax6 = plt.subplot(2, 3, 6)
    ax6.axis('off')
    summary = f"""
MATERIAL: {material_name}
ρ_true: {rho_theoretical} g/cm³
Mass: {powder_mass:.2f} g
h₀: {h0_actual:.2f} mm

DATA POINTS: {len(P_all)}
D₀: {D0:.4f}
D_final: {D_all.max():.4f}
P_max: {P_all.max():.2f} MPa
F_max: {P_all.max()*(np.pi*(PISTON_DIAMETER/2)**2):.1f} N
Strain_max: {strain_all.max()*100:.1f}%

HECKEL:
"""
    if heckel_data[2] is not None:
        K, A, sigma_y, r2 = heckel_data[2:6]
        summary += f"  K = {K:.4f} MPa⁻¹\n"
        summary += f"  σy = {sigma_y:.2f} MPa\n"
        summary += f"  R² = {r2:.4f}\n"
    else:
        summary += "  Not available\n"

    summary += "\nKAWAKITA:\n"
    if kawakita_data[2] is not None:
        a, b, P_y, r2 = kawakita_data[2:6]
        summary += f"  a = {a:.4f}\n"
        summary += f"  b = {b:.4f} MPa⁻¹\n"
        summary += f"  Py = {P_y:.2f} MPa\n"
        summary += f"  Fy = {P_y*(np.pi*(PISTON_DIAMETER/2)**2):.1f} N\n"
        summary += f"  R² = {r2:.4f}"
    else:
        summary += "  Not available"

    if filename:
        summary += f"\n\nFILE:\n  {os.path.basename(filename)}"

    ax6.text(0.05, 0.98, summary, transform=ax6.transAxes, fontsize=10,
             verticalalignment='top', fontfamily='monospace',
             bbox=dict(boxstyle='round', facecolor='wheat', alpha=0.3))

    plt.tight_layout()


    if filename:
```

```
        base_name = os.path.splitext(os.path.basename(filename))[0]
        save_name = f'compression_analysis_{base_name}.png'
    else:
        save_name = f'compression_analysis_{material_name.replace(" ", "_")}.png'

    if output_folder:
        save_path = os.path.join(output_folder, save_name)
    else:
        save_path = save_name

    plt.savefig(save_path, dpi=150)
    print(f"\n✓ Plot saved: {save_path}")
    plt.show()

#
==========
# BATCH ANALYSIS
#
==========

def batch_analysis(file_list=None, results_filename="batch_results_single_cycle.txt"):
    """Analyze multiple files in batch mode - simplified for single cycle."""

    import os
    import glob
    from datetime import datetime

    timestamp = datetime.now().strftime("%Y%m%d_%H%M%S")
    plots_folder = f"compression_plots_{timestamp}"
    os.makedirs(plots_folder, exist_ok=True)
    print(f"\n📁 Plots will be saved in: {plots_folder}/")

    if file_list is None:

        pattern = *insert pattern*
        print(f"\nUsing pattern: {pattern}")
        file_list = glob.glob(pattern)

        if not file_list:
            print(f"❌ No files found matching pattern: {pattern}")
            return None, None, None

    print(f"\n{'='*70}")
    print(f"BATCH ANALYSIS - SINGLE CYCLE MODE")
    print(f"Found {len(file_list)} files to analyze")
    print(f"{'='*70}\n")

    tap_density, rho_theoretical, material_name, powder_mass = select_material()
```

```
    for i, filepath in enumerate(file_list, 1):
        filename = os.path.basename(filepath)
        print(f"\n{'='*70}")
        print(f"ANALYZING FILE {i}/{len(file_list)}: {filename}")
        print(f"{'='*70}")

        try:
            # Load data
            force_all, displacement_all, force_raw, laser_current, h0_idx, laser_initial = load_data(
                filepath, SHEET_NAME, COL_FORCE, COL_POSITION
            )

            h0_actual = laser_initial

            # Clean and smooth
            print("\n--- CLEANING AND SMOOTHING ---")
            force_clean, displacement_clean = clean_data(force_all, displacement_all)
            force_smooth, displacement_smooth = smooth_data(force_clean, displacement_clean)
            force_smooth, displacement_smooth = remove_unloading_phase(force_smooth,
displacement_smooth)

            # Calculate parameters
            result = calculate_basic_parameters(
                force_smooth, displacement_smooth, PISTON_DIAMETER, h0_actual,
                tap_density, rho_theoretical, powder_mass
            )

            if result[0] is None:
                warnings_all = ["Failed to calculate basic parameters"]
                save_batch_results(filepath, material_name, rho_theoretical, powder_mass,
h0_actual, laser_initial,
                                   np.array([]), np.array([]), np.array([]), 0,
                                   (None, None, None, None, None, None),
                                   (None, None, None, None, None, None, None, None, None, None),
                                   0, {'high_p': 0, 'all_data': 0}, warnings_all, results_filename)
                continue

            P_all, strain_all, D_all, D0, A = result
            # Initialize warnings lists
            heckel_warnings = []
            kawakita_warnings = []
            warnings_all = []

            # Heckel analysis
            print("\n--- HECKEL ANALYSIS ---")
            try:
                heckel_result = heckel_analysis(P_all, D_all, HECKEL_MIN_FRACTION,
HECKEL_MAX_FRACTION)
            except Exception as e:
```

```
            print(f"⚠️ Heckel analysis error: {e}")
            heckel_result = (None,)*8

        heckel_data = heckel_result[:6] if heckel_result and len(heckel_result)>=6 else
(None,)*6
        heckel_n_points = heckel_result[6] if heckel_result and len(heckel_result)>=7 else 0
        heckel_warnings = heckel_result[7] if heckel_result and len(heckel_result)>=8 else []

        # Kawakita analysis
        print("\n--- KAWAKITA ANALYSIS ---")
        try:
            kawakita_result = kawakita_analysis(P_all, strain_all, MIN_COMPRESSION)

            if kawakita_result[0] is None:
                kawakita_data = (None, None, None, None, None, None, None, None, None,
None)
                kawakita_n_points = {'high_p': 0, 'all_data': 0}
                kawakita_warnings = kawakita_result[12] if len(kawakita_result) > 12 else []
            else:
                kawakita_data = kawakita_result[:10]
                kawakita_n_points = {
                    'high_p': kawakita_result[10],
                    'all_data': kawakita_result[11]
                }
                kawakita_warnings = kawakita_result[12] if len(kawakita_result) > 12 else []
        except Exception as e:
            print(f"⚠️ Kawakita analysis error: {e}")
            kawakita_data = (None, None, None, None, None, None, None, None, None, None)
            kawakita_n_points = {'high_p': 0, 'all_data': 0}
            kawakita_warnings = [f"Kawakita error: {str(e)}"]

        # Save results
        print("\n--- SAVING RESULTS ---")
        save_batch_results(filepath, material_name, rho_theoretical, powder_mass, h0_actual,
laser_initial,
                           P_all, strain_all, D_all, D0, heckel_data, kawakita_data,
                           heckel_n_points, kawakita_n_points, warnings_all, results_filename)

        # Plot with output folder
        plot_results(P_all, strain_all, D_all, P_all, strain_all, heckel_data, kawakita_data,
                     material_name, rho_theoretical, D0, powder_mass, force_raw, laser_current,
h0_actual,
                     filename=filepath, output_folder=plots_folder)

        print(f"✅ ANALYSIS COMPLETE FOR: {filename}")

    except Exception as e:
        print(f"\n⚠️ ERROR during analysis: {e}")
        import traceback
```

```
            traceback.print_exc()
            continue

    print("\n" + "="*70)
    print("BATCH ANALYSIS COMPLETE!")
    print(f"Results saved to: {results_filename}")
    print(f"Plots saved to: {plots_folder}/")
    print("="*70)

    return P_all, strain_all, D_all

# ============================================================================
# EXECUTION
# ============================================================================

if __name__ == "__main__":
    P_all, strain_all, D_all = batch_analysis()  # Batch analysis
```

Vacuum and cryo-vacuum script:

```
import pandas as pd
import numpy as np
import matplotlib.pyplot as plt
from scipy.signal import savgol_filter
from scipy.stats import linregress
import warnings
from datetime import datetime
import os
import glob
warnings.filterwarnings('ignore')

#
==========================================================================
==========
# TEST CONDITION SELECTION (VACUUM vs CRYO)
#
==========================================================================
==========

def select_test_condition():
    """
    Select test condition: Vacuum or Cryogenic.
    Returns force_offset and pressure_max values.
    """
    print("\n" + "="*70)
    print("SELECT TEST CONDITION")
    print("="*70)
    print("1. Vacuum test (offset: 65 N, max pressure: 10 mbar)")
    print("2. Cryogenic test (offset: 75 N, max pressure: 20 mbar)")
    print("="*70)

    while True:
        choice = input("Enter your choice (1 or 2): ").strip()

        if choice == '1':
            print("\n✓ VACUUM TEST selected")
            print("  - Force offset: 65 N")
            print("  - Max pressure: 10 mbar")
            return 65, 10  # force_offset, pressure_max

        elif choice == '2':
            print("\n✓ CRYOGENIC TEST selected")
            print("  - Force offset: 75 N")
            print("  - Max pressure: 20 mbar")
            return 75, 20  # force_offset, pressure_max

        else:
            print("❌ Invalid choice. Please enter 1 or 2.")
```

```
def select_directory():
    """
    Select directory for batch analysis.
    Returns the directory path pattern for Excel files.
    """
    print("\n" + "="*70)
    print("SELECT DIRECTORY")
    print("="*70)
    print("1. Vacuum test - Filterperlite")
    print("2. Vacuum test - Cryoperlite")
    print("3. Vacuum test - Microsphere")
    print("4. Vacuum test - Fumed silica")
    print("5. Cryo test - Filterperlite")
    print("6. Cryo test - Cryoperlite")
    print("7. Cryo test - Microsphere")
    print("8. Cryo test - Fumed silica")
    print("="*70)

    while True:
        choice = input("Enter your choice (1-8): ").strip()

        if choice == '1':
            path = ""
            print(f"\n✓ Selected: Vacuum - Filterperlite")
            return path

        elif choice == '2':
            path = ""
            print(f"\n✓ Selected: Vacuum - Cryoperlite")
            return path

        elif choice == '3':
            path = ""
            print(f"\n✓ Selected: Vacuum - Microsphere")
            return path

        elif choice == '4':
            path = ""
            print(f"\n✓ Selected: Vacuum - Fumed silica")
            return path

        elif choice == '5':
            path = ""
            print(f"\n✓ Selected: Cryo - Filterperlite")
            return path

        elif choice == '6':
            path = ""
```

```
            print(f"\n✓ Selected: Cryo - Cryoperlite")
            return path

        elif choice == '7':
            path = ""
            print(f"\n✓ Selected: Cryo - Microsphere")
            return path

        elif choice == '8':
            path = ""
            print(f"\n✓ Selected: Cryo - Fumed silica")
            return path

        else:
            print("❌ Invalid choice. Please enter a number between 1 and 8.")

#
==========
# MATERIAL DATABASE WITH TAP DENSITY
#
==========

MATERIALS = {
    1: {
        'name': 'Filtered perlite',
        'density': 2.2,
        'tap_density': 0.163683,
        'h0': 30,  #mm
    },
    2: {
        'name': 'Cryoperlite',
        'density': 2.2,
        'tap_density': 0.074255,
        'h0': 30,  #mm
    },
    3: {
        'name': 'Microspheres',
        'density': 2.4,
        'tap_density': 0.082837,
        'h0': 30,  #mm
    },
    4: {
        'name': 'Fumed silica',
        'density': 2.2,
        'tap_density': 0.049834,
        'h0': 20,
    }
```

```
}

#
==========
# CONFIGURATION PARAMETERS
#
==========

SHEET_NAME = "AMR WinControl"
COL_FORCE = "10.0.0 - Load cell"
COL_POSITION = "80.1 - Laser sensor"
COL_PRESSURE = "80.0 - Vacuum"  # Vacuum pressure column
PISTON_DIAMETER = 54  # mm
VOLUME_CM3 = 68.7  # ml

# Pressure check parameters (set by select_test_condition)
PRESSURE_MIN = 0  # mbar
# PRESSURE_MAX and FORCE_OFFSET will be set by user selection

SMOOTH_WINDOW = 11
SMOOTH_ORDER = 3

ENABLE_DATA_CLEANING = True
MAX_DISPLACEMENT_JUMP = 15.0
MAX_TOTAL_DISPLACEMENT = 55.0
ENABLE_SMOOTHING = False

#
==========
# HECKEL/KAWAKITA PARAMETERS
#
==========

HECKEL_MIN_FRACTION = 0.6
HECKEL_MAX_FRACTION = 0.95
MIN_COMPRESSION = 0.01

#
==========
# BATCH RESULTS EXPORT FUNCTION (SIMPLIFIED)
#
==========
```

```
def save_batch_results(filepath, material_name, rho_theoretical, powder_mass, h0_actual, h0_found,
                       P_all, strain_all, D_all, D0, heckel_data, kawakita_data,
                       n_points_heckel, n_points_kawakita, warnings_log, powder_initial_height, pressure_warning=None,
                       results_file="batch_analysis_results.txt", force_offset=65, pressure_max=10):

    file_exists = os.path.exists(results_file)

    with open(results_file, 'a', encoding='utf-8') as f:
        if not file_exists:
            f.write("="*110 + "\n")
            f.write("BATCH COMPRESSION ANALYSIS RESULTS - SINGLE CYCLE\n")
            f.write(f"Generated: {datetime.now().strftime('%Y-%m-%d %H:%M:%S')}\n")
            f.write("="*110 + "\n\n")

        f.write("\n" + "="*110 + "\n")
        f.write(f"FILE: {os.path.basename(filepath)}\n")
        f.write(f"Analysis time: {datetime.now().strftime('%Y-%m-%d %H:%M:%S')}\n")
        f.write("="*110 + "\n\n")

        # Material info
        f.write("MATERIAL INFORMATION:\n")
        f.write(f"  Material: {material_name}\n")
        f.write(f"  ρ_true: {rho_theoretical} g/cm³\n")
        f.write(f"  Powder mass: {powder_mass:.2f} g\n")
        f.write(f"  Initial height h0 (configured): {h0_actual} mm\n")
        f.write(f"  h0 laser_current (found in Excel): {h0_found:.2f} mm\n")
        f.write(f"  Piston diameter: {PISTON_DIAMETER} mm\n")
        f.write(f"  Volume: {VOLUME_CM3} ml\n\n")

        f.write("PRESSURE CHECK:\n")
        if pressure_warning:
            f.write(f"  ⚠️ WARNING: {pressure_warning}\n\n")
        else:
            f.write(f"  ✓ Test performed under vacuum (P < {pressure_max} mbar)\n")
            f.write(f"  ✓ Force offset applied: {force_offset} N\n\n")

        # Experimental results
        # Calculate displacement range (always available, even if Kawakita fails)
        disp_corrected = np.maximum(strain_all * powder_initial_height, 0.0)

        f.write("EXPERIMENTAL RESULTS:\n")
        f.write(f"  D₀ (initial relative density): {D0:.6f}\n")
        f.write(f"  D_final (final relative density): {D_all.max():.6f}\n")
        f.write(f"  Max pressure: {P_all.max():.4f} MPa\n")
        f.write(f"  Max strain: {strain_all.max()*100:.2f}%\n")
        f.write(f"  Displacement range: {disp_corrected.min():.2f}-{disp_corrected.max():.2f} mm\n")
        f.write(f"  Total data points analyzed: {len(P_all)}\n")
```

```
        f.write(f"  Positive strain points: {np.sum(strain_all > 0)}\n\n")

        # Heckel results
        f.write("HECKEL ANALYSIS:\n")
        if heckel_data and len(heckel_data) > 2 and heckel_data[2] is not None:
            K_h, A_h, sigma_y, r2_h = heckel_data[2], heckel_data[3], heckel_data[4],
heckel_data[5]
            D_A = 1 - np.exp(-A_h)
            f.write(f"  ✓ Analysis successful\n")
            f.write(f"  Points in fit: {n_points_heckel}\n")
            f.write(f"  K (slope): {K_h:.6f} MPa⁻¹\n")
            f.write(f"  A (intercept): {A_h:.6f}\n")
            f.write(f"  σy (yield strength): {sigma_y:.4f} MPa\n")
            f.write(f"  DA (density after rearrangement): {D_A:.6f}\n")
            f.write(f"  R² (fit quality): {r2_h:.6f}\n\n")
        else:
            f.write(f"  ✗ Not available (insufficient data)\n\n")

        # Kawakita results
        f.write("KAWAKITA ANALYSIS:\n")
        if kawakita_data[2] is not None:
            a, b, P_y, r2_k = kawakita_data[2], kawakita_data[3], kawakita_data[4],
kawakita_data[5]
            f.write(f"  ✓ Analysis successful\n")
            f.write(f"  Points in HIGH-PRESSURE fit: {n_points_kawakita['high_p']}\n")
            f.write(f"  Displacement range: {disp_corrected.min():.2f}-{disp_corrected.max():.2f}
mm\n")
            f.write(f"  Points in ALL-DATA fit: {n_points_kawakita['all_data']}\n")
            f.write(f"\n  --- High-Pressure Region Fit (RECOMMENDED) ---\n")
            f.write(f"  a (max compression): {a:.6f}\n")
            f.write(f"  b (compressibility): {b:.6f} MPa⁻¹\n")
            f.write(f"   Py (yield pressure): {P_y:.4f} MPa | Yield Force: {P_y * (np.pi *
(PISTON_DIAMETER/2)**2):.2f} N ← ROBUST ESTIMATE\n")
            f.write(f"  R² (fit quality): {r2_k:.6f}\n")

            if kawakita_data and len(kawakita_data) > 6 and kawakita_data[6] is not None:
                a_all = kawakita_data[6]
                b_all = kawakita_data[7]
                P_y_all = kawakita_data[8]
                r2_k_all = kawakita_data[9]
                f.write(f"\n  --- All-Data Fit (for comparison) ---\n")
                f.write(f"  a (max compression): {a_all:.6f}\n")
                f.write(f"  b (compressibility): {b_all:.6f} MPa⁻¹\n")
                f.write(f"  Py (yield pressure): {P_y_all:.4f} MPa | Yield Force: {P_y_all * (np.pi *
(PISTON_DIAMETER/2)**2):.2f} N\n")
                f.write(f"  R² (fit quality): {r2_k_all:.6f}\n\n")
        else:
            f.write(f"  ✗ Not available (insufficient data)\n\n")
```

```
        # Warnings
        if warnings_log:
            f.write("WARNINGS:\n")
            for w in warnings_log:
                f.write(f"  ⚠ {w}\n")
            f.write("\n")

        f.write("-"*110 + "\n")

#
==========================================================================
==========
# MATERIAL SELECTION
#
==========================================================================
==========

def select_material():
    """Interactive material selection."""
    print("\nAvailable materials:")
    for key, mat in MATERIALS.items():
        print(f"  [{key}] {mat['name']}")
        print(f"      Bulk density: {mat['density']} g/cm³")
        print(f"      Tap density (measured): {mat['tap_density']:.4f}")

    while True:
        try:
            choice = int(input("Select material (1-4): "))
            if choice in MATERIALS:
                selected = MATERIALS[choice]
                density_tap = selected['tap_density']
                powder_mass = VOLUME_CM3 * density_tap

                print(f"\n✓ Selected: {selected['name']}")
                print(f"  ρ_true = {selected['density']} g/cm³")
                print(f"  ρ_tap = {density_tap:.4f} g/cm³")
                print(f"  Calculated mass = {powder_mass:.2f} g")

                return selected['tap_density'], selected['density'], selected['name'], powder_mass,
selected['h0']
            else:
                print("Invalid choice. Enter a number between 1 and 4.")
        except ValueError:
            print("Invalid input. Enter a number.")

#
==========================================================================
==========
# DATA LOADING
```

```
#
==========================================================================
==========

def load_data(filepath, sheet_name, force_col, laser_current_col, pressure_col=None,
              force_offset=65, pressure_max=10):
    """Load data from Excel file - simplified for single monotonic loading."""
    print(f"\nLoading data from {filepath}...")
    df = pd.read_excel(filepath, sheet_name=sheet_name)

    force_raw = df[force_col].values
    laser_current = df[laser_current_col].values

    # Load pressure data if column specified
    pressure_raw = None
    pressure_warning = None
    if pressure_col:
        try:
            pressure_raw = df[pressure_col].values
            print(f"✓ Loaded pressure data from column '{pressure_col}'")
        except KeyError:
            print(f" ⚠️ WARNING: Pressure column '{pressure_col}' not found in file")
            pressure_warning = f"Pressure column '{pressure_col}' not found"

    # STEP 1: Filter data where pressure < pressure_max mbar
    if pressure_raw is not None and pressure_warning is None:
        vacuum_mask = pressure_raw < pressure_max
        n_before = len(force_raw)
        n_vacuum = np.sum(vacuum_mask)

        if n_vacuum == 0:
            print(f"\n ⚠️ ERROR: No data points with pressure < {pressure_max} mbar!")
            pressure_warning = f"No data with pressure < {pressure_max} mbar"
            # Use all data as fallback
            vacuum_mask = np.ones(len(force_raw), dtype=bool)
        else:
            print(f"\n✓ Filtering data with pressure < {pressure_max} mbar")
            print(f"  Points before filter: {n_before}")
            print(f"  Points after filter: {n_vacuum} ({n_vacuum/n_before*100:.1f}%)")
            print(f"  Pressure range in filtered data: {pressure_raw[vacuum_mask].min():.2f} to
{pressure_raw[vacuum_mask].max():.2f} mbar")

        # Apply vacuum filter
        force_raw = force_raw[vacuum_mask]
        laser_current = laser_current[vacuum_mask]
        pressure_raw = pressure_raw[vacuum_mask]
    else:
        print(f"\n ⚠️ WARNING: Pressure data not available, using all data")
```

```
# STEP 2: Apply force offset
force_raw = force_raw + force_offset
print(f"\n✓ Applied force offset: {force_offset} N")
print(f"  Force range after offset: {force_raw.min():.1f} to {force_raw.max():.1f} N")

# STEP 3: Find h0 at first point where force > 10 N (after offset)
first_valid_force_idx = np.where(force_raw > 50)[0]
if len(first_valid_force_idx) > 0:
    h0_idx = first_valid_force_idx[0]
    laser_initial = laser_current[h0_idx]
    print(f"\n✓ Found first force > 30 N at index {h0_idx} (after offset)")
    print(f"  Force: {force_raw[h0_idx]:.1f} N | h0 Position: {laser_initial:.2f} mm")
else:
    h0_idx = 0
    laser_initial = laser_current[0]
    print(f"\n⚠️ WARNING: No force > 30 N found! Using first data point")
    print(f"  Force at first point: {force_raw[h0_idx]:.1f} N | Position: {laser_initial:.2f} mm")

displacement = laser_initial - laser_current

# STEP 4: Extract only positive force region (single monotonic loading)
positive_mask = force_raw > 60
force = force_raw[positive_mask]
displacement = displacement[positive_mask]

# Check final pressure range during positive force if available
if pressure_raw is not None and pressure_warning is None:
    pressure_pos = pressure_raw[positive_mask]
    pressure_min = pressure_pos.min()
    pressure_max_actual = pressure_pos.max()
    pressure_mean = pressure_pos.mean()

    print(f"\n--- Pressure Check During Compression ---")
    print(f"  Pressure range: {pressure_min:.2f} to {pressure_max_actual:.2f} mbar")
    print(f"  Pressure mean: {pressure_mean:.2f} mbar")

    if pressure_max_actual > pressure_max:
        pressure_warning = (f"Pressure exceeded {pressure_max} mbar during compression: "
                            f"max = {pressure_max_actual:.2f} mbar")
        print(f"  ⚠️ WARNING: {pressure_warning}")
    else:
        print(f"  ✓ Pressure remained below {pressure_max} mbar threshold")

print(f"\n✓ Final dataset:")
print(f"  Total points: {len(force)}")
print(f"  h0 Position: {laser_initial:.2f} mm")
print(f"  Force range: {force.min():.1f} to {force.max():.1f} N")
print(f"  Displacement range: {displacement.min():.2f} to {displacement.max():.2f} mm")
```

```
    return force, displacement, force_raw, laser_current, h0_idx, laser_initial, pressure_warning

#
==========
# DATA CLEANING
#
==========

def clean_data(force, displacement):
    """Clean data by removing outliers."""
    if not ENABLE_DATA_CLEANING or len(force) == 0:
        return force, displacement

    print("\n--- Data Cleaning ---")
    n_original = len(force)
    valid_mask = np.ones(len(force), dtype=bool)

    # Remove extreme displacement outliers
    displacement_outliers = displacement > MAX_TOTAL_DISPLACEMENT
    valid_mask &= ~displacement_outliers
    if np.sum(displacement_outliers) > 0:
        print(f"  Removed {np.sum(displacement_outliers)} displacement outliers (>
{MAX_TOTAL_DISPLACEMENT} mm)")

    # Remove severe negative displacement (noise/vibration)
    negative_disp = displacement < -10
    valid_mask &= ~negative_disp
    if np.sum(negative_disp) > 0:
        print(f"  Removed {np.sum(negative_disp)} severe negative displacement points")

    # Remove displacement jumps
    if len(displacement) > 1:
        displacement_diff = np.abs(np.diff(displacement))
        jump_mask = np.zeros(len(force), dtype=bool)
        jump_mask[1:] = displacement_diff > MAX_DISPLACEMENT_JUMP
        valid_mask &= ~jump_mask
        if np.sum(jump_mask) > 0:
            print(f"  Removed {np.sum(jump_mask)} displacement jump points (>
{MAX_DISPLACEMENT_JUMP} mm)")

    # Remove force jumps
    if len(force) > 1:
        force_diff = np.abs(np.diff(force))
        force_jump_mask = np.zeros(len(force), dtype=bool)
        force_jump_mask[1:] = force_diff > 700
        valid_mask &= ~force_jump_mask
        if np.sum(force_jump_mask) > 0:
            print(f"  Removed {np.sum(force_jump_mask)} force jump points (> 700 N)")
```

```
    force_clean = force[valid_mask]
    displacement_clean = displacement[valid_mask]

    n_removed = n_original - len(force_clean)
    print(f"  Total removed: {n_removed}/{n_original} ({100*n_removed/n_original:.1f}%)")
    print(f"  Remaining: {len(force_clean)} points")

    return force_clean, displacement_clean

#
==========================================================================
==========
# DATA SMOOTHING
#
==========================================================================
==========

def smooth_data(force, displacement):
    """Apply Savitzky-Golay smoothing."""
    if not ENABLE_SMOOTHING or len(force) < SMOOTH_WINDOW:
        return force, displacement

    print("\n--- Data Smoothing ---")

    try:
        force_smooth = savgol_filter(force, SMOOTH_WINDOW, SMOOTH_ORDER)
        displacement_smooth = savgol_filter(displacement, SMOOTH_WINDOW,
SMOOTH_ORDER)

        force_rms = np.sqrt(np.mean((force - force_smooth)**2))
        disp_rms = np.sqrt(np.mean((displacement - displacement_smooth)**2))

        print(f"✓ Applied Savitzky-Golay filter (window={SMOOTH_WINDOW},
order={SMOOTH_ORDER})")
        print(f"  Force RMS change: {force_rms:.2f} N")
        print(f"  Displacement RMS change: {disp_rms:.3f} mm")

        return force_smooth, displacement_smooth

    except Exception as e:
        print(f"  ⚠ Smoothing failed: {e}")
        return force, displacement
def remove_unloading_phase(force, displacement, min_force_fraction=0.90):
    """Remove points after force drops below a fraction of maximum."""
    if len(force) < 3:
        return force, displacement

    print("\n--- Checking for unloading phase ---")
```

```
    max_force = force.max()
    threshold = max_force * min_force_fraction

    max_idx = np.argmax(force)

    cut_idx = len(force)
    for i in range(max_idx, len(force)):
        if force[i] < threshold:
            cut_idx = i
            print(f"  Force dropped below {min_force_fraction*100:.0f}% of max at index {i}")
            print(f"  Max force: {max_force:.1f} N, Current: {force[i]:.1f} N")
            break

    if cut_idx < len(force):
        removed = len(force) - cut_idx
        print(f"  Removing {removed} unloading points")
        return force[:cut_idx], displacement[:cut_idx]

    print("  No unloading phase detected")
    return force, displacement
#
================================================================================
===========
# PARAMETER CALCULATION
#
================================================================================
===========

def calculate_basic_parameters(force, displacement, d_piston, h0, tap_density, rho_theo,
powder_mass, powder_initial_height):
    """Calculate pressure, strain and relative density."""

    if len(force) == 0 or len(displacement) == 0:
        print("\n⚠ ERROR: Empty arrays!")
        return None, None, None, None, None

    A = np.pi * (d_piston/2)**2
    P = force / A
    strain = displacement / powder_initial_height
    D0 = tap_density / rho_theo

    # Handle negative displacement (clamp to 0 for density calculation)
    print(f"\n--- Displacement Analysis ---")
    print(f"  Raw displacement range: {displacement.min():.3f} to {displacement.max():.3f}
mm")
    print(f"  Negative displacement points: {np.sum(displacement < 0)}/{len(displacement)}")

    displacement_corrected = np.maximum(displacement, 0.0)

    if np.any(displacement < 0):
```

```
        print(f"   ⚠ WARNING: {np.sum(displacement < 0)} negative displacement values
detected!")
        print(f"  These indicate laser reading > h0 (vibrations/noise)")
        print(f"  Clamping to 0 for density calculation")

    h_current = powder_initial_height - displacement_corrected
    h_current = np.maximum(h_current, 0.1)  # Avoid zero/negative heights

    apparent_density = powder_mass / (A * h_current * 1e-3)
    D = apparent_density / rho_theo

    if np.any(D > 1.0):
        print(f"\n⚠ WARNING: Relative density exceeds 1.0! Max D = {D.max():.3f}")
        print(f"  This suggests measurement errors or incorrect parameters")

    if np.any(D < D0):
        n_below = np.sum(D < D0)
        print(f"\n⚠ WARNING: {n_below} points have D < D0!")
        print(f"  D range: {D.min():.6f} to {D.max():.6f}")
        print(f"  D0: {D0:.6f}")

    print(f"\n--- Basic Parameters ---")
    print(f"Piston area: {A:.2f} mm²")
    print(f"Powder mass: {powder_mass:.2f} g")
    print(f"Initial height h0: {h0} mm")
    print(f"Initial relative density D₀: {D0:.4f}")
    print(f"Final relative density D: {D.max():.3f}")
    print(f"Maximum pressure: {P.max():.2f} MPa")
    print(f"Maximum strain: {strain.max():.3f} ({strain.max()*100:.1f}%)")
    print(f"Data points: {len(force)}")

    return P, strain, D, D0, A

#
==========================================================================
==========
# HECKEL ANALYSIS
#
==========================================================================
==========

def heckel_analysis(P, D, min_frac=0.6, max_frac=0.95):
    """Apply Heckel equation."""

    warnings_list = []

    print(f"\n=== HECKEL ANALYSIS ===")
    print(f"Input data:")
    print(f"  Total points: {len(P)}")
    print(f"  D range: {D.min():.6f} to {D.max():.6f}")
```

```
print(f"  P range: {P.min():.4f} to {P.max():.4f} MPa")

D_min = D.min() * 0.5
D_max = D.max() * 1.1

print(f"\n✓ Using ADAPTIVE filtering:")
print(f"  D_min threshold: {D_min:.6f}")
print(f"  D_max threshold: {D_max:.6f}")

valid_mask = (D >= D_min) & (D <= D_max)
P_valid = P[valid_mask]
D_valid = D[valid_mask]

print(f"  Points after filter: {len(D_valid)}")

if len(P_valid) < 10:
    msg = "Not enough valid points for Heckel analysis (< 10 points)"
    print(f"\n⚠ WARNING: {msg}")
    warnings_list.append(msg)
    return None, None, None, None, None, None, 0, warnings_list

y_heckel = np.log(1.0 / (1.0 - D_valid))

print(f"\nCalculating Heckel variable:")
print(f"  y_heckel = ln[1/(1-D)]")
print(f"  y_heckel range: {y_heckel.min():.6f} to {y_heckel.max():.6f}")

print(f"\nIdentifying linear region:")
P_max = P_valid.max()
P_min_linear = min_frac * P_max
P_max_linear = max_frac * P_max

print(f"  P_max: {P_max:.4f} MPa")
print(f"  Linear region: {P_min_linear:.4f} to {P_max_linear:.4f} MPa")
print(f"  Fraction range: {min_frac} to {max_frac}")

linear_mask = (P_valid >= P_min_linear) & (P_valid <= P_max_linear)
P_linear = P_valid[linear_mask]
y_linear = y_heckel[linear_mask]

print(f"  Points in linear region: {len(P_linear)}")

if len(P_linear) < 5:
    msg = f"Insufficient linear region points ({len(P_linear)} < 5)"
    print(f"\n⚠ WARNING: {msg}")
    warnings_list.append(msg)
    return None, None, None, None, None, None, 0, warnings_list

slope, intercept, r_value, _, _ = linregress(P_linear, y_linear)
K = slope
```

```
    A = intercept
    sigma_y = 1 / K if K > 0 else None
    r2 = r_value**2

    print(f"\n✓ Heckel fit successful:")
    print(f"  K (slope): {K:.6f} MPa⁻¹")
    print(f"  A (intercept): {A:.6f}")
    if sigma_y:
        print(f"  σy (yield strength): {sigma_y:.4f} MPa")
    print(f"  R²: {r2:.6f}")

    if r2 < 0.9:
        msg = f"Poor fit quality (R² = {r2:.3f} < 0.9)"
        print(f"  ⚠ WARNING: {msg}")
        warnings_list.append(msg)

    return P_linear, y_linear, K, A, sigma_y, r2, len(P_linear), warnings_list

#
================================================================================
==========
# KAWAKITA ANALYSIS
#
================================================================================
==========

def kawakita_analysis(P, strain, min_compression=0.01, pressure_threshold=0.20):
    """Apply Kawakita equation with fixed pressure threshold."""

    warnings_list = []

    print(f"\n=== KAWAKITA ANALYSIS ===")
    print(f"Input data:")
    print(f"  Total points: {len(P)}")
    print(f"  Strain range: {strain.min():.6f} to {strain.max():.6f}")
    print(f"  P range: {P.min():.4f} to {P.max():.4f} MPa")

    # Filter positive compression only
    valid_mask = strain >= min_compression
    P_valid = P[valid_mask]
    C_valid = strain[valid_mask]

    print(f"\n✓ Filtered data (strain >= {min_compression}):")
    print(f"  Valid points: {len(P_valid)}")

    if len(P_valid) < 3:
        msg = f"Insufficient data points ({len(P_valid)} < 5)"
        print(f"\n⚠ WARNING: {msg}")
        warnings_list.append(msg)
```

```
        return None, None, None, None, None, None, None, None, None, None, 0, 0, warnings_list

    # FIXED PRESSURE THRESHOLD
    if P_valid.max() < pressure_threshold:
        msg = f"Max pressure {P_valid.max():.3f} MPa < threshold {pressure_threshold} MPa"
        print(f"\n⚠ WARNING: {msg}")
        warnings_list.append(msg)
        high_p_mask = np.ones(len(P_valid), dtype=bool)
    else:
        high_p_mask = P_valid >= pressure_threshold

    P_high_p = P_valid[high_p_mask]
    C_high_p = C_valid[high_p_mask]

    print(f"\nHigh-pressure region (P >= {pressure_threshold:.2f} MPa):")
    print(f"  Points: {len(P_high_p)}")
    print(f"  Pressure range: {P_high_p.min():.3f} - {P_high_p.max():.3f} MPa")
    print(f"  Strain range: {C_high_p.min()*100:.1f}% - {C_high_p.max()*100:.1f}%")

    if len(P_high_p) >= 3:
        y_kawakita_high = P_high_p / C_high_p

        slope_high, intercept_high, r_value_high, _, _ = linregress(P_high_p, y_kawakita_high)

        # Check for valid fit
        if intercept_high == 0 or slope_high < 0:
            msg = "Invalid Kawakita fit parameters"
            print(f"\n⚠ WARNING: {msg}")
            warnings_list.append(msg)
            a_high = b_high = P_y_high = r2_high = None
        else:
            a_high = 1 / intercept_high
            b_high = slope_high / intercept_high
            P_y_high = 1 / b_high if b_high != 0 else None
            r2_high = r_value_high**2

            print(f"\n✓ High-pressure fit successful:")
            print(f"  a (max compression): {a_high:.6f}")
            print(f"  b (compressibility): {b_high:.6f} MPa⁻¹")
            if P_y_high:
                print(f"  Py (yield pressure): {P_y_high:.4f} MPa")
            print(f"  R²: {r2_high:.6f}")

            if r2_high < 0.95:
                msg = f"Moderate fit quality (R² = {r2_high:.3f} < 0.95)"
                print(f"  ⚠ WARNING: {msg}")
                warnings_list.append(msg)
    else:
```

```
        print(f"  ⚠ Insufficient high-pressure points")
        a_high = b_high = P_y_high = r2_high = None

    # All-data fit (for comparison)
    y_kawakita_all = P_valid / C_valid

    try:
        slope_all, intercept_all, r_value_all, _, _ = linregress(P_valid, y_kawakita_all)

        if intercept_all != 0:
            a_all = 1 / intercept_all
            b_all = slope_all / intercept_all
            P_y_all = 1 / b_all if b_all != 0 else None
            r2_all = r_value_all**2
        else:
            a_all = b_all = P_y_all = r2_all = None
    except:
        a_all = b_all = P_y_all = r2_all = None

    print(f"\n✓ All-data fit:")
    if a_all:
        print(f"  a (max compression): {a_all:.6f}")
        print(f"  b (compressibility): {b_all:.6f} MPa⁻¹")
        if P_y_all:
            print(f"  Py (yield pressure): {P_y_all:.4f} MPa")
        print(f"  R²: {r2_all:.6f}")
    else:
        print(f"  Fit failed")

    return (P_high_p, y_kawakita_high, a_high, b_high, P_y_high, r2_high,
            a_all, b_all, P_y_all, r2_all, len(P_high_p), len(P_valid), warnings_list)

#
==========================================================================
==========
# PLOTTING
#
==========================================================================
==========

def plot_results(P_all, strain_all, D_all, P_mono, strain_mono, heckel_data, kawakita_data,
                 material_name, rho_theoretical, D0, powder_mass, force_raw, laser_current,
h0_actual,
                 powder_initial_height, filename=None, output_folder=None):
    """Plot comprehensive results - 2x3 layout."""

    fig = plt.figure(figsize=(18, 10))

    # 1. Pressure vs Strain
    ax1 = plt.subplot(2, 3, 1)
```

```
ax1.plot(strain_all*100, P_all, 'b-', linewidth=2, label='Data')
ax1.set_xlabel('Strain (%)', fontsize=11)
ax1.set_ylabel('Pressure (MPa)', fontsize=11)
ax1.set_title('Pressure vs Strain', fontsize=12, fontweight='bold')
ax1.grid(True, alpha=0.3)
ax1.legend()

# 2. Relative Density vs Pressure
ax2 = plt.subplot(2, 3, 2)
ax2.plot(P_all, D_all, 'r-', linewidth=2, label='Data')
ax2.axhline(y=D0, color='g', linestyle='--', linewidth=2, label=f'D₀ = {D0:.4f}')
ax2.set_xlabel('Pressure (MPa)', fontsize=11)
ax2.set_ylabel('Relative Density D', fontsize=11)
ax2.set_title('Densification Curve', fontsize=12, fontweight='bold')
ax2.grid(True, alpha=0.3)
ax2.legend()

# 3. Force vs Displacement
ax3 = plt.subplot(2, 3, 3)
disp_all = strain_all * powder_initial_height
ax3.plot(disp_all, P_all * (np.pi * (PISTON_DIAMETER/2)**2), 'b-', linewidth=2)
ax3.set_xlabel('Displacement (mm)', fontsize=11)
ax3.set_ylabel('Force (N)', fontsize=11)
ax3.set_title('Force vs Displacement', fontsize=12, fontweight='bold')
ax3.grid(True, alpha=0.3)

# 4. Heckel Plot
ax4 = plt.subplot(2, 3, 4)
try:
    if heckel_data and heckel_data[0] is not None:
        P_heckel, y_heckel, K, A, sigma_y, r2 = heckel_data
        ax4.plot(P_heckel, y_heckel, 'go', markersize=6, label='Data', alpha=0.6)

        P_fit = np.linspace(P_heckel.min(), P_heckel.max(), 100)
        y_fit = K * P_fit + A
        ax4.plot(P_fit, y_fit, 'r-', linewidth=2, label=f'R²={r2:.4f}')

        ax4.set_xlabel('Pressure P (MPa)', fontsize=11)
        ax4.set_ylabel('ln[1/(1-D)]', fontsize=11)
        ax4.set_title(f'Heckel Plot (σy = {sigma_y:.2f} MPa)', fontsize=12, fontweight='bold')
        ax4.legend()
    else:
        ax4.text(0.5, 0.5, 'Heckel analysis\nnot available',
                 ha='center', va='center', transform=ax4.transAxes, fontsize=12)
        ax4.set_title('Heckel Plot', fontsize=12, fontweight='bold')
except Exception as e:
    ax4.text(0.5, 0.5, f'Heckel plot error:\n{str(e)}',
             ha='center', va='center', transform=ax4.transAxes, fontsize=10)
    ax4.set_title('Heckel Plot', fontsize=12, fontweight='bold')
ax4.grid(True, alpha=0.3)
```

```
    # 5. Kawakita Plot
    ax5 = plt.subplot(2, 3, 5)
    try:
        if kawakita_data and kawakita_data[0] is not None:
            P_kaw, y_kaw, a, b, P_y, r2 = kawakita_data[:6]
            ax5.plot(P_kaw, y_kaw, 'mo', markersize=6, label='High-P data', alpha=0.6)

            P_fit = np.linspace(P_kaw.min(), P_kaw.max(), 100)
            slope = b * (1/a)
            intercept = 1/a
            y_fit = slope * P_fit + intercept
            ax5.plot(P_fit, y_fit, 'r-', linewidth=2, label=f'R²={r2:.4f}')

            ax5.set_xlabel('Pressure P (MPa)', fontsize=11)
            ax5.set_ylabel('P/C', fontsize=11)
            ax5.set_title(f'Kawakita Plot (Py = {P_y:.2f} MPa)', fontsize=12, fontweight='bold')
            ax5.legend()
        else:
            ax5.text(0.5, 0.5, 'Kawakita analysis\nnot available',
                     ha='center', va='center', transform=ax5.transAxes, fontsize=12)
            ax5.set_title('Kawakita Plot', fontsize=12, fontweight='bold')
    except Exception as e:
        ax5.text(0.5, 0.5, f'Kawakita plot error:\n{str(e)}',
                 ha='center', va='center', transform=ax5.transAxes, fontsize=10)
        ax5.set_title('Kawakita Plot', fontsize=12, fontweight='bold')
    ax5.grid(True, alpha=0.3)

    # 6. Summary text
    ax6 = plt.subplot(2, 3, 6)
    ax6.axis('off')
    summary = f"""
MATERIAL: {material_name}
ρ_true: {rho_theoretical} g/cm³
Mass: {powder_mass:.2f} g
h₀: {h0_actual:.2f} mm

DATA POINTS: {len(P_all)}
D₀: {D0:.4f}
D_final: {D_all.max():.4f}
P_max: {P_all.max():.2f} MPa
F_max: {P_all.max()*(np.pi*(PISTON_DIAMETER/2)**2):.1f} N
Strain_max: {strain_all.max()*100:.1f}%

HECKEL:
"""
    if heckel_data[2] is not None:
        K, A, sigma_y, r2 = heckel_data[2:6]
        summary += f"  K = {K:.4f} MPa⁻¹\n"
        summary += f"  σy = {sigma_y:.2f} MPa\n"
```

```
        summary += f"  R² = {r2:.4f}\n"
    else:
        summary += "  Not available\n"

    summary += "\nKAWAKITA:\n"
    if kawakita_data[2] is not None:
        a, b, P_y, r2 = kawakita_data[2:6]
        summary += f"  a = {a:.4f}\n"
        summary += f"  b = {b:.4f} MPa⁻¹\n"
        summary += f"  Py = {P_y:.2f} MPa\n"
        summary += f"  Fy = {P_y*(np.pi*(PISTON_DIAMETER/2)**2):.1f} N\n"
        summary += f"  R² = {r2:.4f}"
    else:
        summary += "  Not available"

    if filename:
        summary += f"\n\nFILE:\n  {os.path.basename(filename)}"

    ax6.text(0.05, 0.98, summary, transform=ax6.transAxes, fontsize=10,
             verticalalignment='top', fontfamily='monospace',
             bbox=dict(boxstyle='round', facecolor='wheat', alpha=0.3))

    plt.tight_layout()

    if filename:
        base_name = os.path.splitext(os.path.basename(filename))[0]
        save_name = f'compression_analysis_{base_name}.png'
    else:
        save_name = f'compression_analysis_{material_name.replace(" ", "_")}.png'

    if output_folder:
        save_path = os.path.join(output_folder, save_name)
    else:
        save_path = save_name

    plt.savefig(save_path, dpi=150)
    print(f"\n✓ Plot saved: {save_path}")
    plt.show()

#
================================================================================
==========
# BATCH ANALYSIS
#
================================================================================
==========

def batch_analysis(file_list=None, results_filename="batch_results_single_cycle.txt"):
    """Analyze multiple files in batch mode - simplified for single cycle."""
```

```
    # SELECT TEST CONDITION FIRST
    force_offset, pressure_max = select_test_condition()

    timestamp = datetime.now().strftime("%Y%m%d_%H%M%S")
    plots_folder = f"compression_plots_{timestamp}"
    os.makedirs(plots_folder, exist_ok=True)
    print(f"\n📁 Plots will be saved in: {plots_folder}/")

    if file_list is None:
        # SELECT DIRECTORY
        pattern = select_directory()
        print(f"\nUsing pattern: {pattern}")
        file_list = glob.glob(pattern)

        if not file_list:
            print(f"❌ No files found matching pattern: {pattern}")
            return None, None, None

    print(f"\n{'='*70}")
    print(f"BATCH ANALYSIS - SINGLE CYCLE MODE")
    print(f"Found {len(file_list)} files to analyze")
    print(f"{'='*70}\n")

    tap_density, rho_theoretical, material_name, powder_mass, powder_initial_height =
select_material()

    for i, filepath in enumerate(file_list, 1):
        filename = os.path.basename(filepath)
        print(f"\n{'='*70}")
        print(f"ANALYZING FILE {i}/{len(file_list)}: {filename}")
        print(f"{'='*70}")

        try:
            # Load data with selected test parameters
            force_all, displacement_all, force_raw, laser_current, h0_idx, laser_initial,
pressure_warning = load_data(
                filepath, SHEET_NAME, COL_FORCE, COL_POSITION, COL_PRESSURE,
                force_offset=force_offset, pressure_max=pressure_max
            )

            h0_actual = laser_initial

            # Clean and smooth
            print("\n--- CLEANING AND SMOOTHING ---")
            force_clean, displacement_clean = clean_data(force_all, displacement_all)
            force_smooth, displacement_smooth = smooth_data(force_clean, displacement_clean)
            force_smooth, displacement_smooth = remove_unloading_phase(force_smooth,
displacement_smooth)

            # Calculate parameters
```

```
        result = calculate_basic_parameters(
            force_smooth, displacement_smooth, PISTON_DIAMETER, h0_actual,
            tap_density, rho_theoretical, powder_mass, powder_initial_height
        )

        if result[0] is None:
            warnings_all = ["Failed to calculate basic parameters"]
            save_batch_results(filepath, material_name, rho_theoretical, powder_mass,
h0_actual, laser_initial,
                               np.array([]), np.array([]), np.array([]), 0,
                               (None, None, None, None, None, None),
                               (None, None, None, None, None, None, None, None, None, None),
                               0, {'high_p': 0, 'all_data': 0}, warnings_all, powder_initial_height,
pressure_warning, results_filename,
                               force_offset, pressure_max)
            continue

        P_all, strain_all, D_all, D0, A = result
        # Initialize warnings lists
        heckel_warnings = []
        kawakita_warnings = []
        warnings_all = []

        # Heckel analysis
        print("\n--- HECKEL ANALYSIS ---")
        try:
            heckel_result = heckel_analysis(P_all, D_all, HECKEL_MIN_FRACTION,
HECKEL_MAX_FRACTION)
        except Exception as e:
            print(f"⚠️ Heckel analysis error: {e}")
            heckel_result = (None,)*8

        heckel_data = heckel_result[:6] if heckel_result and len(heckel_result)>=6 else
(None,)*6
        heckel_n_points = heckel_result[6] if heckel_result and len(heckel_result)>=7 else 0
        heckel_warnings = heckel_result[7] if heckel_result and len(heckel_result)>=8 else []

        # Kawakita analysis
        print("\n--- KAWAKITA ANALYSIS ---")
        try:
            kawakita_result = kawakita_analysis(P_all, strain_all, MIN_COMPRESSION)

            if kawakita_result[0] is None:
                kawakita_data = (None, None, None, None, None, None, None, None, None,
None)
                kawakita_n_points = {'high_p': 0, 'all_data': 0}
                kawakita_warnings = kawakita_result[12] if len(kawakita_result) > 12 else []
            else:
                kawakita_data = kawakita_result[:10]
                kawakita_n_points = {
```

```
                'high_p': kawakita_result[10],
                'all_data': kawakita_result[11]
            }
            kawakita_warnings = kawakita_result[12] if len(kawakita_result) > 12 else []
        except Exception as e:
            print(f"⚠️ Kawakita analysis error: {e}")
            kawakita_data = (None, None, None, None, None, None, None, None, None, None)
            kawakita_n_points = {'high_p': 0, 'all_data': 0}
            kawakita_warnings = [f"Kawakita error: {str(e)}"]

        # Save results
        print("\n--- SAVING RESULTS ---")
        save_batch_results(filepath, material_name, rho_theoretical, powder_mass, h0_actual,
laser_initial,
                           P_all, strain_all, D_all, D0, heckel_data, kawakita_data,
                           heckel_n_points, kawakita_n_points, warnings_all, powder_initial_height,
pressure_warning, results_filename,
                           force_offset, pressure_max)

        # Plot with output folder
        plot_results(P_all, strain_all, D_all, P_all, strain_all, heckel_data, kawakita_data,
                     material_name, rho_theoretical, D0, powder_mass, force_raw, laser_current,
h0_actual,
                     powder_initial_height, filename=filepath, output_folder=plots_folder)

        print(f"✅ ANALYSIS COMPLETE FOR: {filename}")

    except Exception as e:
        print(f"\n⚠️ ERROR during analysis: {e}")
        import traceback
        traceback.print_exc()
        continue

print("\n" + "="*70)
print("BATCH ANALYSIS COMPLETE!")
print(f"Results saved to: {results_filename}")
print(f"Plots saved to: {plots_folder}/")
print("="*70)

return P_all, strain_all, D_all
#
==========================================================================
==========
# EXECUTION
#
==========================================================================
==========

if __name__ == "__main__":
    P_all, strain_all, D_all = batch_analysis()  # Batch analysis
```